

**THE EFFECT OF GRAIN GROWTH INHIBITORS TO
THE MICROSTRUCTURAL AND MECHANICAL
PROPERTIES OF WC-Co NANOCOMPOSITES**

BY

KHWAJA MOHAMMAD

A Thesis Presented to the
DEANSHIP OF GRADUATE STUDIES

KING FAHD UNIVERSITY OF PETROLEUM & MINERALS

DHAHRAN, SAUDI ARABIA

In Partial Fulfillment of the
Requirements for the Degree of

MASTER OF SCIENCE

In

MECHANICAL ENGINEERING

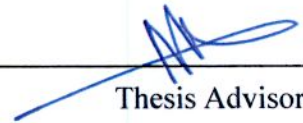
DECEMBER 2012

**KING FAHD UNIVERSITY OF PETROLEUM & MINERALS
DHAHRAN, SAUDI ARABIA**

DEANSHIP OF GRADUATE STUDIES

This thesis, written by **Khwaja Mohammad** under the direction of his thesis advisor and approved by his thesis committee, has been presented to and accepted by the Dean of Graduate Studies, in partial fulfillment of the requirements for the degree of **MASTER OF SCIENCE in MECHANICAL ENGINEERING**.

Thesis Committee



Thesis Advisor
Dr. Nasser Al-Aqeeli



Member
Dr. Saheb Nouari



Department Chairman
Prof. Amro M. Al-Qutub



Member
Dr. Syed Fida Hassan



Dean of Graduate Studies
Prof. Salam A. Zummo





Date

DEDICATION

I strongly dedicate my research at KFUPM to

My best friend ever (My father), for instilling the importance of hard work and higher education, which always pushed me to stair up in my life dreams.

And my mom....for everything you've done from extreme love, to raising me in a manner, to celebrate and embrace life while keeping in-contact to the traditional values.

Simply, I could not have asked for better parents or role-models.

ACKNOWLEDGEMENT

First and foremost I offer my highest gratitude to my thesis advisor, Dr. Naseer Al-Aqeeli, who has always helped me, in technical, ethical, social and financial support though out my thesis, especially his patience and knowledge whilst allowing me the room to work in my own way. I attribute the level of my Masters degree to his encouragement and effort and without him this thesis, too, would not have been completed or written. One simply could not wish for a better or friendlier supervisor.

Beside Dr. Aqeeli, It was an honor for me to be working under auspicious supervision of Prof. Dr. Tahar Lauio. His supervision, advice, and guidance from the very early stage of this research as well as giving me extraordinary experiences throughout the work. . He exceptionally inspired and enriched my growth as a student, a researcher and a scientist.

I would also like to thank Dr. Abbass Hakem for all and the most what he attributes. He provided me unflinching encouragement and support in various ways. His truly scientific comments and ideas have always been fruitful regarding this thesis work. I have always found him ready to help and discuss, when and ever required. Beside special thanks to my other committee members, Dr. Nouari saheb and Dr. Syed Fida Hassan, I would also forward my attributes and thanks to Mr.lateef hashmi, Mr. sadaqat, indeed everyone, who have helped me in touching the peaks during this research work.

I wish to acknowledge the help from Dr. Zain Yamani, Director, Center of Research Excellence in Nanotechnology, KFUPM who have always welcomed me to use any of the required equipment, with-out any time scale, especially SPS, FESEM, XRD and further for extending his full support which contributed to the finishing of my MS-Thesis.

I am Indebted from my deep heart to King Fahd University of petroleum and minerals, and in particularly to Mechanical Engineering department for giving me an opportunity to step-up in my educational carrier. I enjoyed the entire supportive research oriented environment, from best lecture room, best available laboratory equipment's, on-campus accommodation, and family-like care. I am very sure with-out all this, it would have been difficult to achieve targets of my thesis in such a short time. Further, the financial support, which I received from KFUPM during my stay, is an extra edge. Besides KFUPM, I would also like to Thank KACST for extending financial support towards completion of this project.

I would never forget to mention full support from my employer in Pakistan especially Mr. Umar sardar Khattak, Mr. Bakhtiyar Majeed, Mr. Zia Aftab, Dr. Tariq Jamal solaija, and all concerned authorities, , who have actively supported the cause of my higher education.

I cannot forget my life partner, my wife, my beloved friend and mother of my kids, who has always supported me in every walk of life. I truly enjoyed her patience, her motivation and encouragement in completing my thesis research.

Last but not the least, my little baby-girl Zaryab khan, and two best ever friends Hamza Khan and Hasnain khan (my sons), whom I have enjoyed always and who have always proven to be a source of relaxation.

TABLE OF CONTENTS

DEDICATION	III
ACKNOWLEDGEMENT	IV
LIST OF FIGURES	IX
LIST OF TABLES	XI
ABSTRACT (ENGLISH)	XII
ABSTRACT (ARABIC)	XIII
CHAPTER 1	1
INTRODUCTION	1
1.1 <i>Objective of this work.</i>	3
CHAPTER 2	5
LITERATURE REVIEW	5
2.1 <i>Tungsten Carbide:</i>	5
2.2 <i>Binding material:</i>	7
2.3 <i>Mechanical Alloying:</i>	10
2.4 <i>Consolidation:</i>	12
2.5 <i>Spark plasma sintering:</i>	15
2.6 <i>Inhibitors:</i>	20
CHAPTER 3	24
MATERIALS AND EXPERIMENTAL PROCEDURE	24
3.1 <i>Raw Materials.</i>	24

3.2	<i>Powder Milling</i>	25
3.3	<i>Sintering Procedures:</i>	27
3.4	<i>Characterization</i>	30
CHAPTER 4		39
RESULTS & DISCUSSION		39
4.1	<i>Characterization of starting powders</i>	39
4.2	<i>Preparation of WC (nano) powder</i>	44
4.3	<i>Effect of initial particle size on WC-Co composite</i>	51
4.4	<i>Effect of amount of binding material</i>	56
4.5	<i>Effect of sintering temperature, binding material over inhibitor –added WC-Co composites</i>	61
4.6	<i>Effect of adding range of individual Inhibitors to WC-Co Nano Composites</i>	73
4.7	<i>Effect of adding range of combined Inhibitors to WC-Co Nano composites</i>	84
CONCLUSION:		90
	<i>Future Recommendation</i>	92
	<i>Publications</i>	93
REFERENCES		94
CURRICULUM VITAE		100

LIST OF FIGURES

<i>Figure 1 schematics of distribution of current, during SPS [21].....</i>	<i>8</i>
<i>Figure 2 Schematic diagram of ball-milling device with controlled ball movement 1: rotating 2: balls 3: magnets [24].</i>	<i>11</i>
<i>Figure 3 Ball-powder-ball collision of powder mixture during mechanical alloying [8]</i>	<i>11</i>
<i>Figure 4 Schematic illustration of Spark Plasma Sintering (SPS).</i>	<i>17</i>
<i>Figure 5 Illustrates how pulse current flows through powder particles inside the SPS sintering die [36]</i>	<i>18</i>
<i>Figure 6 Temperature, Pressure and shrinkage profile during pulsed current activated sintering process [20]</i>	<i>18</i>
<i>Figure 7 Time-temperature and Time-Pressure variation during SPS</i>	<i>29</i>
<i>Figure 8 Spark Plasma Machine, being used for consolidation.</i>	<i>29</i>
<i>Figure 9 Shows Universal Hardness Testing Machine (Zwick-Roell, ZHU250, Germany).</i>	<i>33</i>
<i>Figure 10 Optical micrographs of indentation on a sintered WC-Co nanocomposite</i>	<i>35</i>
<i>Figure 11 Williamson-Hall plot used for calculating crystallite size of 72hr milled WC powder.....</i>	<i>37</i>
<i>Figure 12 FESEM of starting powder, Cobalt 1.31μm (a), WC 3.5μm as received (b)</i>	<i>40</i>
<i>Figure 13 FESEM micrographs showing as received (a, b) VC and (c, d) Cr₃C₂, which are used as inhibitors</i>	<i>41</i>
<i>Figure 14 . XRD peak broadening effect during different stages of milling of as-received 3.5μm WC.....</i>	<i>45</i>
<i>Figure 15 Showing XRD of different particle size used during the study</i>	<i>46</i>
<i>Figure 16 WC particle size distribution (a) at different stages of ball milling operations (b) final attained powder after milling of 72hrs.</i>	<i>48</i>
<i>Figure 17 FESEM of WC, at different stages of milling, showing morphology of powders.....</i>	<i>50</i>
<i>Figure 18 FESEM of Sintered WC 3.5 (a,c,e) and WC 10nm (b,d,f), each with 9%Co.....</i>	<i>54</i>

<i>Figure 19 Fractured surface of SPSed WC(10nm)-9%Co.....</i>	<i>54</i>
<i>Figure 20 Effect of WC initial size over (a) densification and (b) Vickers hardness Hv_{30}.....</i>	<i>55</i>
<i>Figure 21 showing effect of amount of binding material over mechanical properties of WC-Co nanocomposite.</i>	<i>57</i>
<i>Figure 22 showing mapping distribution of milled powder.</i>	<i>59</i>
<i>Figure 23 EDX of milled powder(WC 10nm-9Co).</i>	<i>60</i>
<i>Figure 24 FESEM images of milled WC powder</i>	<i>62</i>
<i>Figure 25 (a) incomplete densification as a result of WC-9Co-0.6VC sintered at 1200⁰C, while (b) showing complete densification, homogeneous distribution as a result of WC-12Co-0.6VC sintered at 1300⁰C.</i>	<i>64</i>
<i>Figure 26 XRD of spark plasma sintered WC-12Co-0.6Cr₃C₂.....</i>	<i>67</i>
<i>Figure 27 showing change in basic properties of WC-Co composite, as a result of variation in amount of Cobalt and sintering temperatures.</i>	<i>71</i>
<i>Figure 28 comparison of attained densification, with varying sintering temperatures, amount of cobalt, and using different inhibitors</i>	<i>75</i>
<i>Figure 29 comparison of attained hardness values, with varying sintering temperatures, amount of cobalt, and using different inhibitors</i>	<i>76</i>
<i>Figure 30 comparison of attained crystallite sizes, with varying sintering temperatures, amount of cobalt, and using different inhibitors</i>	<i>77</i>
<i>Figure 31 comparison of FESEM images for different type and rages of inhibitors, being sintered at 1300⁰C.</i>	<i>81</i>
<i>Figure 32 Mapping showing distribution of additives in the composites, after being sintered at 1300⁰C.</i>	<i>83</i>
<i>Figure 33 Graphical representation of results from addition of combined effect of inhibitors to the nano composites.....</i>	<i>87</i>

LIST OF TABLES

<i>Table 1 variables affecting sinter ability and microstructure [25].....</i>	<i>13</i>
<i>Table 2 showing characteristics of the starting powders.</i>	<i>25</i>
<i>Table 3 Summary of parameters for Spark Plasma Sintering (SPS).....</i>	<i>28</i>
<i>Table 4 EDX Analysis of vanadium Carbide, as received.....</i>	<i>42</i>
<i>Table 5 EDX Analysis of Chromium Carbide, as received.....</i>	<i>43</i>
<i>Table 6 Mechanical properties of WC-Co composite studies in this work, in comparison to reported by earlier researchers.</i>	<i>60</i>
<i>Table 7 showing experimental results of WC-Co system, where both the amount of cobalt and sintering temperature has been changed.</i>	<i>68</i>
<i>Table 8 showing comparison of research work in WC-Co system for refining grain growth and increasing mechanical properties.</i>	<i>72</i>
<i>Table 9 Input parameters regarding experimental data for adding individual range of inhibitors.....</i>	<i>74</i>
<i>Table 10 Experimental input parameters for addition of combination of both inhibitors.....</i>	<i>85</i>
<i>Table 11 results for combined addition of inhibitors to Nano-scaled WC-Co.....</i>	<i>85</i>

ABSTRACT (ENGLISH)

WC-Co hard metal composites are widely used in cutting and drilling industry, due to their unique combination of properties such as wear-, high thermal shock-; corrosion-resistant and exhibiting high hardness and toughness values.

Nano sized WC powder was prepared through planetary ball milling of as received micron sized WC powder for 72hrs. These hard carbides were further mixed with soft binding material, Cobalt in this case, and other desired additives through mechanical alloying, which results in homogeneous distribution of powders in the mixed composition. The resulted mixed powder composition was then consolidated under spark plasma sintering technique. Sintering and compositional parameters were varied during this study. The resulted sintered composites were characterized for their densification, Vickers hardness and fracture toughness. Micro-structural characterization was done through FESEM and X-rays diffraction.

One of the key challenges for researchers in this area is the development of WC-Co Nano composites by limiting their grain sizes to nanoscale, even after sintering. The development of finer dense microstructures is in addition to the expectations of improving their mechanical properties. The aim of this study is to offer an understanding to the possible fabrication of dense nanostructured hard metals composites and further effect on mechanical properties of these nanocomposites, by varying initial WC particle sizes and use of grain growth inhibitors, in retarding grain growth. The effect of grain growth was also studied in combination of changing amount of binding material and sintering temperature. Vanadium carbide and Chromium carbide as grain growth inhibitors have been studied in ranges of 0.2, 0.4, 0.6 and 0.8wt%, both individually and also in combination. In addition to individual and combined effect of these inhibitors, their effect was also monitored while varying amount cobalt and sintering temperature of these spark plasma sintered nano-crystalline WC(10nm)-Co cemented carbides, in each case. Grain sizes attained in each case and their respective mechanical and physical properties were analyzed and compared respectively. Characterization was carried out using (XRD)X-ray diffraction, (FESEM)Field emission scanning electron microscope. Densification, hardness and fracture toughness were observed, measured and compared in each case to access any improvement in the mechanical properties.

It was found that VC added samples were comparatively more active in controlling grain sizes, however resulted in comparatively lower densification of the resulted nano composite. Beside Cr_3C_2 added samples were found to result in comparatively higher hardness and fracture toughness of the material. Further combination of both inhibitors in a particular sample, rather than individual, was found to result with higher mechanical properties.

ABSTRACT (ARABIC)

المواد المركبة المولفة من كربيد التنجستن والكوبلت تستخدم على نطاق واسع في صناعة ادوات القطع والحفر وذلك لانها تتميز بخصائص مثل: مقاومة البرى و مقاومة الصدمات الحرارية و مقاومة التاكل وكذلك لما له من صلادة ومتانه عاليه.

كربيد التنجستن المستخدم ذو حجم حبيبات فى مدى المايكرون تم استخدام طريقة التسابك الميكانيكى للحصول على حجم حبيبات فى مدى النانو. ثم اضافة الكوبالت كمادة رابطه وكذلك بعض الاضافات الاخرى لكربيد التنجستن وخطهم باستخدام عملية التسابك الميكانيكى للحصول على خليط متجانس. تم تلييد هذا الخليط باستخدام تقنيه تعتمد على البلازما مع الشراة الكهربيه. و تم دراسه تاثير تغيير عمليه التلييد ومكونات ماده المركبه بعد عمليه التلييد تمت دراسه الخصائص الميكانيكيه عن طريق قياس الصلادة و متانه الكسر وفحص البنيه المجهرية وكذلك باستخدام المجهر الالكترونى.

من التحديات التى تواجه الباحثين فى هذا المجال هى تطوير مواد مؤلفه من كربيد التنجستن مع الكوبلت مع الحفاظ على حجم الحبيبات فى مدى النانو بعد عمليه التلييد.

الهدف من هذه الدراسه بحث امكانية تصنيع مواد صلبه نانومركبه ذات كثافه عاليه وكذلك دراسه الخصائص الميكانيكيه مع تغيير حجم حبيبات كربيد التنجستن واستخدام مواد تمنع نمو الحبيبات. تم دراسه تاثير نمو الحبيبات مع تغيير ماده الرابطه ودجه حراره عمليه التلييد. تم اسنخدام كربيد اتنجستن وكربيد الكروم كماده مانعه لنمو الحبيبات بنسب وزنيه 0.2 و0.4 و0.6 و0.8% كلا على حده وكذلك معا وتم مقارنه حجم الحبيبات الناتج مع استخدام هذه المواد بدونها فى المواد المؤلفه من كربيد التنجستن والكوبلت. ومقارنه الخصائص الميكانيكيه والفيزيائيه.

تمت عمليه التوصيف باستخدام اشعة اكس والميكروسكوب الالكترونى ولتقييم وتحسين الخصائص الميكانيكيه تم قياس الصلاده ومتانه الكسر للمواد الملبده. تم التوصل الى ان كربيد الفاناديوم اكثر فاعليه للتحكم فى حجم الحبيبات بالرغم من انخفاض التكاليف للمواد النانو المركبه الناتجه وكذلك العينات المضاف اليها كربيد الكروم حققت صلاده ومقاومه كسر عاليه علاوه على ذلك وتم التوصل الى ان خليط المواد مانعه لنمو الحبيبات اعطى خصائص ميكانيكيه مرتف.

CHAPTER 1

INTRODUCTION

Tungsten Carbide, which is one of the hardest materials known, is the base material being used in the formation of a very important class of nanocomposites. Further it also exhibit combination of high melting point, wear-, and corrosion- resistant at high temperature.

These extremely hard carbides need to be modified and processed further, which would ensure their effective applicability in tooling industry. During drilling and cutting operations, these carbides come across interaction with different forces and jerks, being applied over it, hence it requires high toughness to absorb the variation in forces and energy. Improving toughness of these materials is accomplished by mixing a soft metal to it. These soft metals, e.g cobalt, increase its toughness although at the expense of hardness. However effective applicability in cutting industry requires having high hardness along with high toughness. So the decreases in hardness, by the addition of soft binding material, needs be controlled and compensated with higher values. This can be done by controlling microstructure of the WC-Co composites to finer grains, where refinement of grains results in higher hardness values while presence of Co keeps toughness at higher.

Refinement of grains can be controlled by sintering process and or by the addition of grain growth inhibitors to the base composition. Decreasing initial particle size also results in finer microstructures attained after sintering. Therefore reducing WC particle size from micron to nano, is also considered in this study. Finer particles will have higher active surface area, and hence the kinetics of diffusion and hence densification during sintering processes will be higher. Initial WC particle size of 3.5 μm was reduced to 10nm after milling for 72 hours in planetary ball mill under inert atmosphere. XRD, particle size analysis and FESEM analysis of the resulted powder confirmed its nano-metric size.

Another aspect, which can control the final attained microstructure is sintering process and sintering parameters. There are different consolidation process, such as conventional and non-conventional techniques which can be used to sinter these mixed powders compositions. Non-conventional sintering processes have the dominancy because it allows use of high heating rates while keeping sintering temperature and holding times at short. We also used a non-conventional sintering technique, spark plasma sintering, for consolidating our different powder compositions. The combination of parameters, such as high heating rates while keeping sintering temperature and holding times at short ends up in finer microstructures.

One of the important aspects in these microstructures is controlling their grain growth during sintering processes by the addition of grain growth inhibitors to the basic composition.

Grain growth inhibitors, used during this research work have been concentrated over using Vanadium carbide and chromium carbide in the WC-Co composites. They have been used in range of additions both individually and in combination to study their effect on the refinement of grains in the final attained consolidated product.

These sintered composites were further characterized using densification analysis through Archimedes principle, Vickers Hardness through micro-indentation, Fracture toughness by incorporating crack-lengths in a mathematical relation. Further samples were also examined by XRD. The microstructural analysis was observed through FESEM.

1.1 Objective of this work.

The aim of the present study is to investigate the possibility of restricting grain growth during sintering process, in addition to developing dense WC-Co nanocomposites. The effect of changing the initial particle size of WC from micron- to nano-scale on the overall behavior and final attained microstructure of the composites was investigated. The control of grain growth during sintering process has been targeted by the use of finer initial WC powder particle sizes, use of a non-conventional sintering process such as spark plasma sintering and finally by the use of grain growth inhibitors. The refinement of grains of the final sintered hard composites will result in improved mechanical properties such as high hardness along with improved fracture toughness of the material. Different parameters, which are used to reach the objectives, are densification kinetics,

sintering process and parameters, type and amount of soft binding material, and finally type and amount of Inhibitors. Addition of Vanadium carbide and Chromium carbide as grain growth inhibitors, to WC-Co composite, was carried out to study their effect on restricting the grain growth during sintering.

CHAPTER 2

LITERATURE REVIEW

2.1 Tungsten Carbide:

Tungsten carbide is thought to be a very versatile material due to the fact that it is one of the hardest known materials in addition to possessing unique combination of properties, such as: corrosion-, wear-, and thermal shock-resistance at high temperatures [1]. The high melting temperature (2785°C) and high hardness values (16-22 GPa) of WC allows it to dominate over other common types of hard carbides like SiC, TaC, TiC, etc. [2]. Mechanical properties of cemented carbide have shown to be dependent over the WC crystallite size and of course over their composition [1]. Other parameters such as starting WC crystallite size, shape, compositional mixing route, sintering process and parameters, used during their consolidation, are equally important, which further controls the resulting microstructure[3]. It was reported that the WC particle size has a rather weak effect on SPS densification stages with more inhomogeneity into the nanosized starting mixture and the influent of WC-Co particles size and the current(s) distribution into the sintering matrix[4].

There has been extensive attention given to fabrication of nanomaterial, as they possess higher strength, hardness, excellent ductility and toughness. Nano WC-Co have been developed by spray conversion process, however this process increases the grain size of the consolidated material and hence degrade mechanical properties, even if starting grain size of powder is smaller[5–7].

The work on WC-Co cemented carbides have been varied between focusing on their development and studying the different parameters governing their performance in the micron-scale[3][8]. WC-Co cemented carbides have been extensively used as cutting tool tip, needs to have higher wear resistance, as it experiences high temperature of 600 °C between the tool and chip during cutting processes [9]

However, some work was also devoted to nanostructured WC-Co composites towards their synthesis and sintering for higher performance applications[10].

These nano crystalline cemented carbides were found to have comparatively higher hardness, toughness compared to their conventional counterparts and therefore are more desirable for application such as drilling and cutting These nano crystalline cemented carbides were found to have comparatively higher hardness, toughness compared to their conventional counterparts and therefore are more desirable for application such as drilling and cutting[11][12].

It was reported that reducing WC powder size to the nano-scale reduces the activation energy and sintering temperature, which results in further improving the microstructure and the mechanical properties of these carbides[13][14].

Research has been devoted to nano-grained WC-Co composites towards their synthesis and sintering for higher performance application [10].

2.2 Binding material:

These hard ceramics are primarily mixed with soft and ductile metal(s) by mechanical mixing. These soft metals act as binding materials in a matrix of hard metal which enhances the mechanical properties of the resultant composite material. Increasing the amount of soft matrix increases toughness at the expense of hardness which decreases in the composite material [15–17]. one of the commonly added matrix materials is Co and WC-Co composites are extensively used in cutting tool industry which requires materials to have high toughness and high hardness values, as the tool experiences different forces and jerks during cutting operations [16]. Most of the cemented carbides, which are used in cutting tool industry, have shown remarkable required properties like hardness and toughness, as tool experiences different forces and jerks during cutting. These carbides also have abrasion resistance and heat resistance properties [16]. the concentration of cobalt is a crucial controlling parameter and many studies were devoted for characterizing the effect of binder concentration on the properties of the developed composites [18], [19].

Co is ultimately used to lower the consolidation temperature during sintering in the WC-Co system, in addition to enhancing the percentage densification of the composite[17].

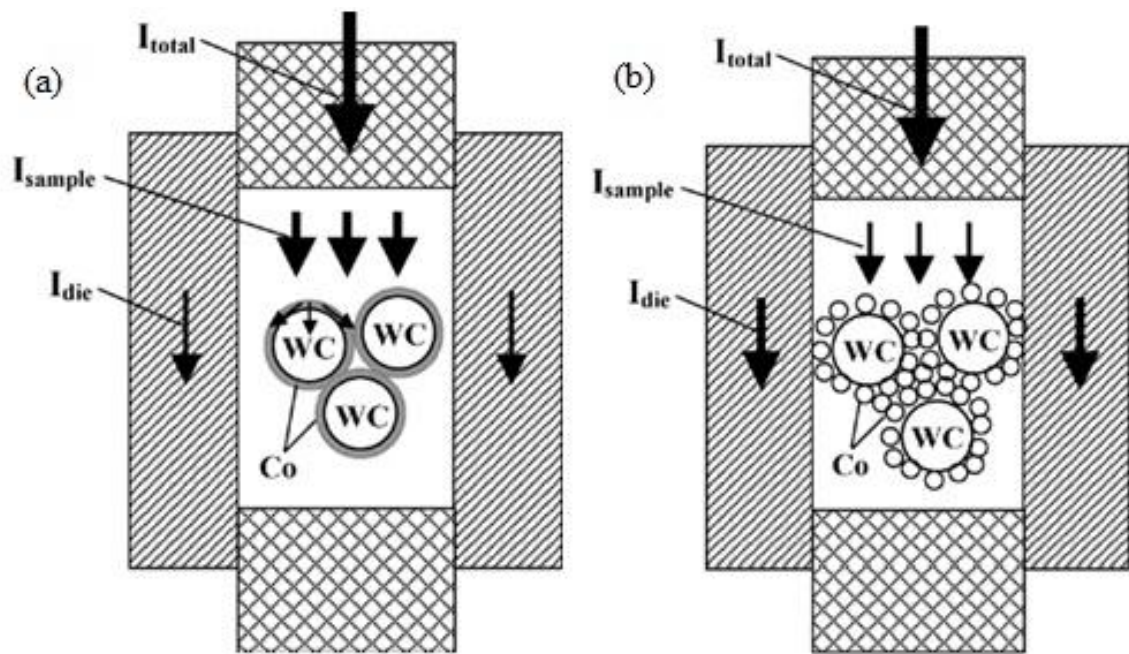


Figure 1 schematics of distribution of current, during SPS [21]

Cobalt, as a binder, in the WC-Co system is used to lower the densification temperature during sintering and it also enhances the the % densification of the composite[17].

Co plays a vital role in densification of WC-Co cemented carbides during PCAS processes. WC particles flows easily in the viscous cobalt, rearranges itself and hence enhances diffusion. Higher %Cobalt in cemented carbides will promote above mechanism and hence ends up with higher %densification, although at the expense of hardness values[20].

Figure 1 Shows effect of Co particle size, which plays an important role, such that Cobalt size shall be enough to fully coat the WC surface or otherwise may not cause thin film formation over WC. In the later case, the exposed WC, which has lower elictrical conductivity than cobalt, may loose portion of elictric current, which rather may pass through the die itself rather than the powder sample.and hence lower current intensities at localized regions which further reduces the densification.[21]

These WC are then mixed with Co, and the particle size effect of cobalt has its own significance on the final product which has already been reported by Zhao et al.[21].

It is reported that increasing sintering temperature will result in W grains to grow, hence decreasing W/W contact or simply the WC surface area. The amount of cobalt present in the mixture, which at time needed to coat higher surface area, will now have lower surface area to be coated.[22]

2.3 Mechanical Alloying:

One of the preferred techniques is mechanical mixing which is known to be simple, versatile, economically viable and scalable for production of larger quantities [23].

Mechanical alloying (MA) is a powder processing method, where powder particles are cold welded, fractured, and re-welded during ball mill operations [15] leading to a uniform dispersion of second phase particles. Figure 2 shows the Schematic diagram of ball-milling device with controlled ball movement and Ball-powder-ball collision of powder mixture during mechanical alloying respectively.

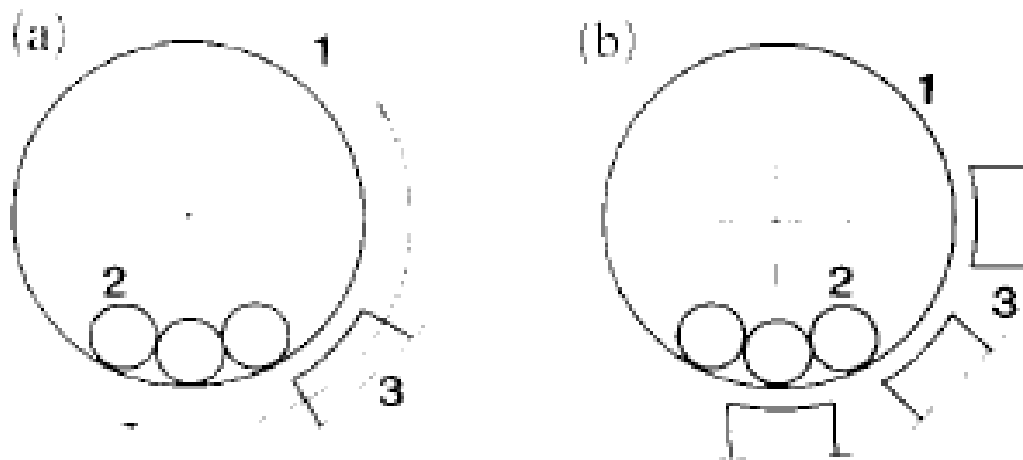


Figure 2 Schematic diagram of ball-milling device with controlled ball movement 1: rotating 2: balls 3: magnets [24].

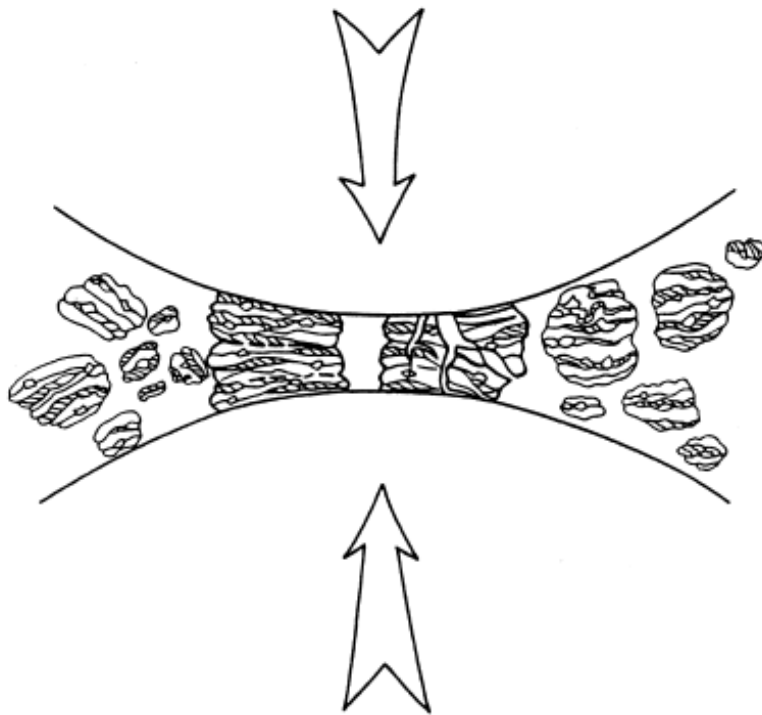


Figure 3 Ball-powder-ball collision of powder mixture during mechanical alloying [8]

2.4 Consolidation:

Sintering is a technique of consolidating powder compacts by using thermal energy, which is supplied during sintering to the green compacts or even powders. This process dates back to the historic firing of pottery during early timings and considered as one of the oldest human technologies which is now extensively used to fabricate bulk ceramic components and parts from powder metallurgy route. During this process, powder particles merge and results in increasing the grain size, where both grain growth and densification occurs. This process is called as sintering [25]. Sintering has also been extensively defined by G.S. Upadhyaya [26] which reads as follows, ‘sintering is the bonding of particles in a mass of powders by molecular or atomic attraction in the solid state, by application of heat, causing strengthening of the powder mass and possibly resulting in densification and re-crystallization by transport of materials’.

Broadly sintering is a complex phenomenon comprising of a number of variables such as particle size, particle shape, pore volume, surface tension, etc. [26]. These variables determines the degree of sinterability and reflects the resulted the sintered microstructure which further defines the resultant properties of the compact.

There are a number of sintering processes, and the degree of sinterability in each case is dependent upon different variables, which are listed in table 3.

Table 1 variables affecting sinter ability and microstructure [25]

Material variables	Powder: shape, size and distribution, agglomeration Chemistry: composition, impurity, non-stoichiometry, homogeneity
Process variables	Temperature, time, pressure, atmosphere, heating, and cooling rate.

Mixed powder compositions need to be consolidated to attain full densification, and shape before it can be used in different applications. Powders particles, after ball milling, attains higher hardness and are strong enough, due to the smaller sizes and also because of the incorporation of a high density of crystal defects during milling process. Consequently, the pressures required for compaction are expected to be higher. These small powder particles, having increased active surface area, once compacted, are expected to sinter at comparatively smaller sintering temperature. the process of sintering is expected to take place quickly due to the small size of the particles, which further results in lower grain sizes and hence increased grain boundary. Occasionally, a combination of more than one parameters is required to achieve full densification[27]. Sintering is the process, whereby powder particles merge into each other, as a result of thermal energy being provided by high temperature sintering process. Thus micro structural development and hence densification of the final product depends over these two vital parameters, which are the powder material and the sintering process, which governs the kinetics of thermal energy supplied to the particles during sintering process[28]. Environment during sintering process is another important parameter which controls the impurity/reinforcement content and composition. High gas transportation

rates, pore structure, grain structure, impurity content, kinetics and surface structures are major changes caused by the sintering atmosphere. Therefore, determination of sintering atmospheres is most effective for control of impurity. However, consolidation of powders through isotactic techniques is a feasible technique for composite materials which are intricate or costly to fabricate by other methods[29].

WC-Co cemented carbides have been extensively studied by researcher and parameters have been developed for sintering these carbides under micron-scale grain structure [1],[8]. However, the methods that are used to consolidated micro-scale WC-Co have certain limitations, when used in preparing ultrafine and nanocrystalline WC-Co.

Literature shows that substantial research efforts have been expended towards the synthesis and sintering of nanosized WC-Co powders in order to manufacture cemented tungsten carbide material by applying unique sintering techniques which may aid to produce cemented carbides with better properties. Certain gases O₂ N₂ and water that could have been adsorbed over WC particles, which further hurdles the molten flow of cobalt during sintering, giving rise to formation of micro porosity[30]

Generally sintering techniques can broadly be divided into two major categories, which are conventional sintering processes and non-conventional sintering processes.

Presence of Oxygen during sintering may give rise to de-carbonization and formation of W₂C phase which lowers the hardness values of the composite[2].

2.5 Spark plasma sintering:

Spark plasma sintering is an advanced mode of sintering which sinter a compact of powder by passing high electric pulsed current through the compact. Spark plasma sintering is a non-conventional sintering technique which allows use of high heating rates, while keeping sintering temperature and holding time at short. There are some conventional sintering processes as well, e.g Isostatic pressing, whereby powder compacts are pressed through uniform pressure from all directions to maintain uniformity and homogeneity in all directions. This isostatic pressing can either occur at lower temperature (CIP, Cold isostatic 2.5CIP and HIP are the two types of sintering collectively called the conventional sintering processes or techniques. The pressure transmitting medium is liquid and gas in CIP and HIP respectively [31]. CIP usually is carried out as preliminary pressing step before occurrence of sintering at higher temperatures. While in HIP, powder compacts commence with application of pressure while heating compact at higher temperatures during, and collectively the process is called HIP. The processing route involves a lot of variables such as powder properties e.g. size, shape, and amount and processing parameters such as pressure, temperature and time. Good information experimental and theoretical knowledge about densification process will give optimum choice of variables. The usual defect in CIPing and HIPing is the distortion of produced components [31].

Advantages of isostatic pressing methods

1. High melting point materials can be processed e.g. ceramic-ceramic.
2. Immiscible systems can also be processed.

3. The properties of the compacted components are isotropic especially for randomly mixed powders.
4. Components with complex shapes or geometries can be made near-net shape thereby, cutting down machining cost and scrap losses.
5. Grain coarsening and interfacial reaction can be avoided by careful choice of pressure-temperature-time cycle resulting in production of fine grained material with uniform microstructure[32].

Several non-conventional advanced sintering techniques such as: field-assisted sintering, microwave sintering, and spark plasma sintering (SPS) have been utilized in multiple studies[18], [19]. Spark plasma sintering (SPS) technique is preferred over usual conventional sintering processes because it exhibits higher heating rates and densification kinetics, in addition to lower sintering temperature and shorter holding timings under controllable high pressure[33].

These non- conventional sintering techniques, particularly spark plasma sintering have extensively been used to fabricate finer grained microstructure materials due to lower sintering temperature and short holding timings[8], [34].Sintering techniques such as spark plasma (SPS) and microwave sintering are examples of non conventional sintering processes. The basic difference between both the sintering processes is the mechanism of heating in each case. In conventional sintering, heat is generated and transferred to the material through conduction, convection and or radiation while in non-conventional sintering, either the material themselves absorb microwave energy and then transform them into heat within their bodies (MWS) or employs an electrical discharge combined with resistance heating and pressure for sintering (SPS).

Spark plasma sintering (SPS) technique, which is a non-conventional sintering technique has the dominancy over usual conventional sintering processes because it exhibits higher heating rates and densification kinetics, as well lower sintering temperature and shorter holding timings under controllable high pressure than as comparative to the usual conventional sintering processes. SPS technique has enhanced the sinter ability of a lot of metals and also leads to the development of new advanced materials and improving their properties[35].

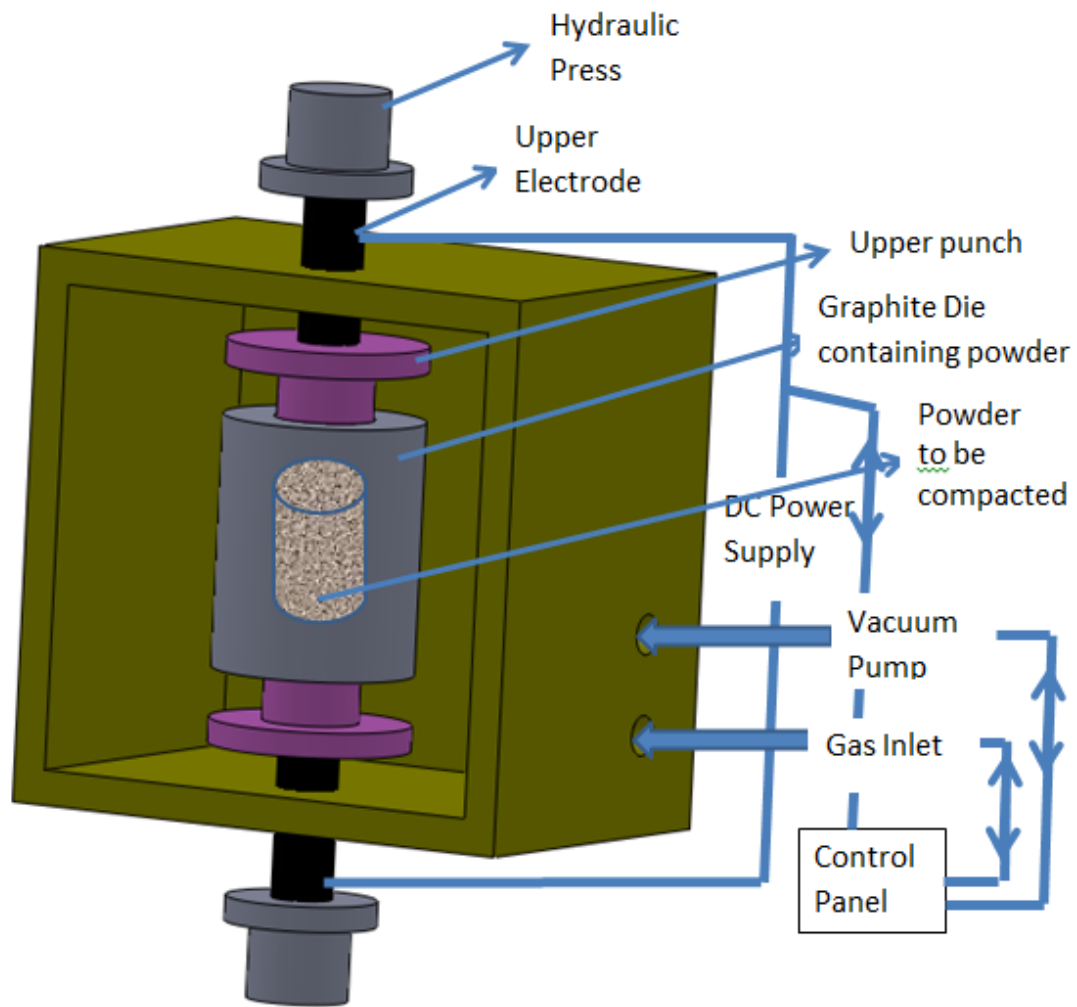


Figure 4 Schematic illustration of Spark Plasma Sintering (SPS).

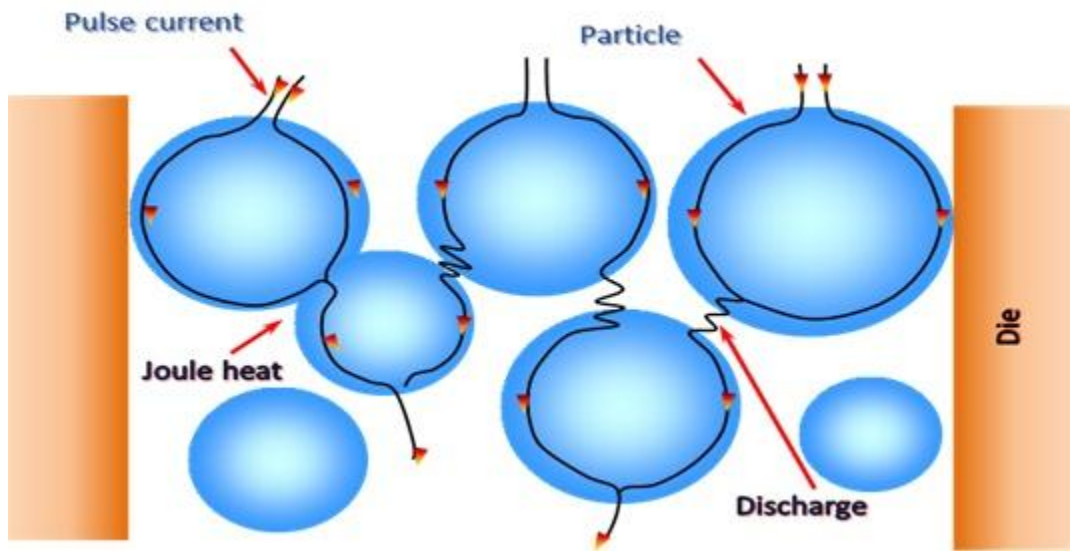


Figure 5 Illustrates how pulse current flows through powder particles inside the SPS sintering die [36]

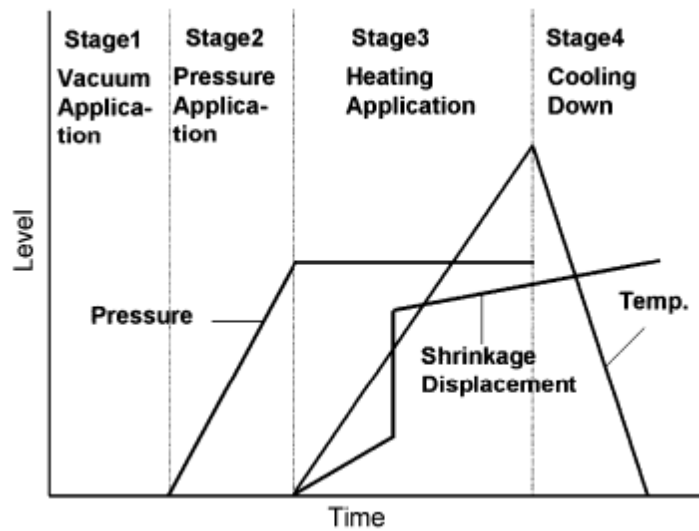


Figure 6 Temperature, Pressure and shrinkage profile during pulsed current activated sintering process [20]

This technique has been used to consolidate both ultrafine and nanocrystalline WC–Co alloy [37][38]. Figure 6 Shows variation of pressure during span of time and also shows clearly the increase in densification with increase in temperature and abruptly increases to higher values after reaching ceratin temperature. The shrinkage rate reaches negligible values,when densification reaches to maximum at sintering temperature.

Presence of Oxygen during the sintering may react with carbon, leaving behind metallic tungsten, which can react with WC present and generates W_2C during the process. The presence of this new phase in a sintered product may degrade the mechanical properties. Possibility of this unwanted phase is further enhanced by using smaller particle sizes due to increase in acive surface area of the powder particles. [2].

There have been some studies focusing on the effect of particle-size combination of the raw WC and Co powders on the SPS sintering process. This was accompanied by microstructure characteristics, and mechanical properties of the consolidated materials. Additionally, the influence of using SPS on different WC particle size and distribution and the densification behavior of the mixed WC–Co powder were analyzed quantitatively.

2.6 Inhibitors:

In addition, metal carbides, nitrides, oxides, and borides such as VC, Nb₃C₂, Mo₂C, TaC, TiC, Cr₃C₂, TiN and Y₂O₃, LaB₆, control the grain growth during sintering by modifying the WC–Co interface or by providing resistance to diffusion and growth by any mean say oswald and dynamic riping [15], [19].

Different grain growth inhibitors were used in WC-10Ni to restrict the grain growth, and it was found that hardness increases with increasing the % of these inhibitors into the composite system, until a certain maximum addition, after which there is almost no significant increase in hardness [39].

Faster grain growth kinetics under spark plasma sintering increases the W grain sizes. Further retaining nano-scaled grain sizes from nano crystalline powder, comparatively to, micron-scaled powder, is a challenge[40][41]

Grain growth occurs during sintering of WC composite, due to the dissolution of the smaller particles having smaller number of atoms attached to it, than as comparative to that of a large particles and hence which are more stable, to reduce overall energy of the system.[40] The detached free atoms in the system are then attracted towards the large stable particles, which hence increases the grain size. Addition of grain growth inhibitor reduces the surface energy of the WC particles, and hence changes the driving force which is needed for the smaller particle to be dissolved. This reduces the possibility of the smaller particles to be dissolved which are then to be re-attached to the large particles, hence restricts the particle or grain growth to occur [15].

Grain growth inhibitors such as VC, Cr₃C₂, NbC or TaC are the most frequently manipulated parameters influencing WC grain growth in WC–Co based cemented carbides[42][19]

Vanadium carbide (VC) and chromium carbide (Cr₃C₂) are the most effective grain growth inhibitors due to their high solubility and mobility in the cobalt phase at lower temperatures[43][44]

Both Cr₃C₂ and VC are proven to be restricting the grain growth of WC and enhancing the hardness and the fracture toughness of the composite under a certain range. The excessive addition cannot inhibit the grain growth [15].

Grain growth is inhibited by reducing the solubility of WC atom in the Co binder. Addition of equally distributed VC into Co reduced the solubility of WC atoms in Co binder from 40 to 10% [45].

Different grain growth inhibitors (VC, Cr₃C₂, NbC or TaC) have been studied by researchers, and it was found that Vanadium carbide (VC) and chromium carbide (Cr₃C₂) are the most effective grain growth inhibitors due to their high solubility and equally distribution ability in the cobalt phase at lower temperatures [44]. Different grain growth inhibitors have been used by early researchers, and it was found that VC and Cr₃C₂ are the most effective in restricting grains to grow. Because they have the most solubility and easy mobility in cobalt under sintering temperatures.[46].

Researchers have pointed thin layer formation over WC particles, which limits the diffusion process, as source of grain growth inhibition. These inhibitors are found to lower the densification of final product by limiting diffusion and migration of Co[3] .

Grain growth inhibitors like VC/Cr₂C₃ forms an interface between WC and Co particles, which rather prevents the transfer of phases across and hence reduces the possibility of grain growth [47]. Addition of VC and Cr₃C₂ causes porosity in the cobalt layer around the WC particles, hence reduces densification of the material. These pores helps to arrest the crack propagation, hence increases the fracture toughness of the final product. This effect is higher in SPSed than as comparative to CSed process. Longer timings in CSed process may increase densification but longer timings in not feasible in SPSed process, as it will loosen the effectiveness of process itself, by increasing grain sizes, thereby will reduces the hardness. [40]

Different grain growth inhibitors have been used by early researchers, and it was found that VC and Cr₃C₂ are the most effective in restricting grains to grow. Because they have the most solubility and easy mobility in liquid cobalt at lower sintering temperatures. These inhibitors forms an interface between WC and Co particles, which rather prevents the transfer of phases across and hence reduces the possibility of grain growth [47]. However their excessive addition cannot inhibit the grain growth[15]. The mechanism for grain growth inhibition has been related to the slowing down of the solution/re-precipitation reactions at the WC–Co interfaces.[48]

The finer the grain is, the greater the total area of the grain boundaries is. As a result, the energy from the plastic zone of a certain size to the expand zone of the crack increases at

the top of the crack. Therefore, the fracture toughness is also higher. However, the added particles of VC/Cr₃C₂ are distributed along the WC grain boundaries. As a result, the cracks will be easily formed at the grain boundary, and the main crack propagation along the grain boundaries is relatively easy. Therefore, when the addition is excessive, the fracture toughness may decrease.[15]. These inhibitors are found to lower the densification of final product by limiting diffusion and migration of Co[3]. .The incomplete densification in the solid state by inhibitors effect is associated with the limitation of the atomic diffusion phenomena and migration of Co[49]. It is reported that abnormal grain growth may occur during sintering process, due to creation of local “cobalt pool”. The effect further was explained as when co viscous flow is thick enough at lower sintering temperatures that it retards to fill the capillary skeleton of nano WC particle or thin enough due to extended plastic deformation will retards the formation of bond between WC and Co.[15]

CHAPTER 3

MATERIALS AND EXPERIMENTAL PROCEDURE

3.1 Raw Materials.

The starting powder materials used for the study were tungsten carbide (hard base material), Cobalt(soft binder), Vanadium carbide and chromium carbide(grain growth inhibitors).Table 2 showing characteristics of the starting powders. Safety measurements such as using hand gloves, face masks, glasses, lab coats etc. were used during and after the experiments at all stages, which ensures implementations of safety laboratory procedures.

Table 2 showing characteristics of the starting powders.

S/No	Powder	Symbol	Size (μm)	Company
1	Tungsten Carbide	WC	3.5	William-Rowland Co., UK
2	Tungsten Carbide	WC	0.05	Fuer, China
3	Cobalt	Co	1.3	William-Rowland Co., UK
4	Vanadium Carbide	VC	0.05	William-Rowland Co., UK
5	Chromium Carbide	Cr_3C_2	0.05	William-Rowland Co., UK

3.2 Powder Milling

One of the important aspect of this research work was to prepare nano WC powders from micron sized WC powder, which were then used in preparation of nanocomposites. As received WC powders were milled using a planetary ball mill (Fritsch Planetary Mill, Pulverisette-5, Germany) under argon atmosphere up to 72 hours at constant speed of 300 rpm and ball to powder ratio of 10:1 was maintained. Milling experiments were halted every 6 h to avoid temperature build up and to scrap powders from the walls of the vials.

Small amount of powder was taken from each vial during milling at different intervals for characterization. Particle size distribution of these samples was carried out using

Microtrac machine (model S3500/Turbotrac). It was found that Particle size of WC was reduced to 10nm after 72hrs milling of the as received 3.5micron WC particle size. Powder samples were further analyzed by a D8 Advance X-ray diffractometer (Bruker AXS, Germany) with copper radiation ($\lambda = 0.15418$ nm) at 40 kV and 40 mA. Powder samples were further analyzed by a Bruker-D8 XRD with Cu radiation ($\lambda = 0.15418$ nm) at operating conditions of 40 kV and 40 mA. Scanning electron microscope (SEM, JEOL, JSM 6460LV, Japan) in a secondary electron mode at an accelerating voltage of 30 kV was used for morphological testing, in addition to compositional analyses using EDX (Oxford Inc., UK). Moreover, indirect measurements of crystallite sizes were performed using Scherer relation and Williamsons-Hall plots from the broadening of XRD peaks.

Powder samples taken from each vial during milling at different interval was further analyzed through SEM scanning electron microscope (SEM, JEOL, JSM 6460LV, Japan)and (FESEM) Field Emission Scanning electron microscopy. The analysis was done to see the change in morphology of powders and micro structural examinations, as a result of milling operation with milling time, under a in a secondary electron mode at an accelerating voltage of 30 kV. gold coating over these powders was also carried out to enhance conductivity and resolution of micro structural images. An Energy dispersive X-ray (EDX) spectroscope (Oxford Inc., UK) was used to verify the compositions and purity of these samples.

At the end of 72 h milling the particle size of WC has reached an average of 10 nm. Later, 9 wt.% Co was added to form two composite systems based on: a) as-received 3.5 μ m WC and b) 72 h-milled WC (10 nm), to investigate the effect of changing the

crystallite size of WC. These compositions were mixed for 6 h in the planetary mill/mixer using ethyl-alcohol as a milling medium, and keeping balls to powder ratio (BPR) of 6:1. Further homogeneity of these mixed powders and effective dispersion of WC within the Co matrix was achieved by using high energy probe sonication.

Scherer relation and Williamsons-Hall plot were used to determine crystallite size from the broadening of XRD peaks.

$$L = \frac{K \lambda}{\text{intercept}} = \text{Crystallite Size}$$

$$\lambda = \text{Cu Wave Length} = 0.154\text{nm}, K = 1.0 \text{ constant}$$

3.3 Sintering Procedures:

Spark Plasma Sintering (SPS): Powder prepared from the above milling/mixing process has to be consolidated in order to reach the final densified sintered products. Spark plasma sintering process is used as a source of consolidation technique during this study. It allows the use of high heating rates while keeping sintering temperatures and holding times at low. Powder mixtures in each case were poured into cylindrical graphite dies of 20X50X50mm(inner-dia x outer-dia x height) and sintered in spark plasma sintering (Type HP D-50, FCT Systeme, Rauenstein, Germany) under vacuum while keeping constant pulsed electric current and pulse duration. Table below shows the parameters,

which are used during SPS. An air compressor was also used during the experiment. Sintering cycle, which was followed during the Spark plasma sintering is shown in Figure 7.

Table 3 Summary of parameters for Spark Plasma Sintering (SPS)

WC-Sizes	10nm, and 3.5 μm
Compositions Used	WC-XCo-YA (X=9,12; Y=0, 0.2, 0.4, 0.6, 0.8, and A=VC and or Cr_3C_2)
Sample dimension (mm)	20X5(diameter X height)
Pressure (MPa)	50
Holding time (mins)	10
Temperature ($^{\circ}\text{C}$)	1200 $^{\circ}\text{C}$, 1300 $^{\circ}\text{C}$
Heating Rate ($^{\circ}\text{C}/\text{min}$)	100
Atmosphere	Inert Argon

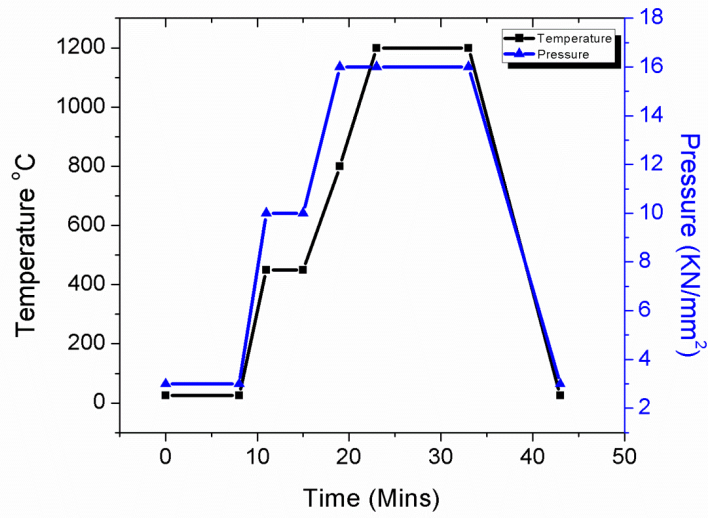


Figure 7 Time-temperature and Time-Pressure variation during SPS



Figure 8 Spark Plasma Machine, being used for consolidation.

3.4 Characterization

3.4.1 Sample Preparation:

All sintered samples were mounted using a Buehler transoptic powder (polymer) pressed in a hot press (Evolution, IPA 40 Remet, Bologna, Italy) at a temperature of 200°C taking 30-35mins for the whole process including heating and cooling. Further, the mounted samples were ground and polished using 12 inch (305mm) diameter Buehler Magno-discs, USA employing 74, 40 and 20um grinding papers with the aid of an Automet 300 Buehler grinding machine. Buehler diamond suspension of 9, 6 and 3 microns water base were used for smooth polishing of the samples and checked under light optical microscope. After the preparation; density, hardness, fracture toughness and microstructure examinations were investigated. Murakami's reagent (10 g NaOH, 10 g potassium ferricyanide and 100 ml distilled water) at room temperature for 3–4 min was used as etchant for microstructural examination.

3.4.2 Density Measurements.

The density of sintered samples was measured on densimeter based on the Archimedes principle using MD-300S, Alfa Mirage, SG resolution-0.001g/cm³, capacity-300g **Error! eference source not found..** The samples are as sintered without mounting but careful grinding to remove all the graphite on the samples as graphite sheets were used during sintering.

This is Archimedes' principle and in words it states that any object totally or partially immersed in a fluid is buoyed up by a force equal to the weight of the fluid displaced by the object. i.e $W_{fluid} = F_B = F_u - F_D = W_{air} - W_{water}$; where W_{fluid} is the weight of fluid being displaced by immersion of object in the same fluid. F_B is the Buoyance force, while

F_u is the upward force and F_D is the downward force on the object, W_{air} is the weight of object in air and W_{water} is the weight of object in fluid.

Now volume of Object = V_{object} = Volume of fluid being displaced = V_{fluid}

But $V_{object} = V_{fluid} = (W_{air} - W_{water}) / \rho_{fluid}$

Now density of object = $\rho_{object} = W_{object} / V_{object} = W_{air} / V_{object} = \frac{W_{air} * \rho_{fluid}}{W_{air} - W_{water}}$

3.4.3 Hardness Measurements:

The Vickers hardness (HV30) was measured on the universal hardness testing machine (Zwick-Roell, ZHU250, Germany) with an indentation Figure 9. Twelve readings were taken and the average used as the hardness of the sample. Vickers hardness indentation experiment with a load of 300 N (HV50) in a line across three different zones was carried out on M4U 025 hardness tester. After Vickers hardness testing, the specimen was etched with Murakami's reagent (10 g NaOH, 10 g potassium ferricyanide and 100 ml distilled water) at room temperature for 3–4 min. Impression image observation and length measurement of the diagonal further gives us Hardness values. The mathematical relationship between indent area and hardness is

$$\mathbf{Vickers\ Hardness} = \frac{\mathbf{c * Kgf}}{\mathbf{(2a)^2}}$$

Where, c is a constant (0.1854) for Vickers hardness, Kgf is the load (in Newton) applied during indentation and 2a is the diagonal length, in mm of the indent being made in the material.

$$\mathbf{Hv30} = \frac{\mathbf{0.1854 * Kgf}}{\mathbf{(2a)^2}}$$

Hv₃₀ is the notation for Vickers harness at a load of 30kg or 300N.

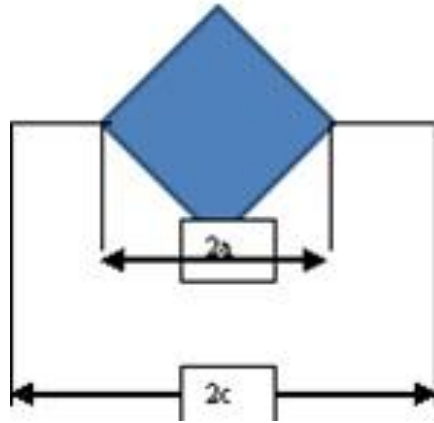


Figure 9 Shows Universal Hardness Testing Machine (Zwick-Roell, ZHU250, Germany).

3.4.4 Fracture toughness

Fracture toughness were evaluated using crack length and indent length under optical microscope employing the mathematical relationship between fracture toughness and crack length. These indents were further viewed under optical microscope.

Fracture toughness of these hard brittle carbides cannot be measured by conventional impact testing, which is usually followed for traditionally prepared specimens like chevron notch, compact tension and round notch specimens. Further preparation of tests samples for the listed conventional impact testing is difficult, time consumable and costly. Researchers have resulted in a different method of calculating fracture toughness of these hard brittle carbides, which is easy and simple to apply, which consists of measuring the crack lengths that form at the corners of a Vickers indentation on the polished surface of these hard carbides. In some cases, using values of material properties like elastic modulus and Poisson's ratio is also required. Due to the fact that hard materials were tested, high loads are needed for crack formation. The high load levels have the potential to cause deviations in the calculated crack lengths. Discrepancies could also be attributed to substantial deformation, residual stresses and damage around the generated cracks. In the present work, Anstis et al. models which is

$K_c = 0.016 \sqrt{\frac{E}{H_v}} \frac{P}{C^{3/2}}$ is used to find the crack intensity factor. Further Palmqvist

fracture toughness can be inferred from the total length of cracks produced at opposite corners of a Vickers indent and from the hardness of the specimen. For conversion of the sum of crack lengths values into Palmqvist fracture toughness values, formula (a) is used

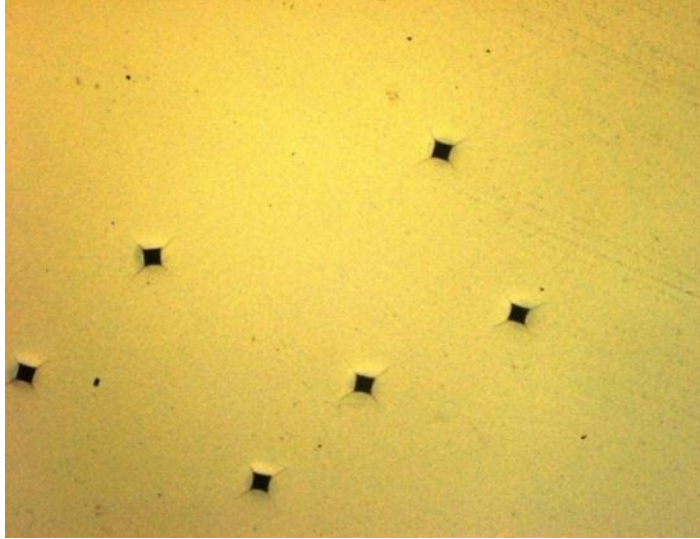


Figure 10 Optical micrographs of indentation on a sintered WC-Co nanocomposite

$K_{1c} = A \cdot \sqrt{HV} \sqrt{\frac{P}{\sum l}}$ where K_{1c} is the fracture toughness $\text{MNm}^{-3/2}$; HV is the hardness in MPa; P is the indentation load in N; $\sum l$ is the sum of crack lengths in mm and A is the constant factor 0.0028. Hardness was measured by Vickers indentation with 30 kg load.

3.4.5 X-Rays Diffraction:

X-Rays diffraction Analysis was used to determine the crystallite sizes of attained consolidated composite material. The peak broadening effect using the FWHM concept in scherrer equation was find helpful in finding the crystallite size. However many factors may contribute to the observed peak profile, which includes

1. Instrumental Peak Profile
2. Crystallite Size
3. Microstrain
 - a. Non-uniform Lattice Distortions
 - b. Faulting

- c. Dislocations
 - d. Antiphase Domain Boundaries
 - e. Grain Surface Relaxation
4. Solid Solution Inhomogeneity
 5. Temperature Factors

All of the above factors can contribute to define the peak profile. Peak Width due to crystallite size varies inversely with crystallite size, i.e as the crystallite size gets smaller, the peak gets broader and according to scherrer equation $B(2\theta) = K\lambda / L \cos(\theta)$, where the constant of proportionality, K (the Scherrer constant) depends on the how the width is determined, the shape of the crystal, and the size distribution. It is usually taken as 1. FWHM is the width of the diffraction peak, in radians, at a height half-way between background and the peak maximum, while integral breadth is the total area under the peak divided by the peak height. Warren suggests that the Stokes and Wilson method of using integral breadths gives an evaluation that is independent of the distribution in size and shape. $B_p = B_T + B_D$, where B_p is the pure breadth, B_T is the breadth due to size while B_D is the breadth due to micro strains. And therefore

$$B = \frac{\lambda}{L \cos \theta} + k \tan \theta \quad \text{or} \quad B \cos \theta = \frac{\lambda}{L} + k \sin \theta$$

Now comparing with general $y=mx+c$ and plotting $B \cos \theta$ against $\sin \theta$, we get a straight line, ending up with intercept equal to strain.

It is important to notify that crystallite size is different from particle size, which can be made of several different crystallites. However crystallite size often matches grain sizes, although there are exceptions.

Crystallite Size from XRD spectrum using PAN analytical expert software and Scherer equation and Williamsons-Hall plot was determined. Typical Williamsons-Hall plot used for the determination of crystallite size is shown below while determining the crystallite size from the relation described in the experimental part of this work.

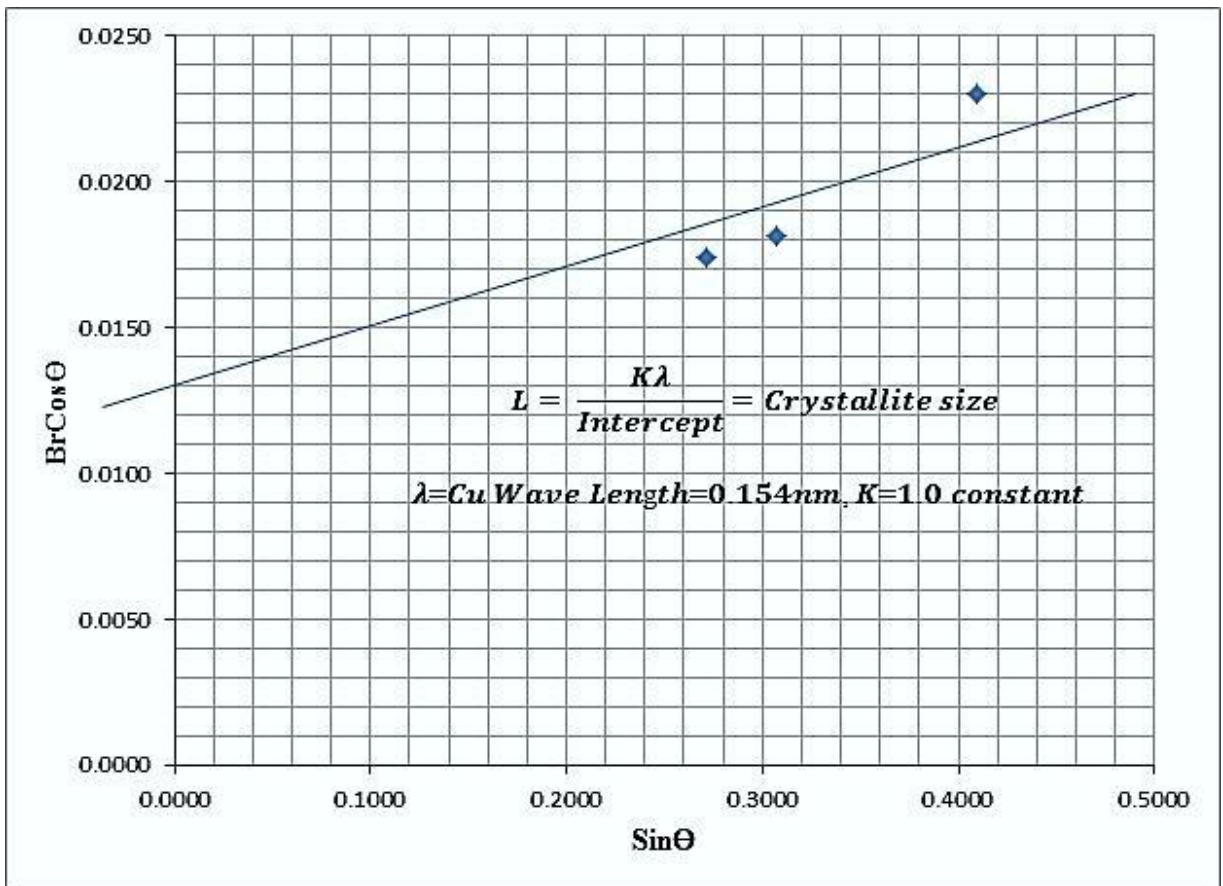


Figure 11 Williamson-Hall plot used for calculating crystallite size of 72hr milled WC powder.

3.4.6 Microstructural analyses (SEM and XRD)

A field-emission cathode in the electron gun of a scanning electron microscope further provides narrower probing beams at low as well as high electron energy, resulting in both improved spatial resolution and minimized sample charging and damage. We also used FESEM Tescan Lyra-3 (Czech Republic); scanning electron microscopes and Optical microscope (MEIJI-Techno microscope, Japan) for investigation the morphology of different powders composition used and further the microstructure of these hard carbides at higher magnifications and higher resolution.

X-ray diffractograms were also taken from the XRD measurements of the sintered samples to see if other phases are present as well as to check for grain growth after calculating the crystallite sizes from the XRD data.

CHAPTER 4

RESULTS & DISCUSSION

4.1 Characterization of starting powders

The FESEM images of the starting powders of Co and WC are shown in Figure 12 which shows the powder morphology and the presence of some size distribution as there has been some variation, especially in the WC powders. These micrographs further shows round nature of WC particles.. Figure 13 shows the morphology of as received growth inhibitors vanadium carbide (VC) and chromium carbide (Cr_3C_2). EDS analyses were performed on the as-received powders and revealed the adequacy of these powders. EDS analysis of Cr_3C_2 is shown in Appendix-1, while that of VC is shown in Appendix-2.

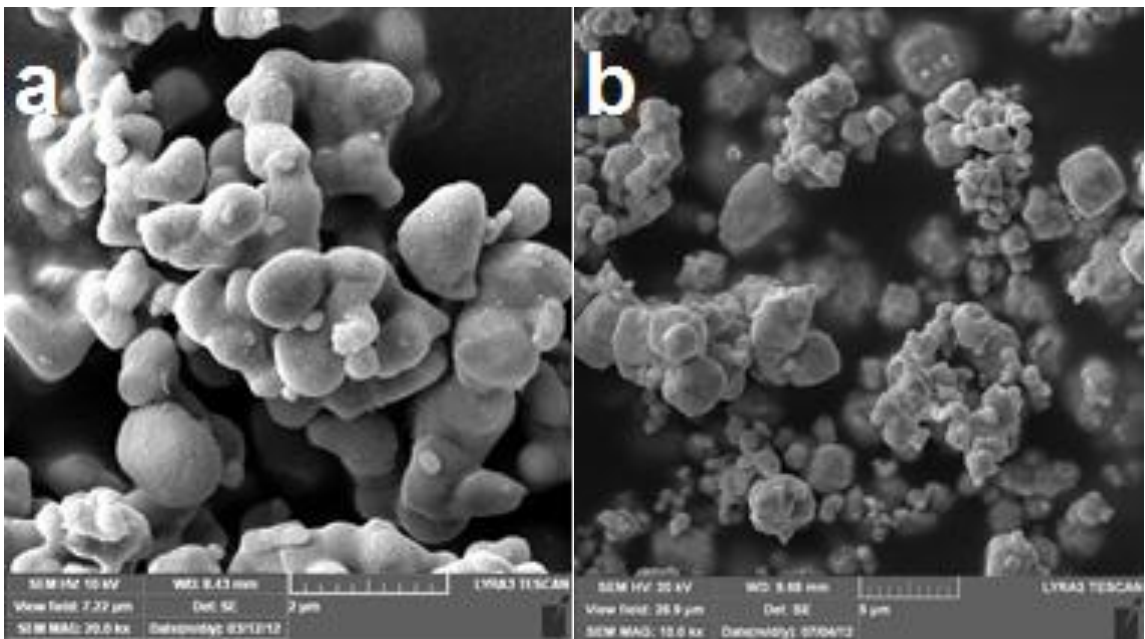


Figure 12 FESEM of starting powder, Cobalt 1.31 μ m (a), WC 3.5 μ m as received (b)

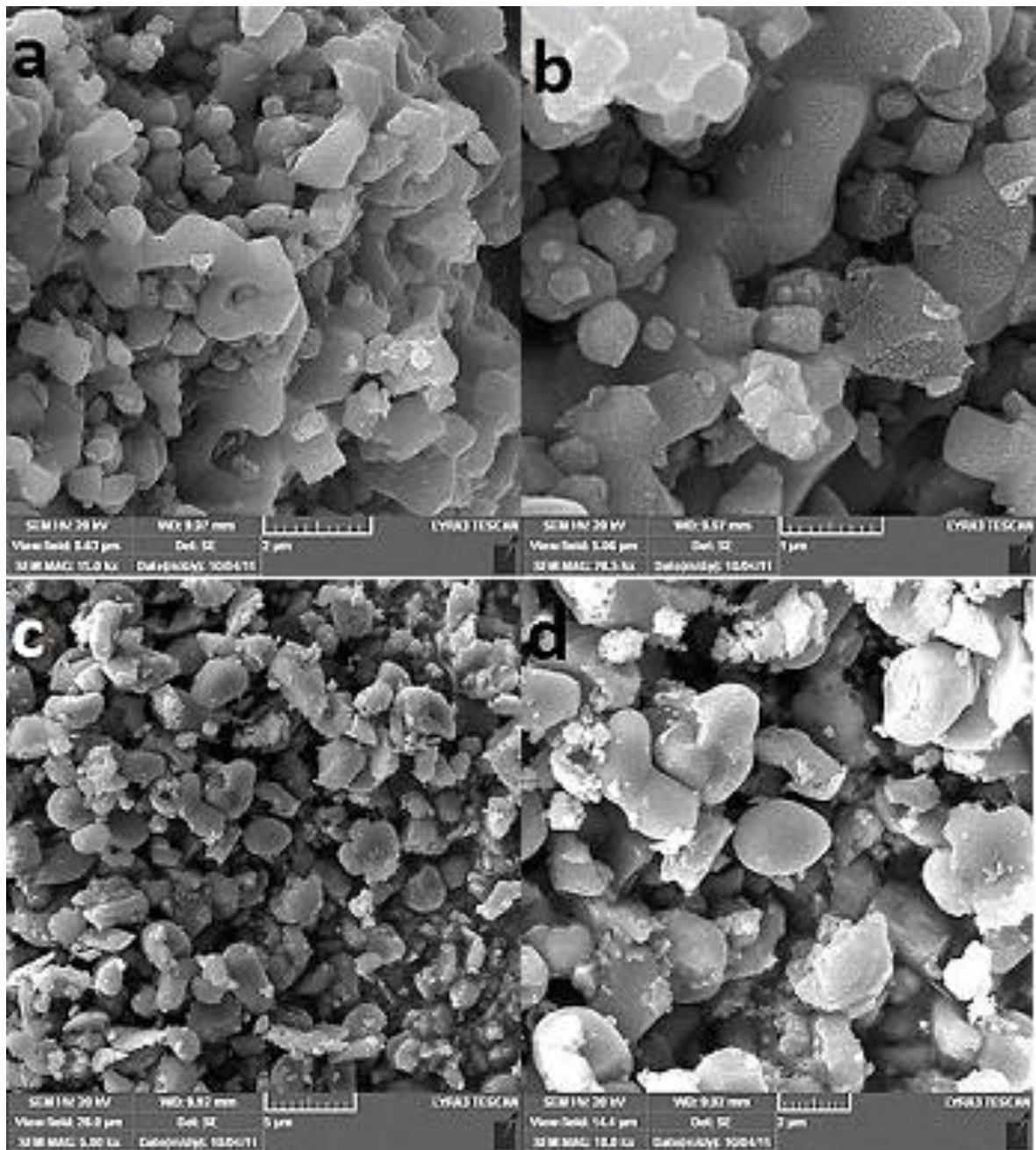
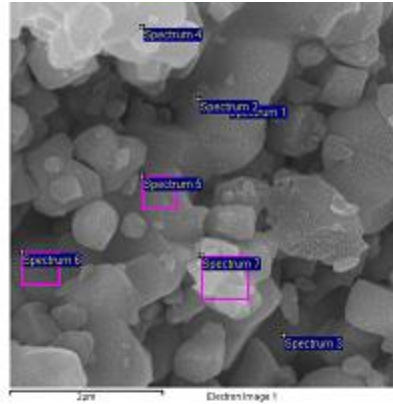


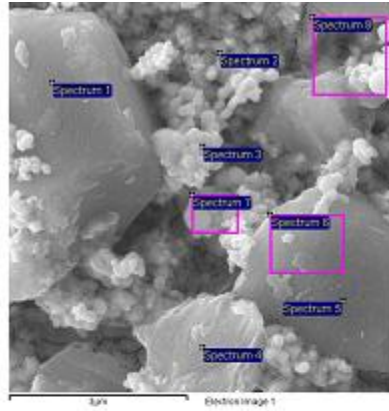
Figure 13 FESEM micrographs showing as received (a, b) VC and (c, d) Cr₃C₂, which are used as inhibitors

Table 4 EDX Analysis of vanadium Carbide, as received



Spectrum	In stats.	C	V	Au	Total
Spectrum 1	Yes	24.08	65.32	10.65	100.00
Spectrum 2	Yes	21.07	78.93		100.00
Spectrum 3	Yes	26.26	73.74		100.00
Spectrum 4	Yes	32.87	67.13		100.00
Spectrum 5	Yes	32.36	67.64		100.00
Spectrum 6	Yes	22.56	77.44		100.00
Spectrum 7	Yes	36.38	63.62		100.00
Max.		36.38	78.93	10.65	
Min.		21.07	63.62	10.65	

Table 5 EDX Analysis of Chromium Carbide, as received



Spectrum	In stats.	C	O	W	Total
Spectrum 1	Yes	22.57	74.34	3.09	100.00
Spectrum 2	Yes	21.65	3.23	75.13	100.00
Spectrum 3	Yes	28.94	6.25	64.81	100.00
Spectrum 4	Yes	11.81	75.57	12.62	100.00
Spectrum 5	Yes	25.38	71.16	3.46	0
Spectrum 6	Yes	26.44	62.93	10.62	100.00
Spectrum 8	Yes	18.80	36.10	45.10	100.00
Max.		28.94	75.57	75.13	
Min.		11.81	3.23	3.09	

4.2 Preparation of WC (nano) powder

WC (nano) powder was prepared from as received WC (micron) through planetary ball milling for long hours of 72hrs under inert atmosphere. Effect of ball milling at different stages of milling pure WC was observed through XRD, Figure 14. Focusing on the major peaks of WC, it can be seen that as milling time increases the peaks became broader and the intensity is significantly reduced. Other factors attributing to the peak broadening are accumulated internal lattice strain and machine effects. This is true for the 10nm XRD peaks where more plastic deformation and accumulated strains are present due to the increased fracturing and rewelding of the powders during the milling process. The X-ray diffractions matched with PDF reference code 25-1047 that the main phase is pure WC.

Particle size distribution was carried at each different milling time as shown Figure 16. It further shows that range for distribution of particle size reduces, while frequency increases with increasing milling time. Crystallite size was also calculated at each different time of milling, and it was found that crystallite size is continuously reducing as milling time increase. However, the major reduction has occurred during the first stage of milling at (18 hrs.) and the following reductions were smaller.. However milling was continued for longer hours, as range of distribution narrowed down and frequency of attained particle size was increasing. We reached to 10nm particle size at milling of 72hrs. Hard agglomerates crushed into smaller during early milling; however their size was found to increase with further milling. This increase in size could probably be due to surface charges on powder surfaces, which increases as milling proceeds. Results were

further confirmed by analyzing powder morphology through FESEM, at different stages of milling, as shown in Figure 17.

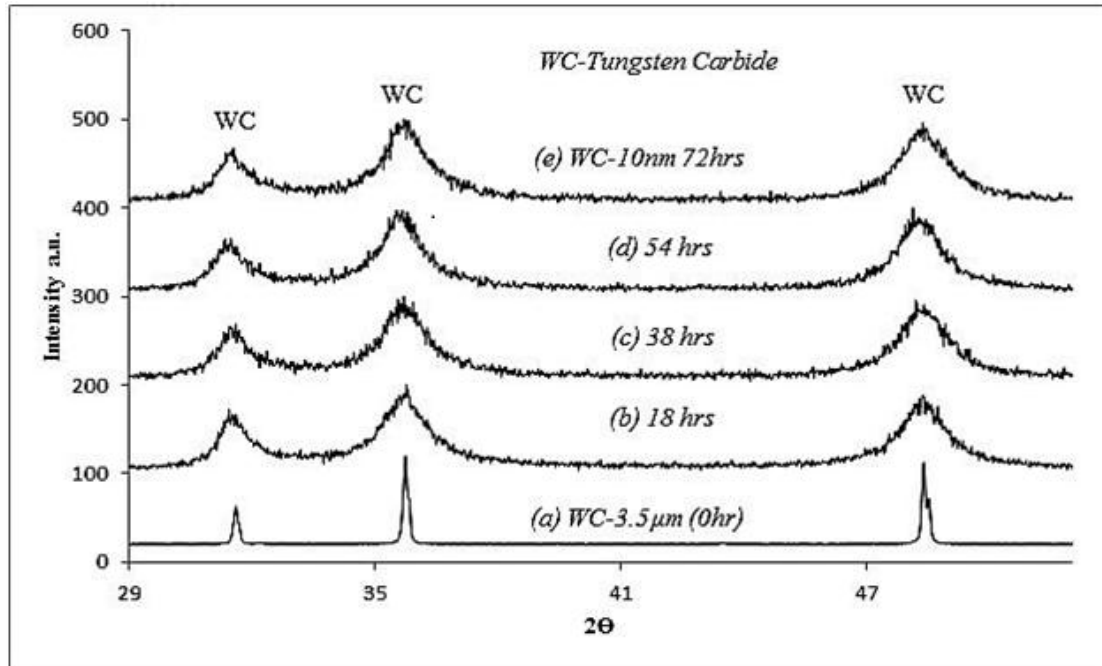


Figure 14 . XRD peak broadening effect during different stages of milling of as-received 3.5μm WC

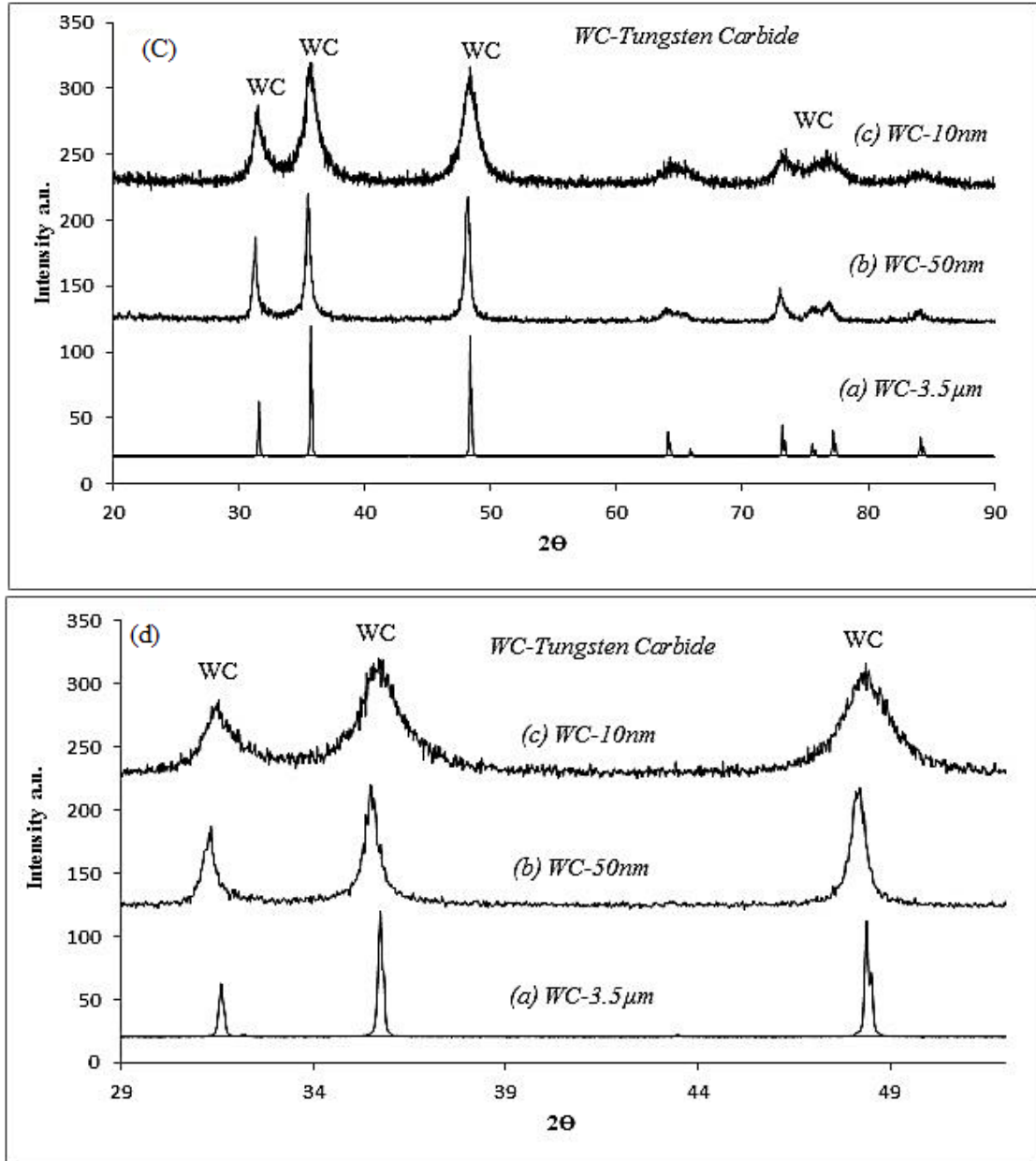
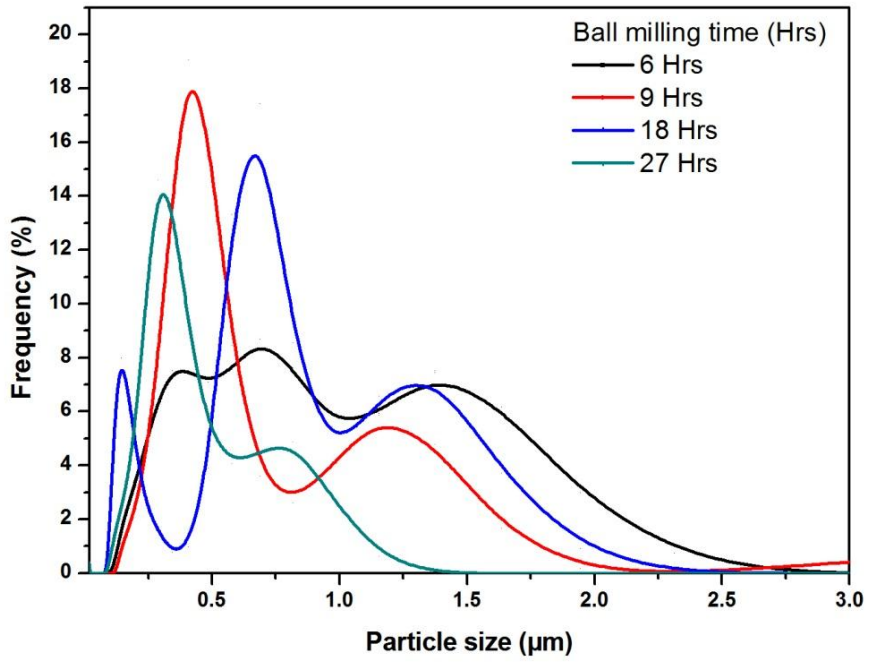
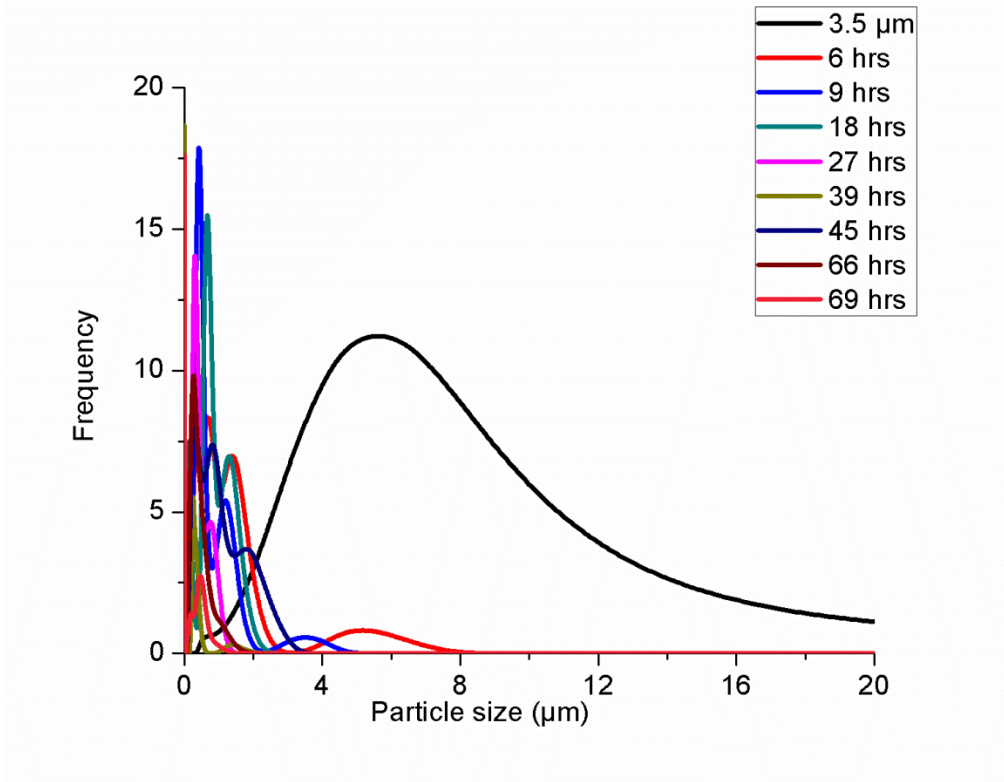


Figure 15 Showing XRD of different particle size used during the study



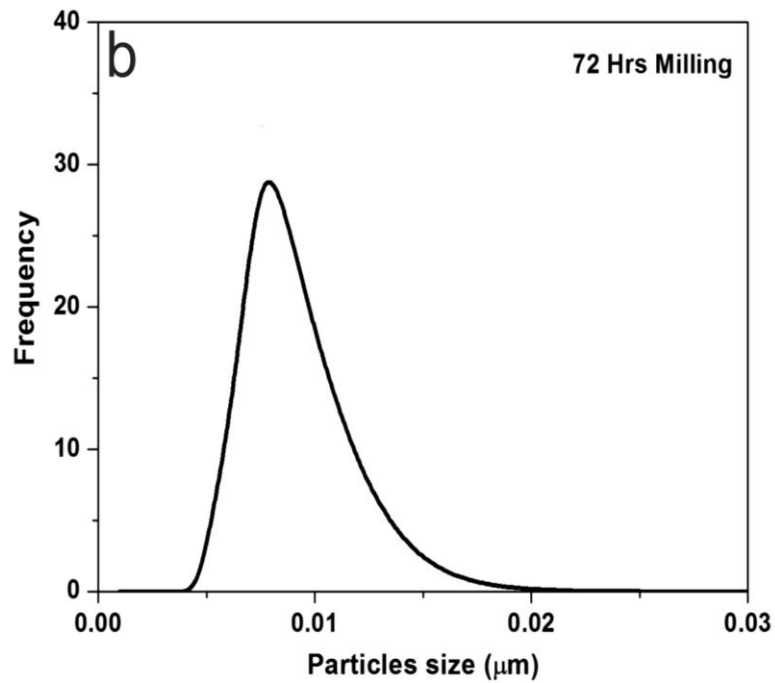
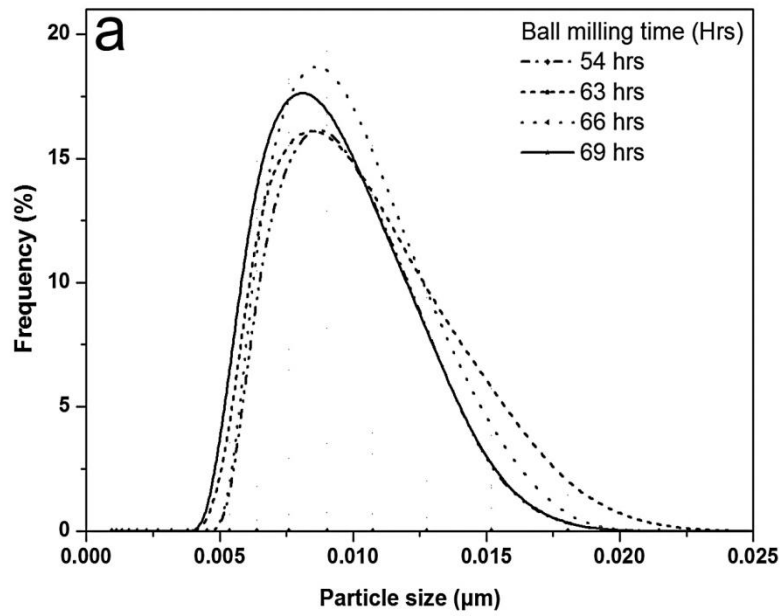
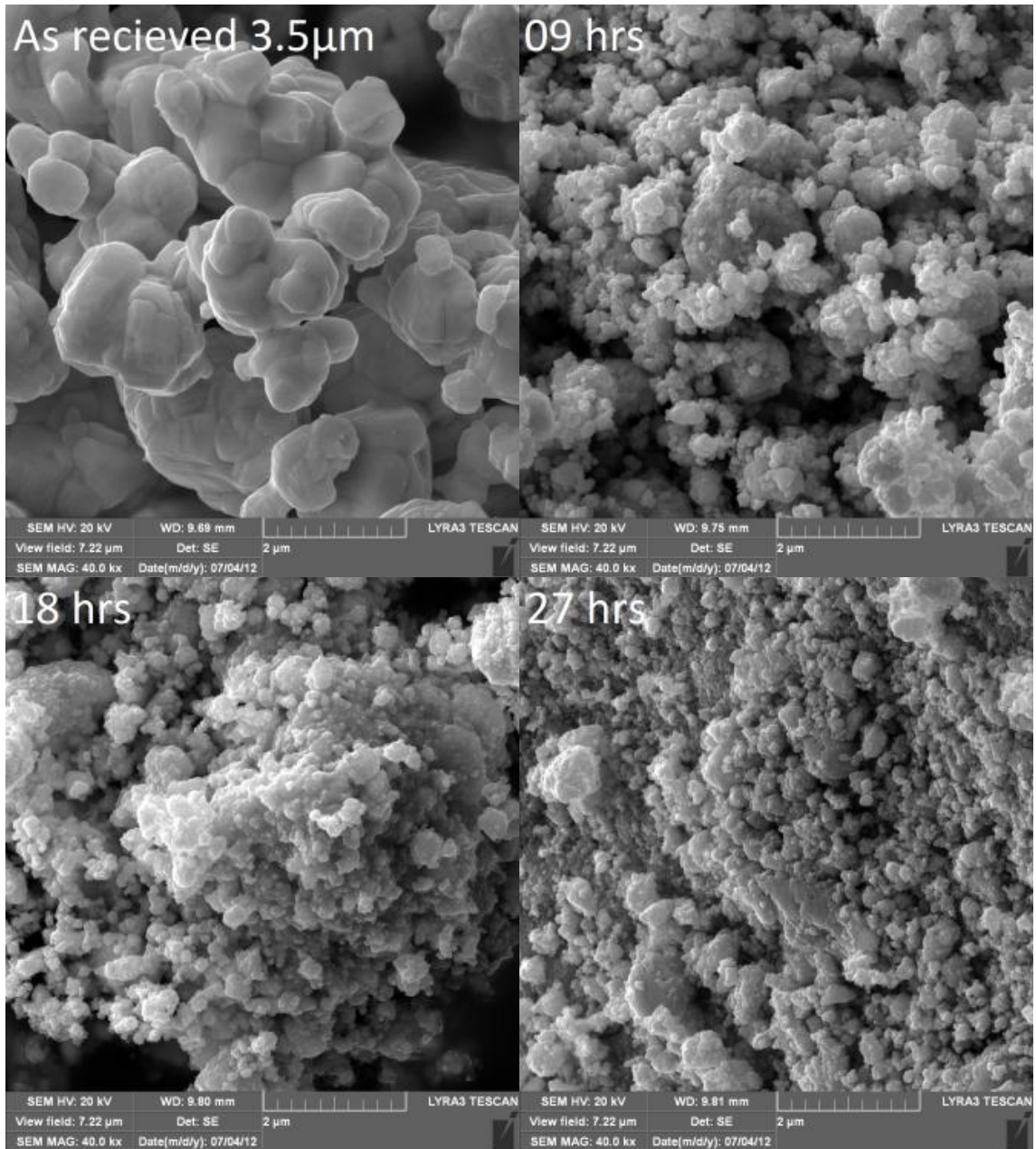


Figure 16 WC particle size distribution (a) at different stages of ball milling operations (b) final attained powder after milling of 72hrs.



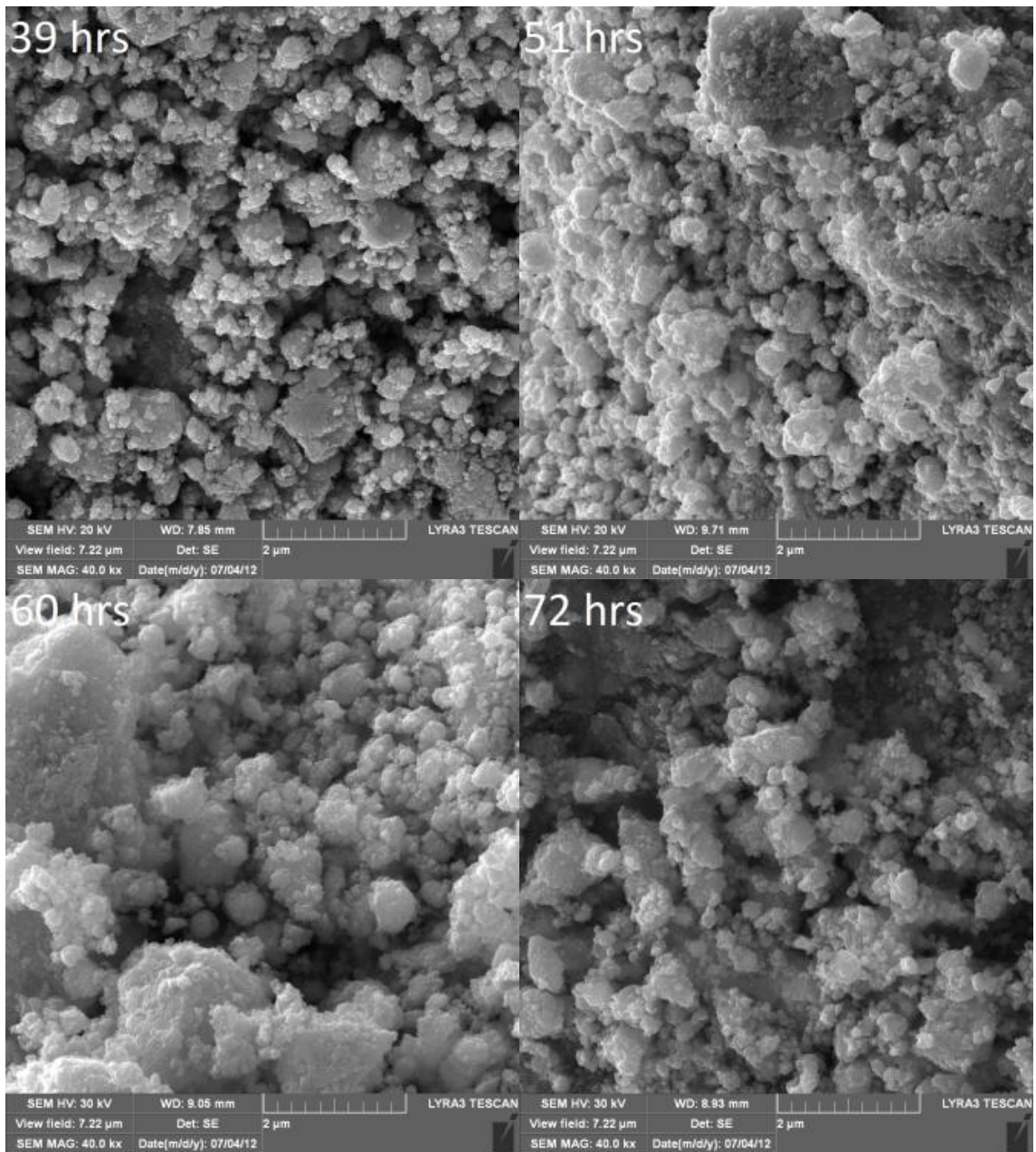


Figure 17 FESEM of WC, at different stages of milling, showing morphology of powders.

Figure 16(a) shows the distribution of milled WC from 54 to 69hrs where a shift to lower size scale was observed as the milling time increased. Samples were analyzed after 3hrs of milling.

Figure 16(b) shows the distribution of 72hr milled WC particles and it was observed that the distribution of particles sizes was higher at the start of the milling and decreases at a later stage of milling. This may indicate unification of the particles distribution. Moreover, it was observed that as the milling time increases the frequency of the distribution increases and the curve slight shifted towards smaller size scale.

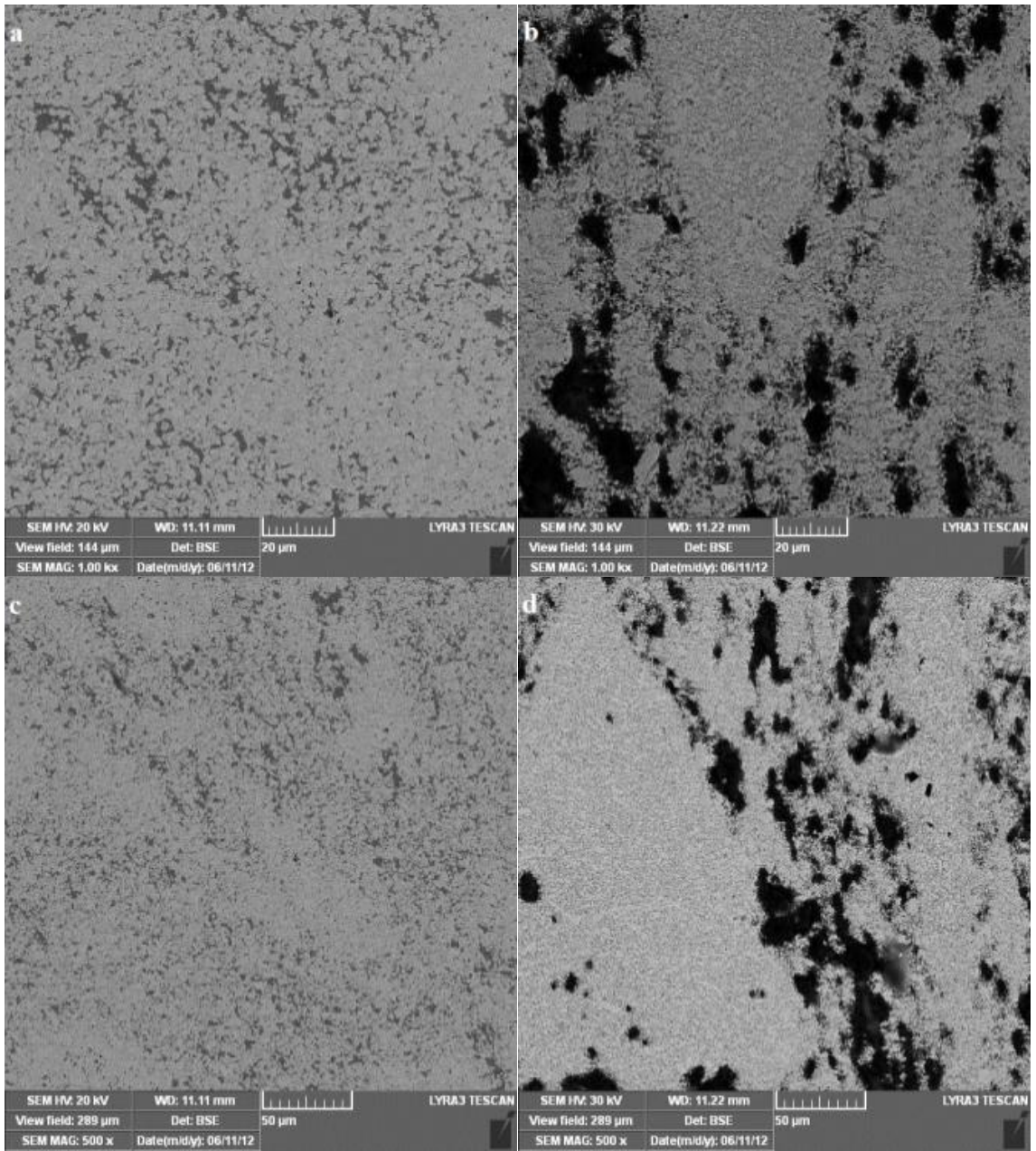
4.3 Effect of initial particle size on WC-Co composite

FESEM images of sintered WC 3.5 μm with 9 wt.%Co are shown in Figure 18 (a,c,e) while images of milled WC-9Co are shown in Figure 18 (b,d,f). Although both the samples were SPSeD under the same parameters and further were analyzed by FESEM at same magnification Figure 18(a) shows dense structure than as compared to Figure 18(b), which shows higher percentage of porosity . One of the probable reasons could be the local deficiency of molten cobalt around WC particles, in case of 10nm, due to comparatively higher surface area. These patches of cobalt-free WC powders could not densify at 1200°C and leaves porosity after sintering. Figure 18(c) showing continuous and homogenous distribution of Cobalt around all WC grains. The inhomogeneity distribution of Figure 18(d) further adds to the explanation of cobalt-free patches in the 10nm sintered sample. The resultant absence of cobalt as a matrix around certain WC

particles resulted in low densification. The same results were found in [8]. Figure 18(e) and Figure 18(f) showing FESEM of WC 3.5 μm and 10nm grinded samples. Grinding effect has shown peeling of certain WC grains from the surface in case of WC 10nm-9CO. This probably may be due to limited binder, cobalt in this case, which resulted in loosely packed particles even after sintering.

Peeling off effect from the surface and presence of internal porosity was further confirmed by FESEM analysis of fractured (with-out grinding and polishing) sample of WC10nm-9Co in Figure 19. Absence of patches in this fractured samples is clear, which were found in the same sample after grinding, as shown in figure Figure 18(d).

Further Almost rounded or oval shaped WC powders, shown in figure 12, have been faceted during sintering, which ended up with relatively rectangular or triangular shaped grains. The same effect have been observed by [8]. Fracture surface reveals brittle nature of the composite, and typically showing both transgranular and intergranular crack propagation in and around the WC grains. Addition of increased cobalt quantity for 10nm samples would retard the brittle fracture of the product.



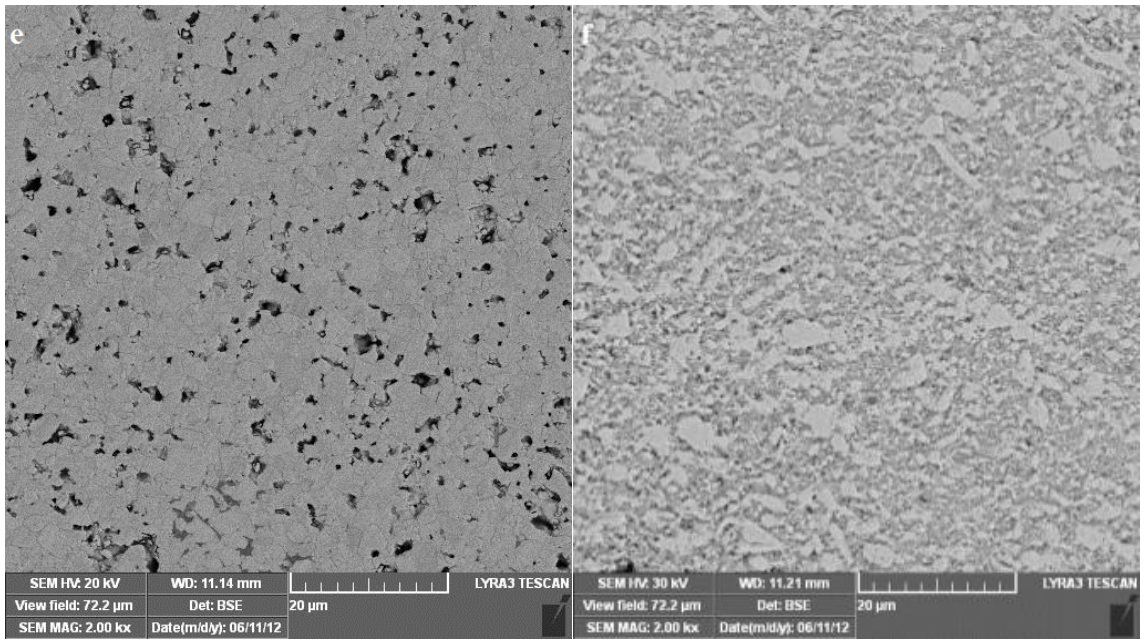


Figure 18 FESEM of Sintered WC 3.5 (a,c,e) and WC 10nm (b,d,f), each with 9%Co.

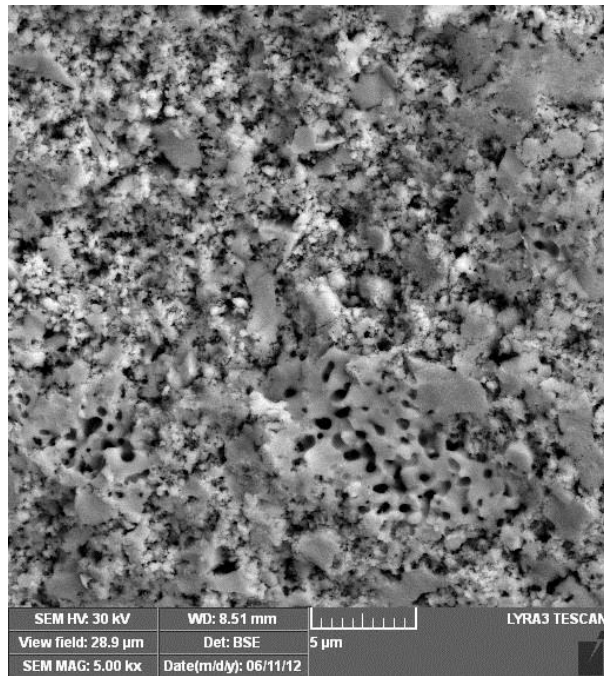


Figure 19 Fractured surface of SPSed WC(10nm)-9%Co

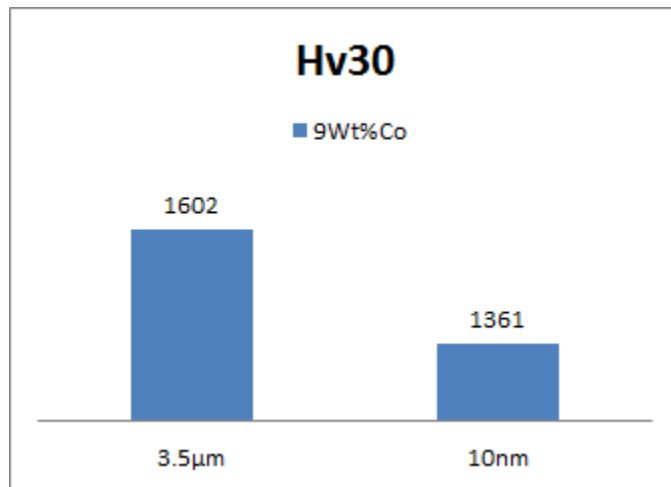
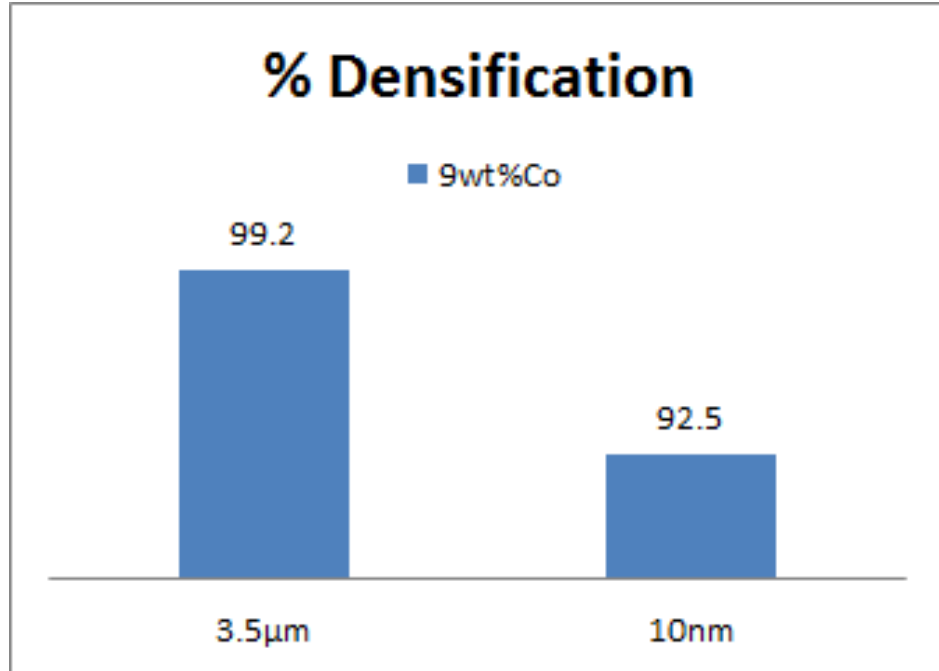


Figure 20 Effect of WC initial size over (a) densification and (b) Vickers hardness Hv_{30}

4.4 Effect of amount of binding material

Mechanical properties of the sintered cemented carbides, both with WC 3.5 μm and 10nm as starting crystallite size were analyzed. Lower densification and low Hv30 value, in WC-9Co nano cemented carbide could be due to several reasons. First, limited available binder cobalt, which could not coat all the increased surface area and hence could not densify in the limited sintering time of SPS. Increase in powder surface area, has been compensated by increasing the binder cobalt, as shown below, which has helped in achieving full densification with improved Hardness and fracture toughness values. Second reason could be certain gases O_2 N_2 and water could have been adsorbed over WC particles, which further hurdles the molten flow of cobalt during sintering,

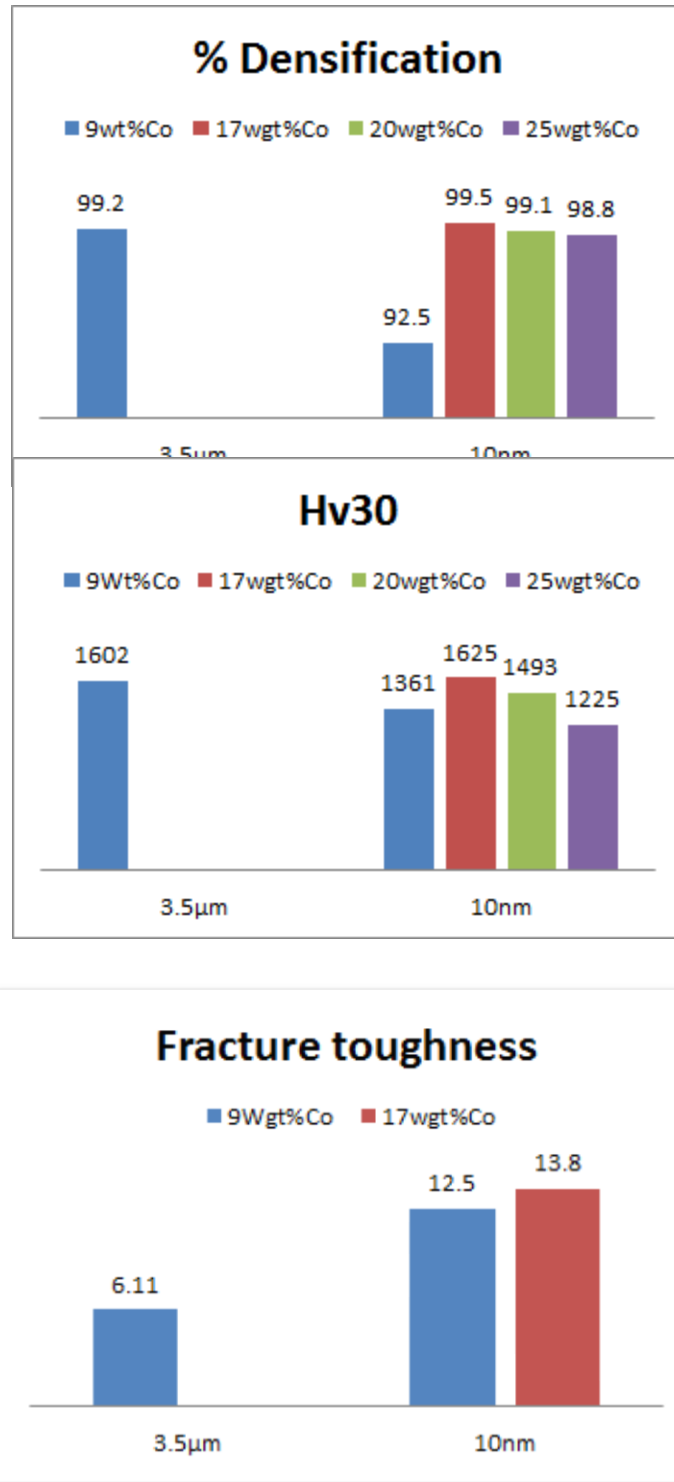


Figure 21 showing effect of amount of binding material over mechanical properties of WC-Co nanocomposite.

giving rise to closed micro porosity[30]. Presence of Oxygen in the milled powder was confirmed through EDX and mapping distribution, as shown in Figure 22 showing mapping distribution of milled powder. Presence of oxygen due to long milling hours is verified by its distribution. Further it seems as if Oxygen has reacted with W rather than Co, as distribution of Oxygen follow that of W rather than that of cobalt, as shown. Presence of oxygen is further verified by the EDX analysis, as shown in Figure 23 EDX of milled powder(WC 10nm-9Co). Last but not the least these impurities in WC powder can give rise to the formation of W_2C phase during de-carbonization which takes place at high temperature during sintering and hence lowers the hardness values of the composite [2].

The overall Vickers hardness was lower in case of nano crystallite carbide, due to presence of voids in the sintered samples, as discussed above. Cracks generated due to indent in nano crystallites have shown comparatively higher toughness value. The reason could probably be the presence of voids in these samples, which absorbs higher energies at the crack tips and did not allow the crack propagation.

Average grain size of sintered composite, calculated through scherrers equation is 92nm, which is far lower than reported by literature as shown in Table 6

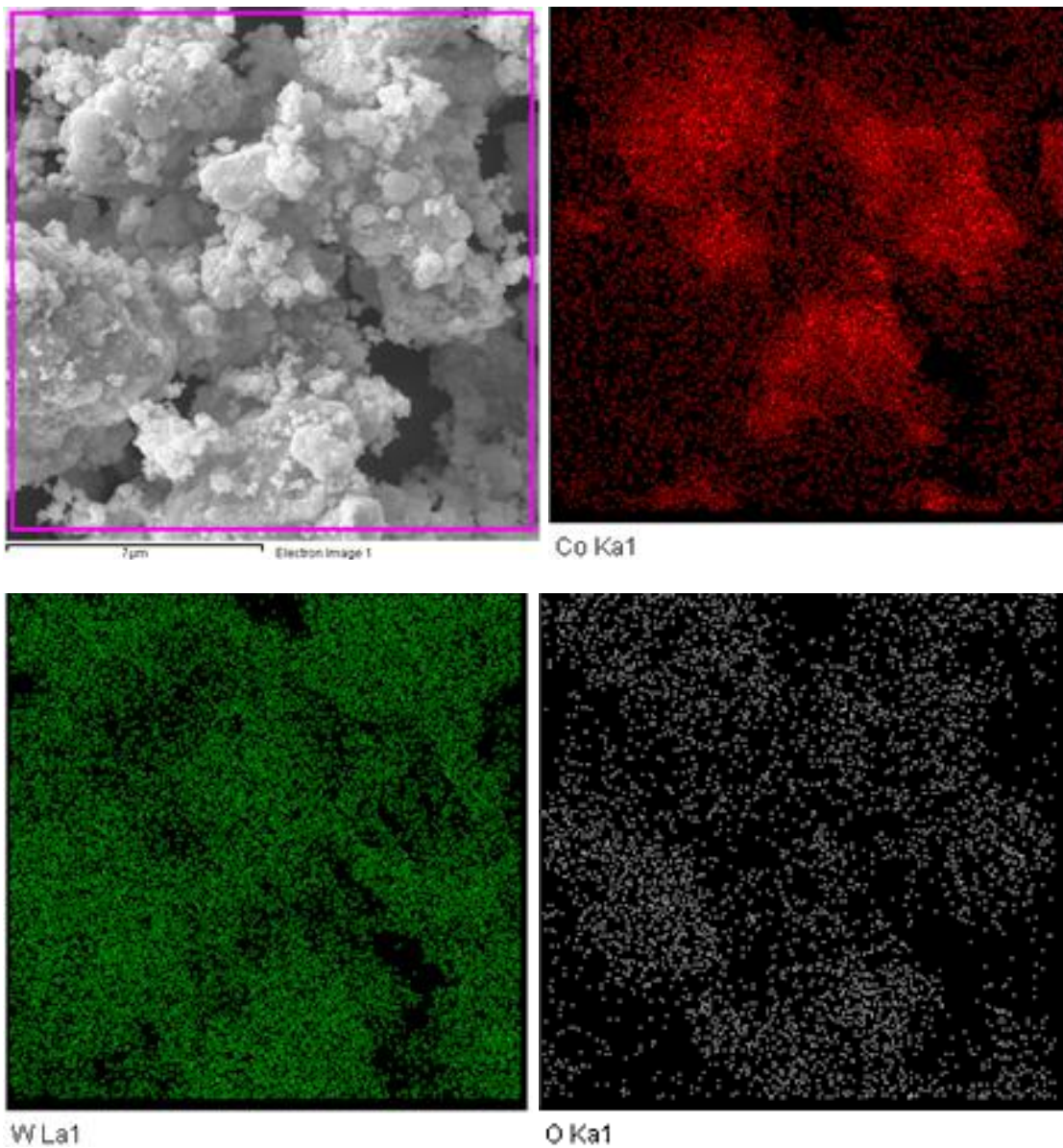


Figure 22 showing mapping distribution of milled powder.

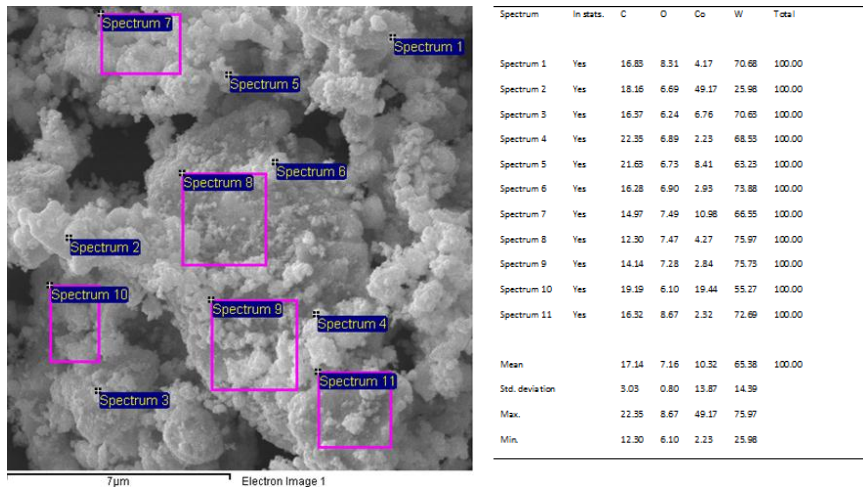


Figure 23 EDX of milled powder(WC 10nm-9Co).

Table 6 Mechanical properties of WC-Co composite studies in this work, in comparison to reported by earlier researchers.

Reference	Cobalt %age	Densification	Grain size	Hv30 (kg/mm ²)	Fracture toughness ((MPa m ^{1/2}))
19	10	-	430	1800	6
8	10	98.9	380	1756	11.6
20	10	99.5	1910	1333	13.5
21	10		300	1800	12
This study (nano WC)	17	99.5	92	1625	13.8
This study (micron WC)	9	99.2	128	1602	6.11

4.5 Effect of sintering temperature, binding material over inhibitor – added WC-Co composites.

Morphology of as received WC powder is shown in Figure 12 which elaborates presence of a range of particle sizes however highest intensity observed in the particle size distribution was 3.5 μ m. it can noted that particles are round in nature and further EDX analysis performed over it, reveals the absence of any compositional fluctuation. The nano WC powder, prepared by planetary ball milling of the as received WC powder is shown in Figure 24. Although figure shows that powders have formed agglomerates of an average size of 500nm, but actual crystallite size, measured using sherrer equation through XRD peaks was around 8-10nm. The attained WC nano powder was further analyzed using FESEM and particle size distribution. XRD patterns at different milling timings and respectively attained grain sizes are shown in Figure 15.

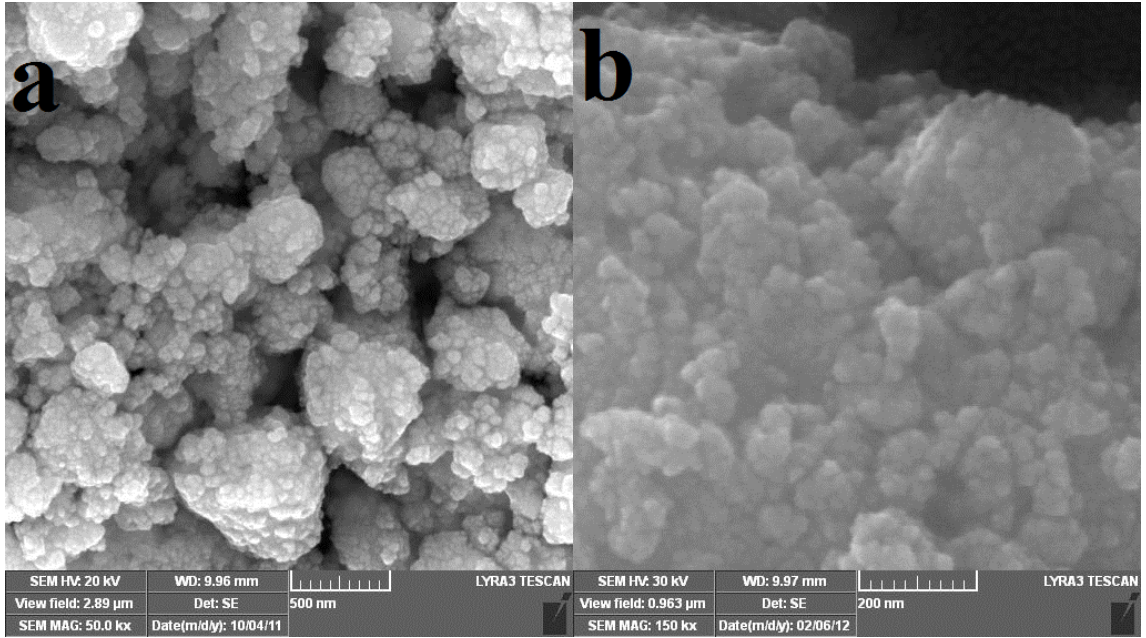


Figure 24 FESEM images of milled WC powder

The powder mixtures using WC(3.5 μ m) were consolidated through spark plasma sintering technique, where shrinkage behavior, during sintering, was closely monitored through displacement of the SPS ram during sintering process. It was noted that shrinkage started to occur around 850oC and the rate continue to increases until 985oC, where then it declined with further increase in temperature. There wasn't any noticeable displacement in the SPS ram, as temperature reached 1200oC, thereby suggesting it to be the sintering temperature for achieving full densification. However when mixture containing WC(milled) powder was consolidated at the same temperature, it resulted in composite with low densification and low mechanical properties. Further it was noted that addition of both Cr₃C₂ and VC has shown to reduce densification of the sintered composite at lower temperatures. This effect is due to formation of thin layer over WC particles, which limits the diffusion process, and hence leads to grain growth inhibition. Although samples with Cr₃C₂ has shown comparatively better densification as shown in Table 7. These inhibitors are found to lower the densification of final product by limiting diffusion and migration of Co[3].

Addition of inhibitors, degrades the atomic diffusion, and hence with in short time of SPS, has resulted to leave voids/porosity in the material, as shown in Figure 25(a) which decreases density of the composite. These results were also reported by[50] .The incomplete densification in the solid state by inhibitors effect is associated with the limitation of the atomic diffusion phenomena and migration of Co [49]. Theses voids further, probably act as crack arrestor, which has shown to increase fracture toughness of the material. This increase in fracture toughness was also referred by [40].

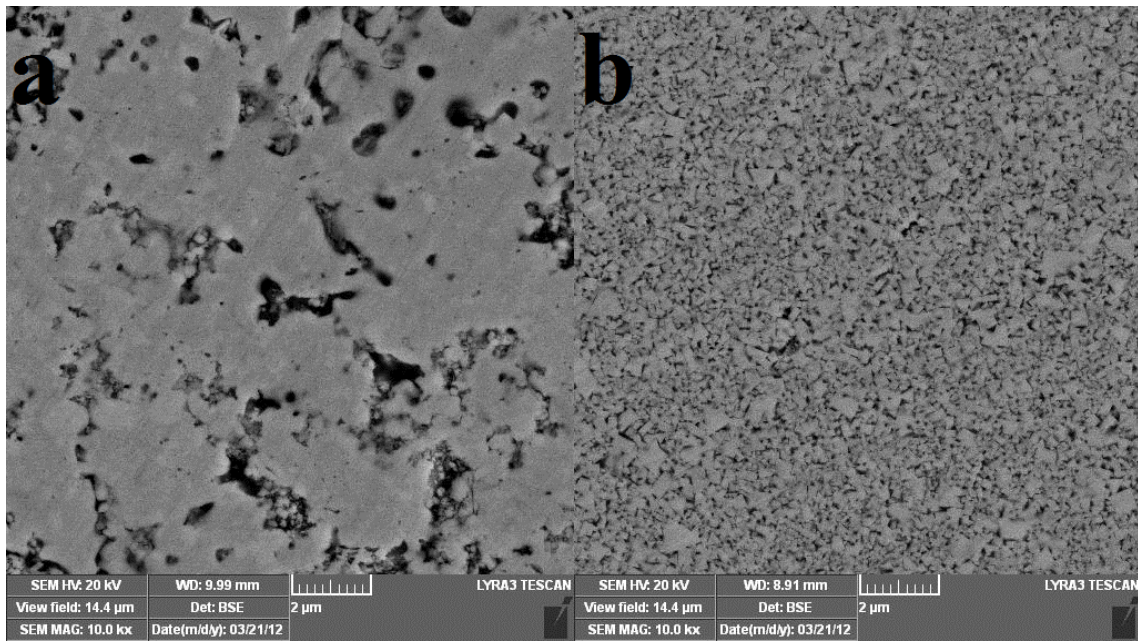


Figure 25 (a) incomplete densification as a result of WC-9Co-0.6VC sintered at 1200⁰C, while (b) showing complete densification, homogeneous distribution as a result of WC-12Co-0.6VC sintered at 1300⁰C.

Nano scaled WC-9Co with the addition of grain growth inhibitors could not attained mechanical properties, when consolidated at 1200⁰C, however increasing quantity of cobalt to 12wt% and sintering temperature to 1300⁰C for 10mins resulted in well dense nao-composite with higher mechanical properties. This may be due to that Cobalt, as binding material, could have been viscous enough at low sintering temperature of 1200⁰C, where it could not flow into the nano pores between nano scaled WC grains, thus leaving behind binder less WC grains. The direct contacts of WC to WC grains have resulted in the abnormal grain growth thus decreasing HV30 values and K1C values. [15] reported that abnormal grain growth may occur during sintering process, due to creation of local “cobalt pool”. The effect further was explained as when co viscous flow is thick enough at lower sintering temperatures that it retards to fill the capillary skeleton of nano WC paticle or thin enough due to extended plastic deformation will retards the formation of bond between WC and Co. Both cases favors the direct contact between WC grains which enhances the abnormal grain growth. This increase in grain sizes, and corresponding lower hardness values are shown in Table 7. It can be noted from Table 7 that increasing amount of cobalt, from 9wt% to 12wt% have shown increase in densification, and mechanical properties of the nano WC powders. This is because higher binding material can float higher WC grains, which eases them to re-arrange and enhance diffusion mechanism and hence densification, even at lower sintering temperatures. Further, increasing sintering temperatures in combination with higher cobalt quantity, have shown to increase mechanical properties of the composite. This is because, besides increasing the diffusion kinetics at higher temperatures, it probably would also have decreased the viscosity of cobalt, thus eases to flow in the nano pore structure between WC grains. However this increase in diffusion rate due to higher binding

material and higher sintering temperature has resulted to increase the grain sizes as shown in Table 7. Further increasing cobalt amount and sintering temperature have resulted to shown faceted WC grains and homogenously distributed as shown in FESEM Figure 25(b). The increase in grain sizes, ultimately reduces the WC surface area which is to be coated/bonded by the amount of cobalt present in the mixture. [30] reported that increasing sintering temperature will result in W grains to grow, hence decreasing W/W contact or simply the WC surface area. The amount of cobalt present in the mixture, which at time needed to coat higher surface area, will now have lower surface area to be coated. The amount of cobalt which was thought to be limited for initial comparatively high WC surface area and which probably was viscous enough to flow into the nano pores between nano WC powders at lower sintering temperatures, was found to improve microstructural and mechanical properties at this stage. The However further increases in either cobalt or sintering temperature may retard hardness at the expense of fracture toughness of the composite showing absence of any other phase formation, after powder mixture was consolidated through Spark plasma sintering technique. Presence of graphite is probably due to the traces of graphite sheet, which was used during consolidation.

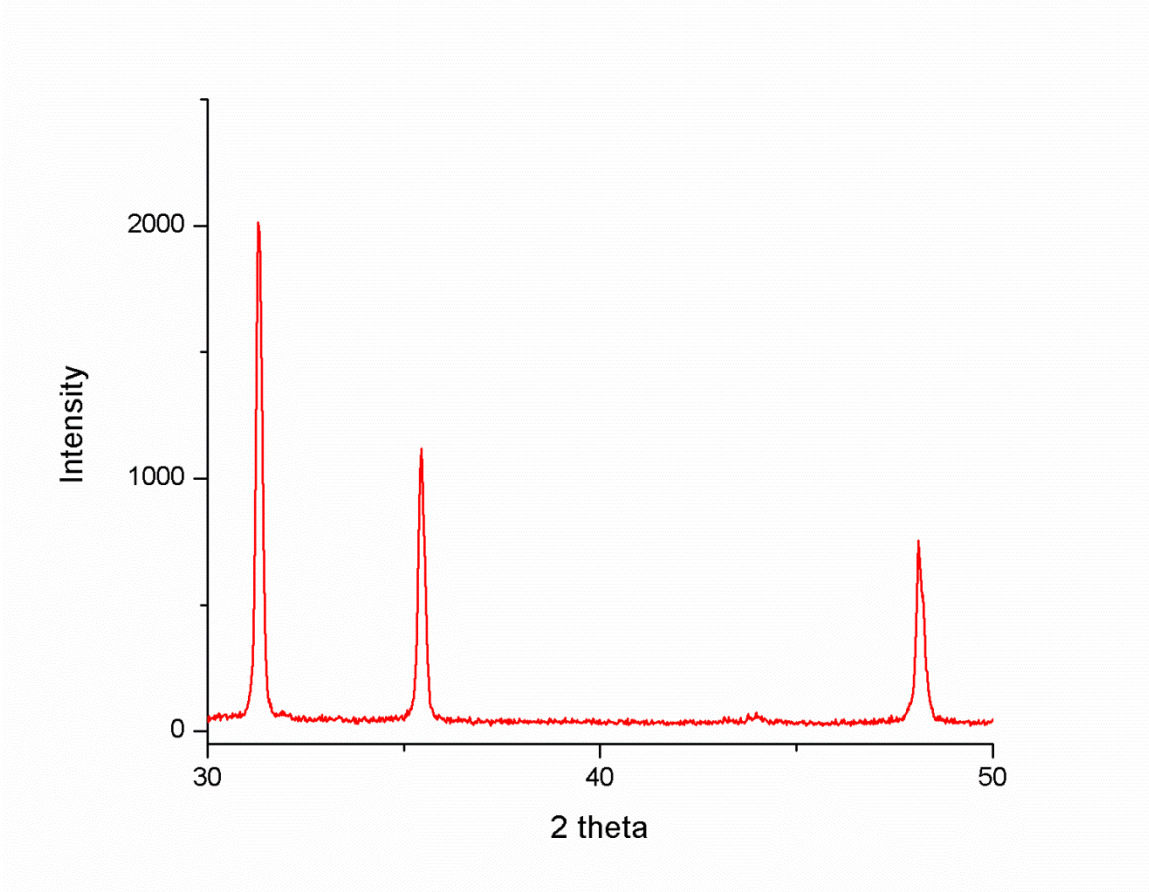
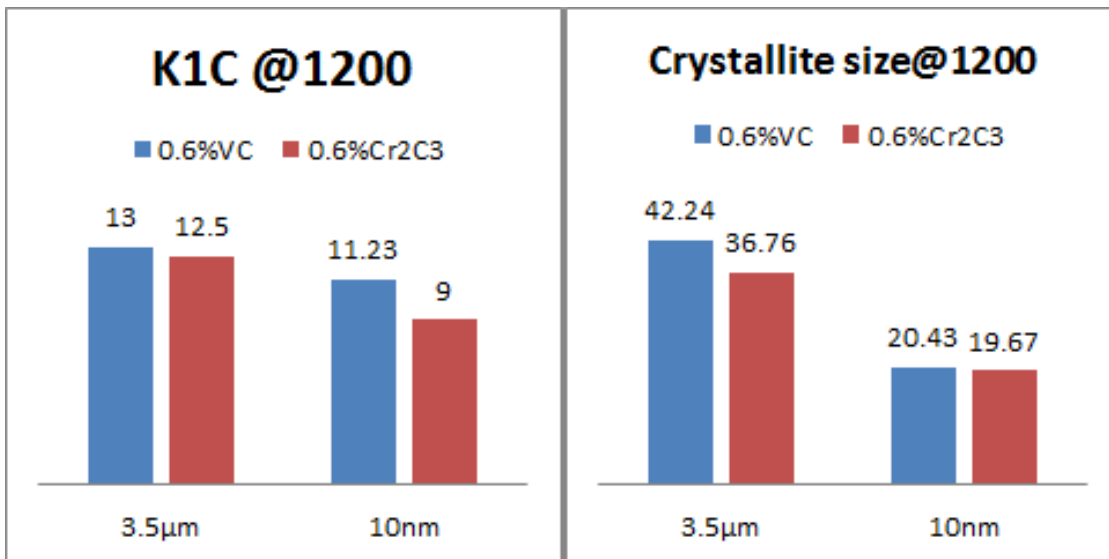
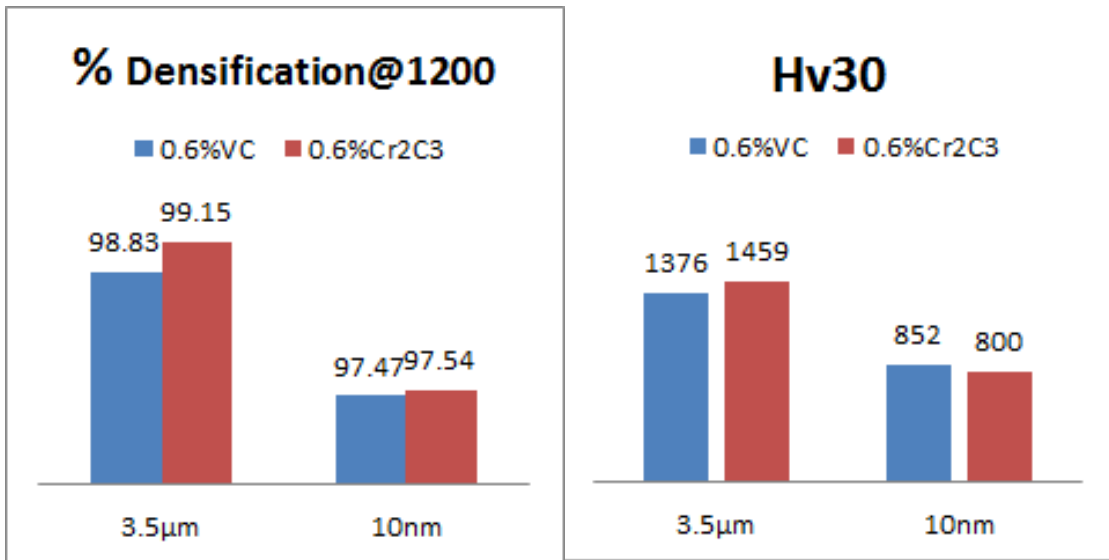
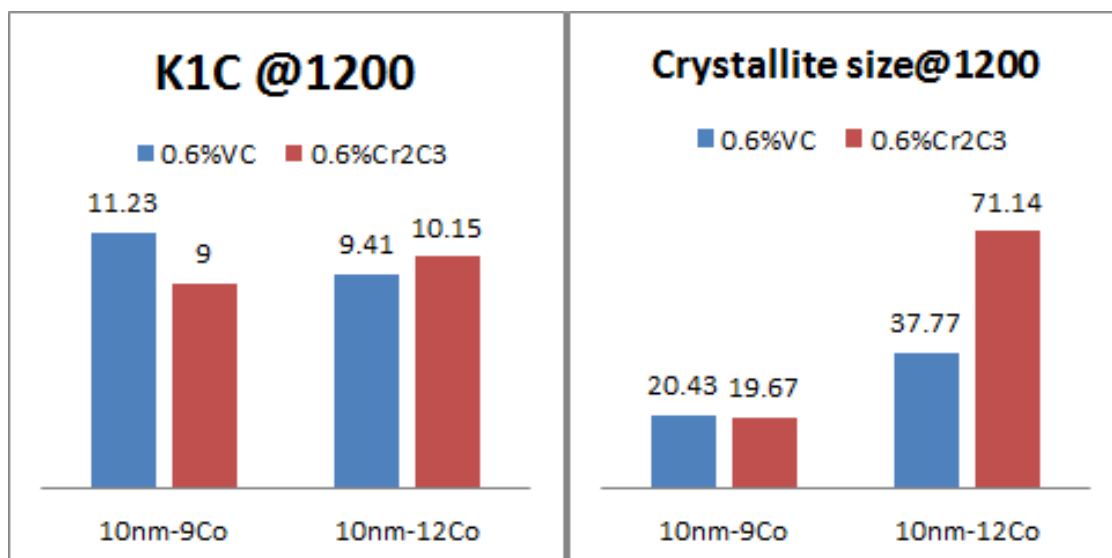
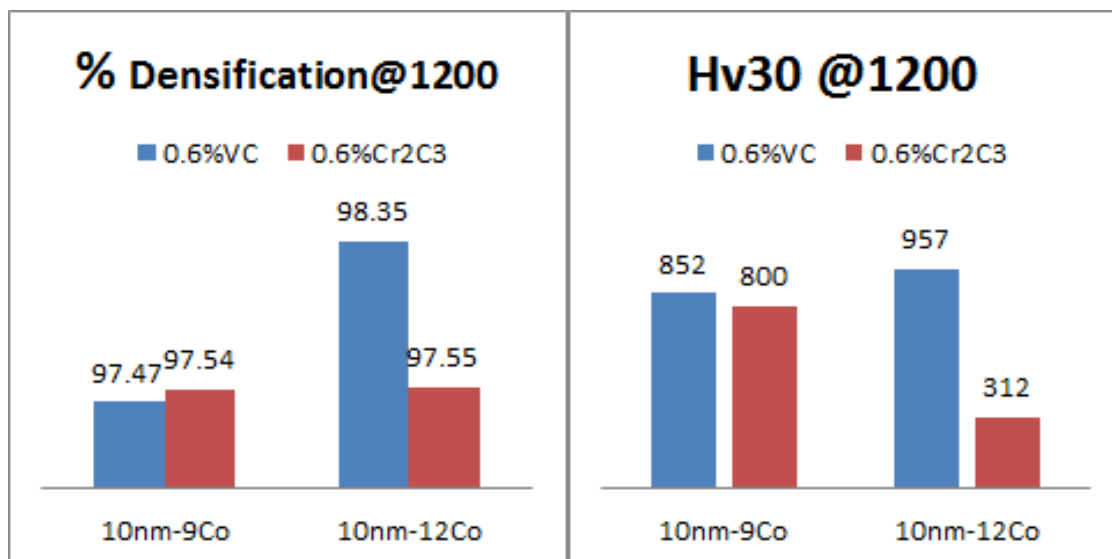


Figure 26 XRD of spark plasma sintered WC-12Co-0.6Cr₃C₂

Table 7 showing experimental results of WC-Co system, where both the amount of cobalt and sintering temperature has been changed.

Sample Number	Initial Fsss	WC	wgt% Co	Wgt% VC	Wgt% Cr ₃ C ₂	SPS temperature (°C).	Hv30	K1c Mpam ^{1/2}	%densification	Crystallite size after SPS(nm)
1	3.5µm		9	0.6	0	1200	1376	13	98.83	42.24
2	3.5µm		9	0	0.6	1200	1459	12.3	99.15	36.76
3	10nm		9	0.6	0	1200	852	11.23	97.47	20.43
4	10nm		9	0	0.6	1200	800	9	97.54	19.67
5	10nm		12	0.6	0	1200	957	9.41	98.35	37.77
6	10nm		12	0	0.6	1200	312		97.55	71.14
7	10nm		9	0.6	0	1300	605	10.25	98.43	42.37
8	10nm		9	0	0.6	1300	1445	13.15	98.36	39.29
9	10nm		12	0.6	0	1300	1432	8.53	98.78	
10	10nm		12	0	0.6	1300	1592	9.23	99.13	71.09





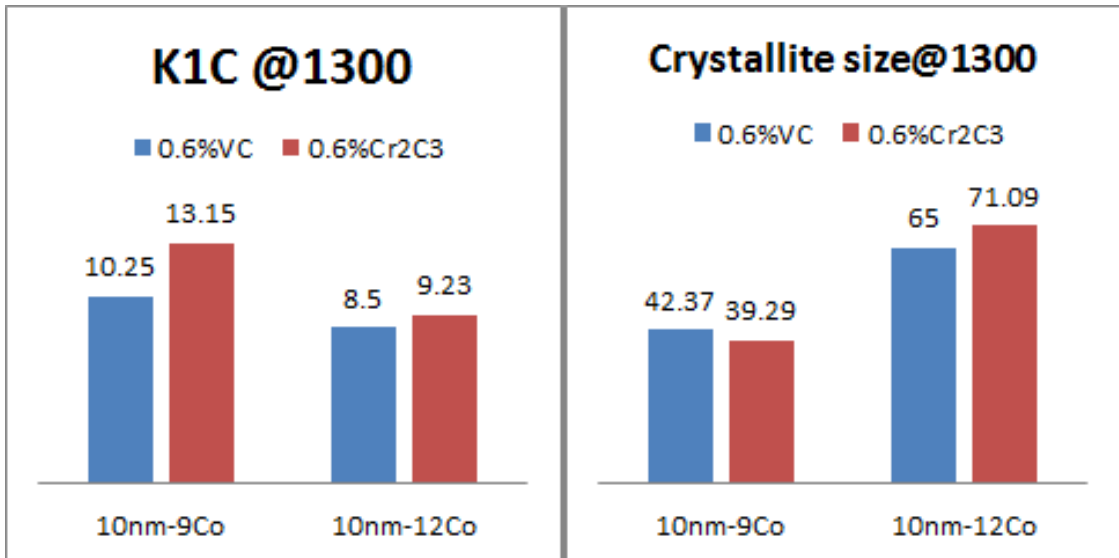
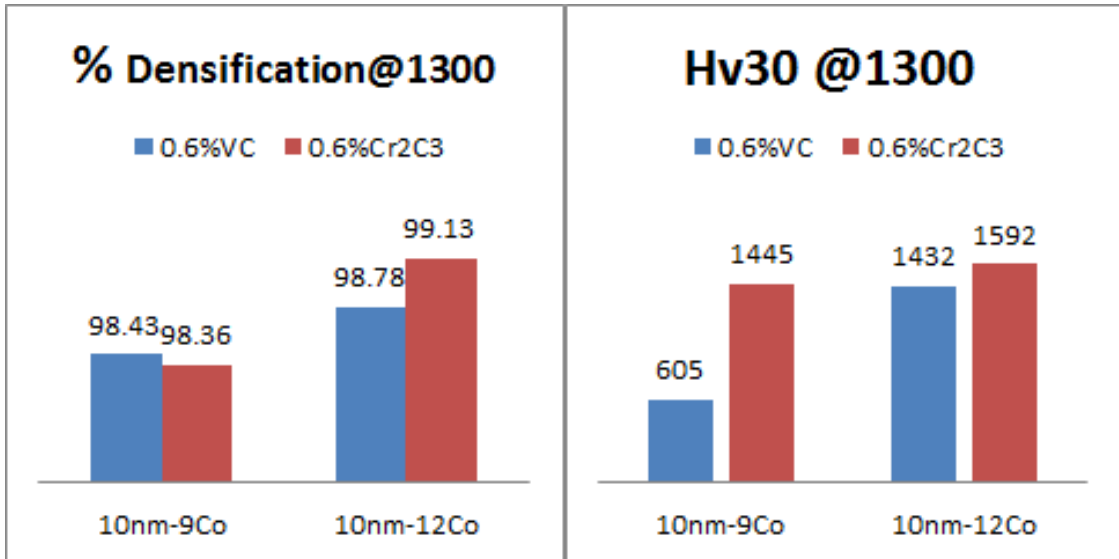


Figure 27 showing change in basic properties of WC-Co composite, as a result of variation in amount of Cobalt and sintering temperatures.

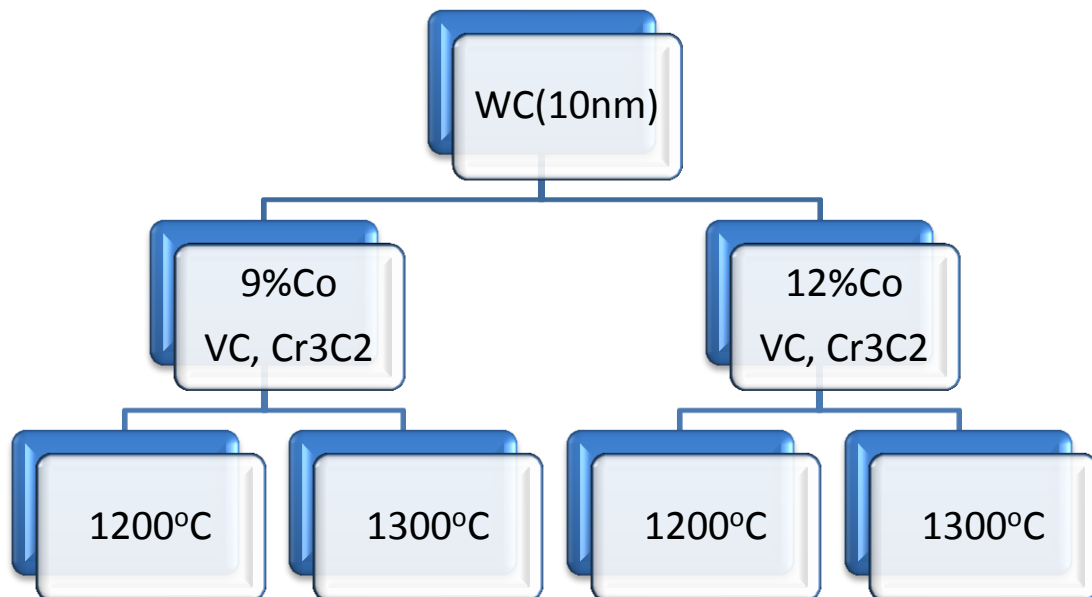
This improvement in hardness is accompanied by a loss of fracture toughness, due probably to loss of strain capacity of the binder as a result of decreasing mean free path and/or the dissolution of VC [50]. The decrease in fracture toughness or early crack initiation, due to addition of inhibitors was reported by [15], who argues that cracks initiation and propagation is easy along the grain boundaries rather than with-in the grains, where inhibitors forms thin layer over WC grains.

Table 8 showing comparison of research work in WC-Co system for refining grain growth and increasing mechanical properties.

Ref.	Initial WC particle size	Grain Size attained	Hv30	KIc Mpam ^{1/2}	Composition
01	0.25microns	350nm	1939	16.34	WC-11Co
03	40-80nm	120nm	2100	10	WC-12Co
10	2.3microns				
15	30nm(spray conversion)	154nm	2000	10	WC-12Co VC/Cr ₃ C ₂
13	40nm	800nm			WC-12Co
This work	8-10nm	71nm	1592	9.23	WC-12Co

4.6 Effect of adding range of individual Inhibitors to WC-Co Nano Composites.

Various amounts of vanadium and chromium carbides have been added to 10nm WC particles. All range of powders were added to 9 and 12wt% Co and the resulting mixed powder were prepared by planetary mixing, as explained in the experimental procedures. The mixed powder compositions were consolidated using spark plasma sintering at 1200°C and 1300°C under high vacuum.



Effect of adding range of individual Inhibitors (0.2,0.4,0.6,0.8wt%) to WC(10nm)-9,12Co and SPS at 1200°C, 1300°C

Table 9 Input parameters regarding experimental data for adding individual range of inhibitors

Sample No.	WC particle size	9% cobalt addition	12% cobalt addition	VC added	Cr ₃ C ₂ added	Sintering Parameters in SPS
sample 3-1	10nm	WC-9Co		0.2		1200/50Mpa/10min
sample 3-2	10nm	WC-9Co		0.4		1200/50Mpa/10min
sample 3-3	10nm	WC-9Co		0.6		1200/50Mpa/10min
sample 3-4	10nm	WC-9Co		0.8		1200/50Mpa/10min
sample 3-5	10nm	WC-9Co			0.2	1200/50Mpa/10min
sample 3-6	10nm	WC-9Co			0.4	1200/50Mpa/10min
sample 3-7	10nm	WC-9Co			0.6	1200/50Mpa/10min
sample 3-8	10nm	WC-9Co			0.8	1200/50Mpa/10min
sample 3-9	10nm		WC-12Co	0.2		1200/50Mpa/10min
sample 3-10	10nm		WC-12Co	0.4		1200/50Mpa/10min
sample 3-11	10nm		WC-12Co	0.6		1200/50Mpa/10min
sample 3-12	10nm		WC-12Co	0.8		1200/50Mpa/10min
sample 3-13	10nm		WC-12Co		0.2	1200/50Mpa/10min
sample 3-14	10nm		WC-12Co		0.4	1200/50Mpa/10min
sample 3-15	10nm		WC-12Co		0.6	1200/50Mpa/10min
sample 3-16	10nm		WC-12Co		0.8	1200/50Mpa/10min
sample 3-17	10nm	WC-9Co		0.2		1300/50Mpa/10min
sample 3-18	10nm	WC-9Co		0.4		1300/50Mpa/10min
sample 3-19	10nm	WC-9Co		0.6		1300/50Mpa/10min
sample 3-20	10nm	WC-9Co		0.8		1300/50Mpa/10min
sample 3-21	10nm	WC-9Co			0.2	1300/50Mpa/10min
sample 3-22	10nm	WC-9Co			0.4	1300/50Mpa/10min
sample 3-23	10nm	WC-9Co			0.6	1300/50Mpa/10min
sample 3-24	10nm	WC-9Co			0.8	1300/50Mpa/10min
sample 3-25	10nm		WC-12Co	0.2		1300/50Mpa/10min
sample 3-26	10nm		WC-12Co	0.4		1300/50Mpa/10min
sample 3-27	10nm		WC-12Co	0.6		1300/50Mpa/10min
sample 3-28	10nm		WC-12Co	0.8		1300/50Mpa/10min
sample 3-29	10nm		WC-12Co		0.2	1300/50Mpa/10min
sample 3-30	10nm		WC-12Co		0.4	1300/50Mpa/10min
sample 3-31	10nm		WC-12Co		0.6	1300/50Mpa/10min
sample 3-32	10nm		WC-12Co		0.8	1300/50Mpa/10min

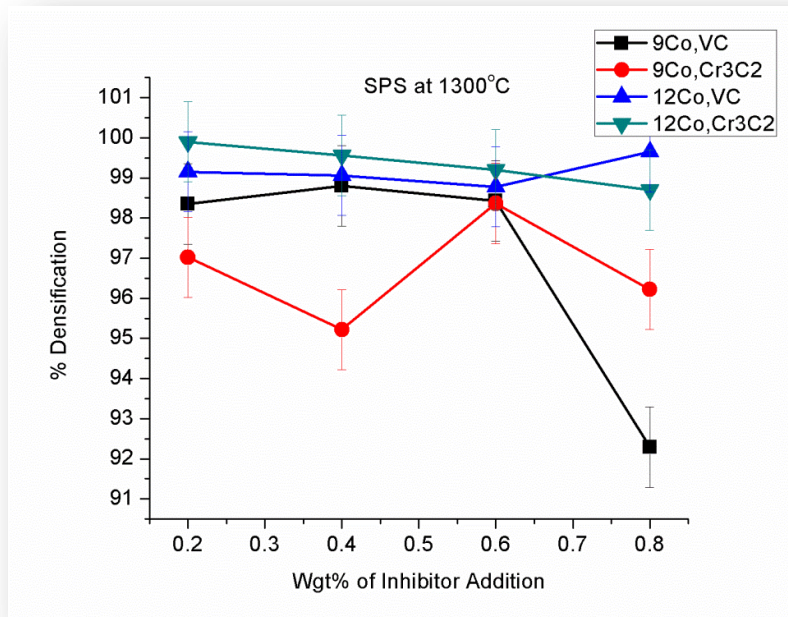
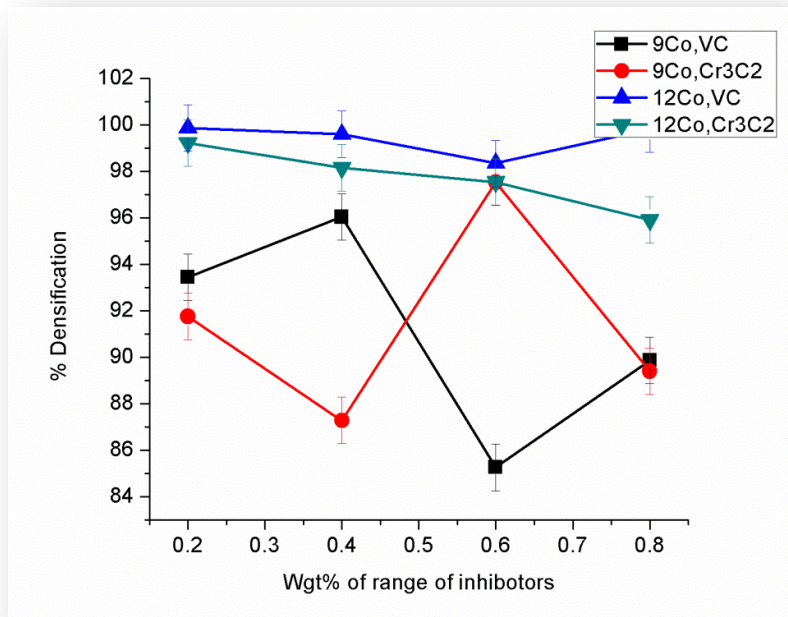


Figure 28 comparison of attained densification, with varying sintering temperatures, amount of cobalt, and using different inhibitors

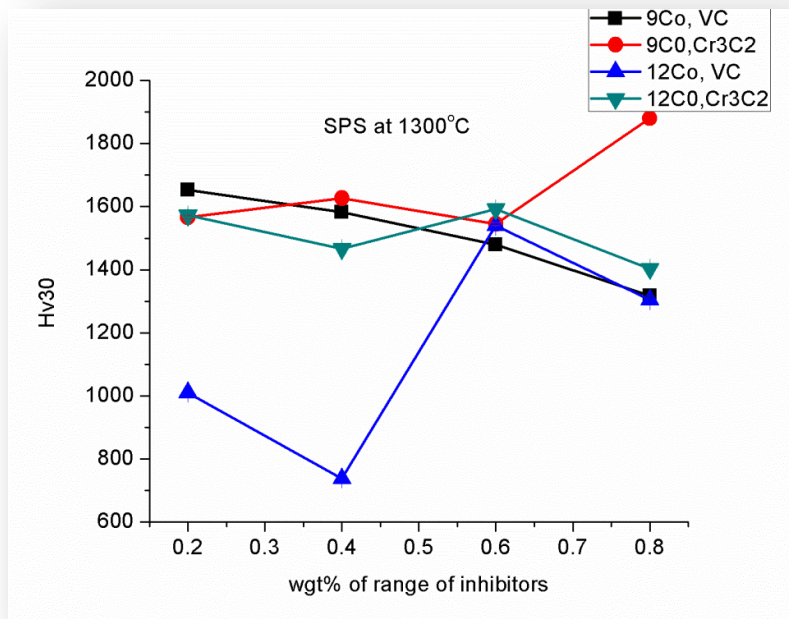
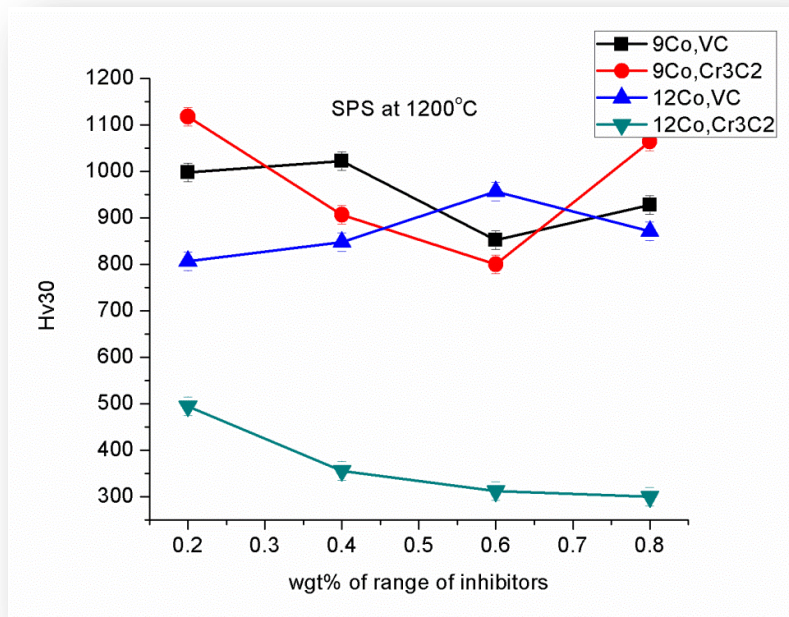


Figure 29 comparison of attained hardness values, with varying sintering temperatures, amount of cobalt, and using different inhibitors

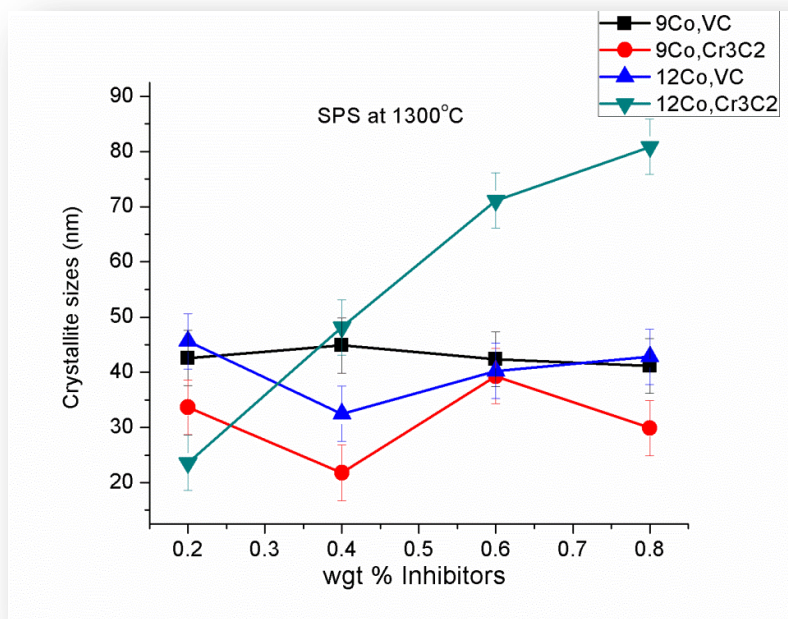
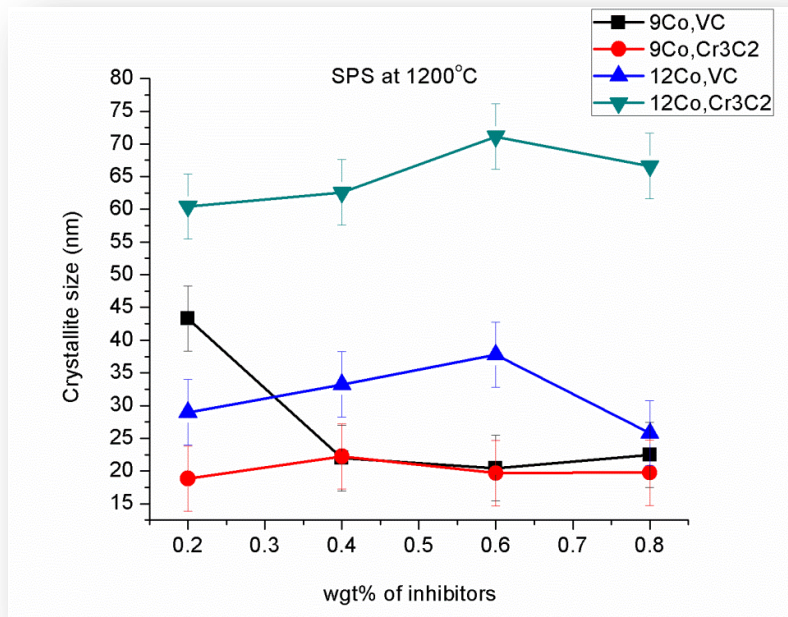


Figure 30 comparison of attained crystallite sizes, with varying sintering temperatures, amount of cobalt, and using different inhibitors

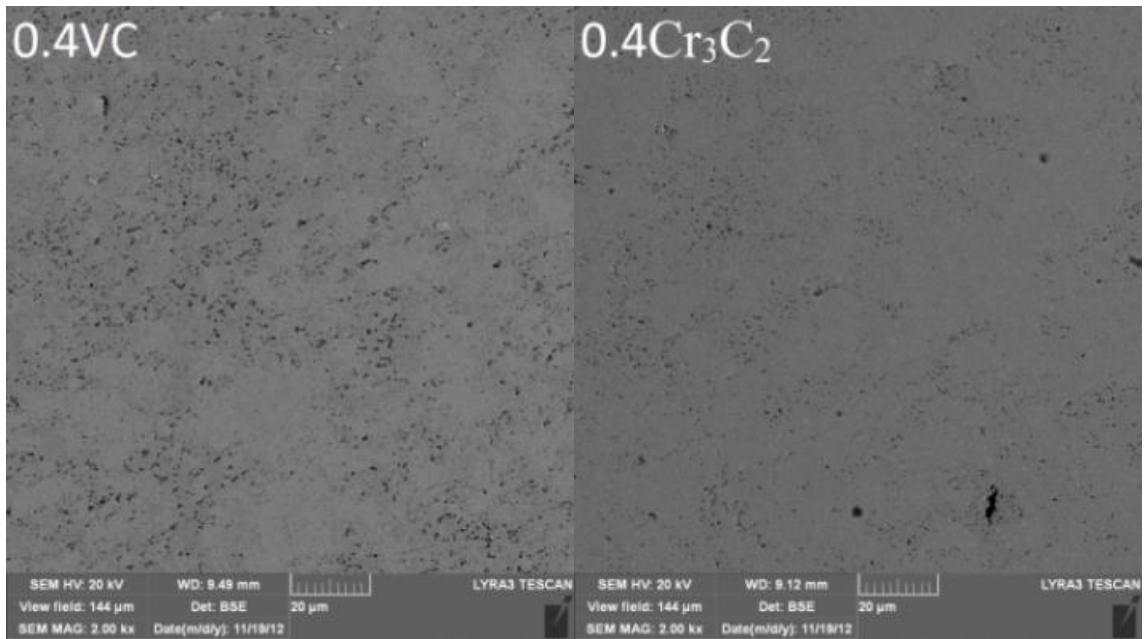
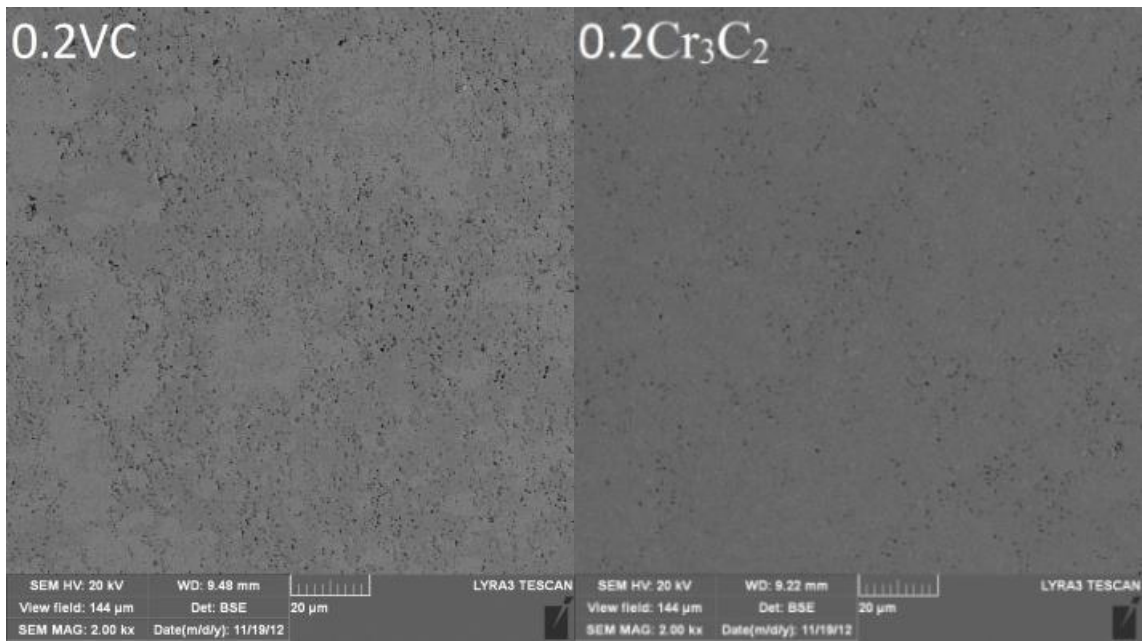
A range of both inhibitors vanadium carbide and Chromium carbide have been studied thoroughly, to analyze their effect on the consolidation of nano-WC crystallites. This portion of the study also covers varying amounts of binder phase, cobalt in this case, along with changing sintering temperatures. The parameters have been varied to see the overall effect on microstructure and respective required mechanical properties. The attained results have been presented graphically in Figure 28-Figure 30.

General increase in densification of all different compositions has been noticed, as sintering temperature was increased from 1200°C to 1300°C. This effect has been represented, as all points on the densification graph have moved upward, as sintering temperature was raised. Another general statement from analyzing the densification graphs is that higher cobalt content has shown higher densification, both at lower and higher temperatures. This effect can be explained as an increase in liquid binder phase would allow more WC particles to easily re-arrange themselves during the sintering process, which further enhances the densification.

Comparing Cr₃C₂ to VC at each resulting value of densification, it can be noticed that addition of Cr₃C₂ comparatively shows higher densification. Lower densification in samples with addition of VC can further be linked to the presence of micro porosity in these samples. 0.6% VC addition to 9CO at 1300°C can be assumed as a saturation point, where it shows highest densification, however further addition of VC may re-precipitate at the WC/Co grain boundary, which further will restrict the material transfer and hence the densification will be affected, as shown. This effect of saturation was not noticed at higher amounts of cobalt, where higher amounts of liquid binder wouldn't have crossed the

solubility limit, and hence decrease in densification at 0.6% VC was not noticed, when amount of cobalt was raised from 9 to 12%.

Further looking at the hardness values, it can be noticed generally that higher sintering temperatures have added to hardness of the composites. This effect is noticed as graphs has moved upward, as sintering temperatures was raised to 1300°C. However higher cobalt addition to the powder mixture have resulted to reduce the Hv30 values. This is obvious as amount of soft material in the mixture increases, will lower the hardness values. Higher cobalt amount with the addition of Cr₃C₂ has been noticed to give higher hardness values, comparatively. This effect was also noticed by [51], who reported that Cr₃C₂ usually exists in binder cobalt rather than VC, which is found both in binder and WC phase. Addition of Cr₃C₂ to binder phase incorporates distortional stresses in the softer binder phase, which further enhances the strengthening effect of binder phase and hence over-all hardness of the composite. It was also reported that VC increases the %age of micro porosity and hence will reduce the average hardness of the composite. This effect was also noticed in the densification graphs, where addition of VC has shown lower densification. The decrease in hardness values, regarding addition of VC from 0.2 to 0.4% at higher amount of cobalt is abnormal and are unexpected values. However general decrease in hardness values with the addition of inhibitors can be attributed to respective lower densifications.



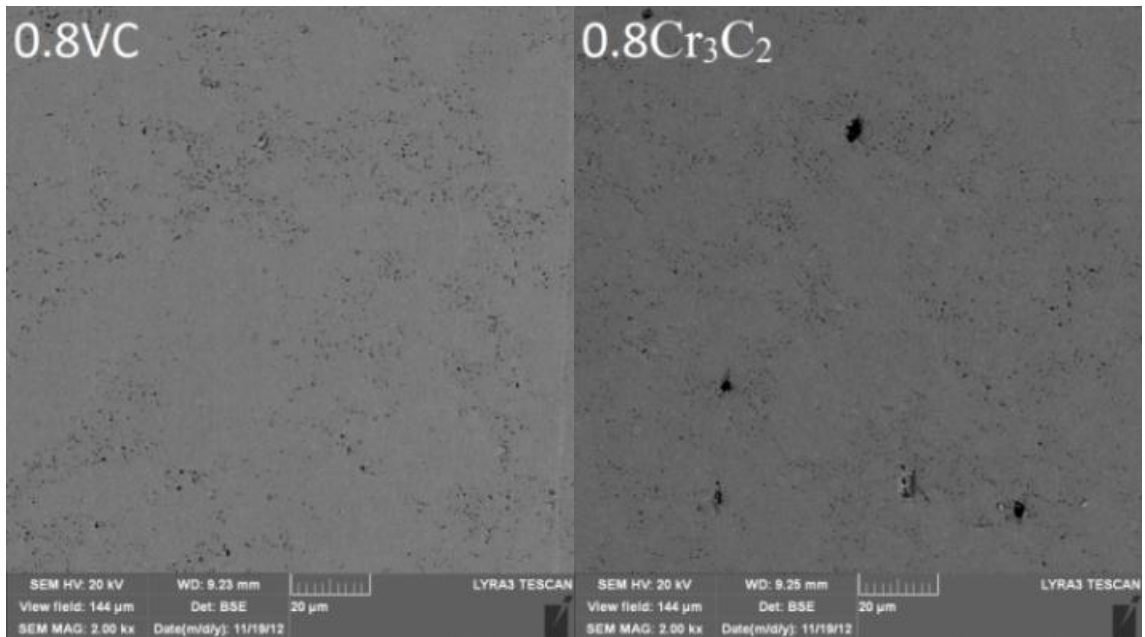
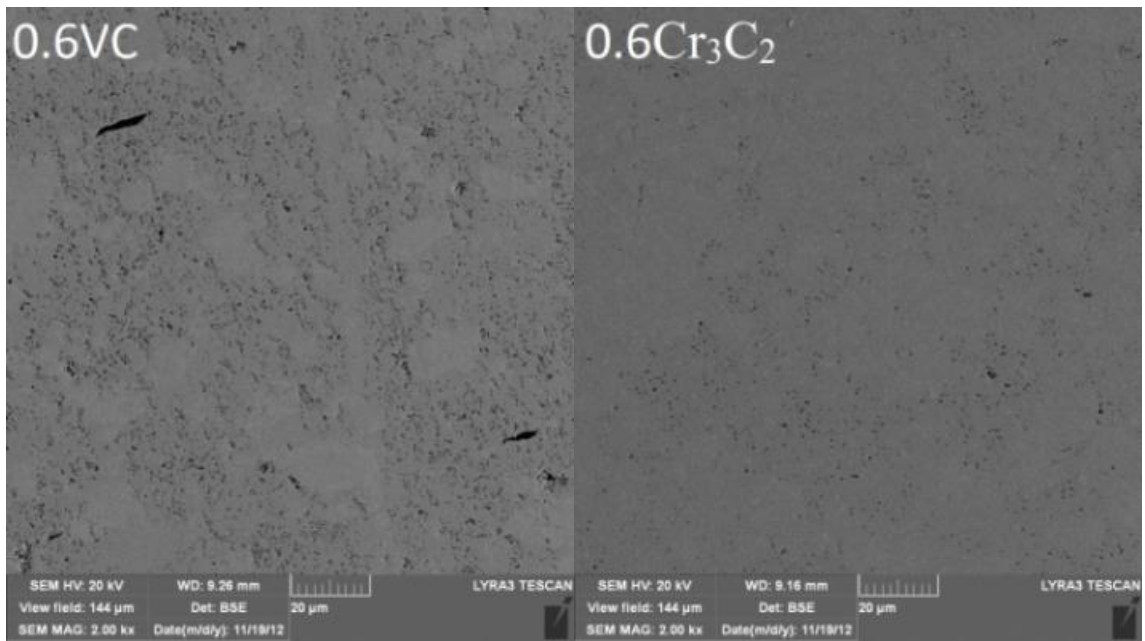
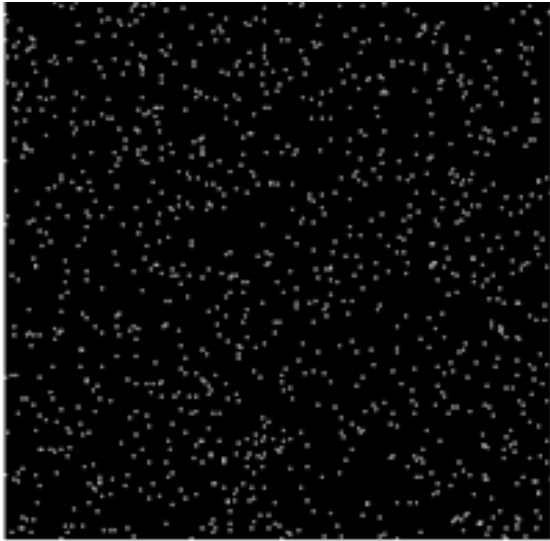
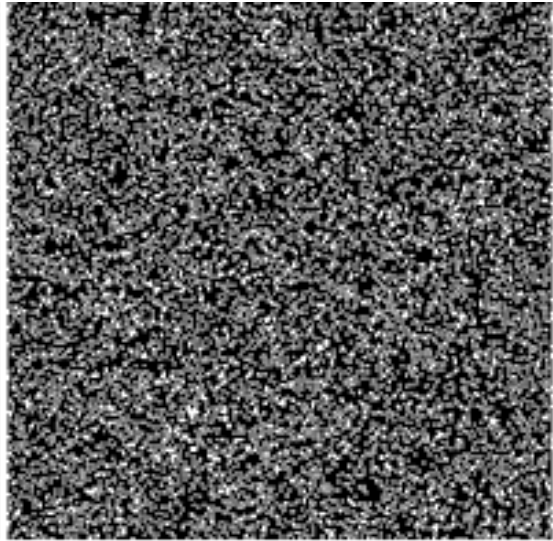


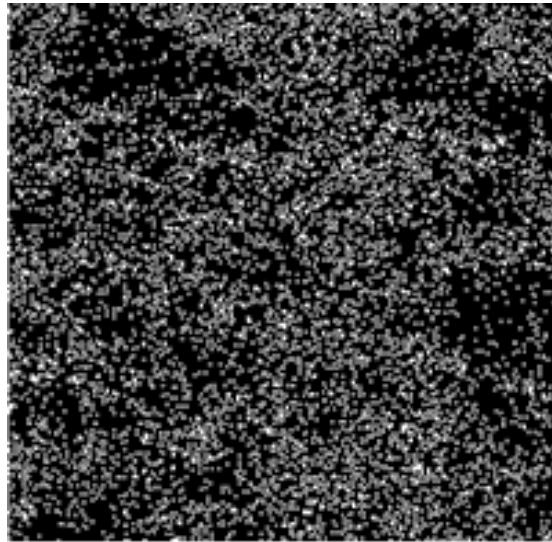
Figure 31 comparison of FESEM images for different type and rages of inhibitors, being sintered at 1300°C.



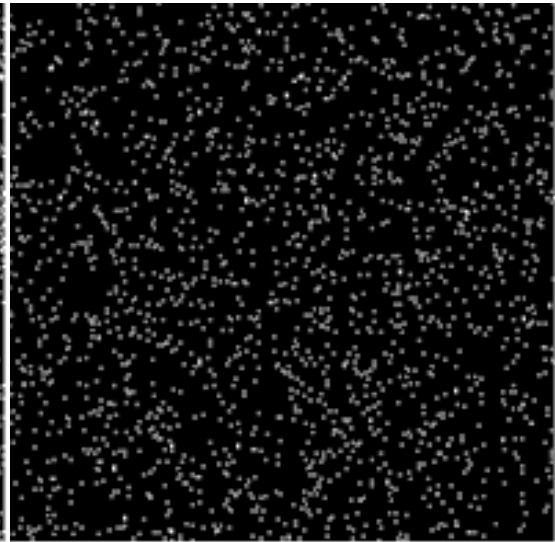
C Ka1_2



W La1



Co Ka1



Cr Ka1

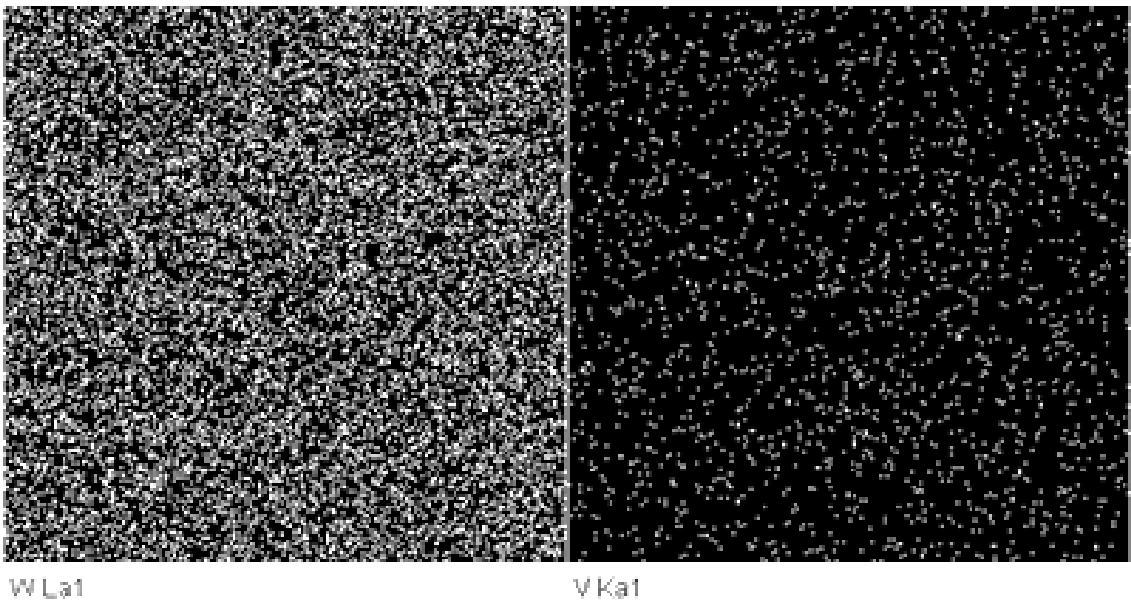
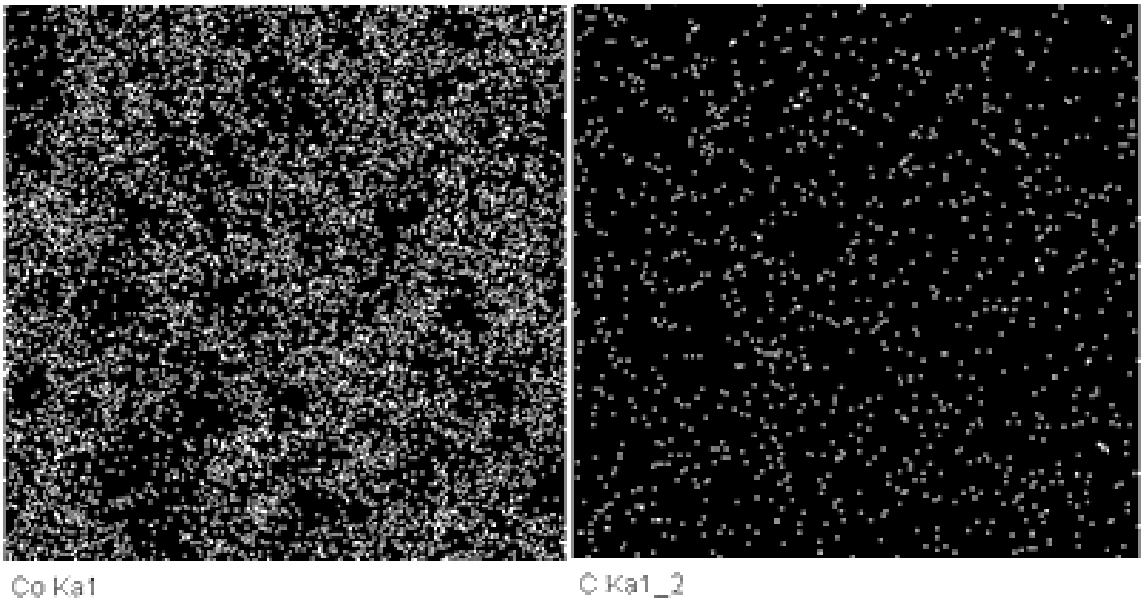
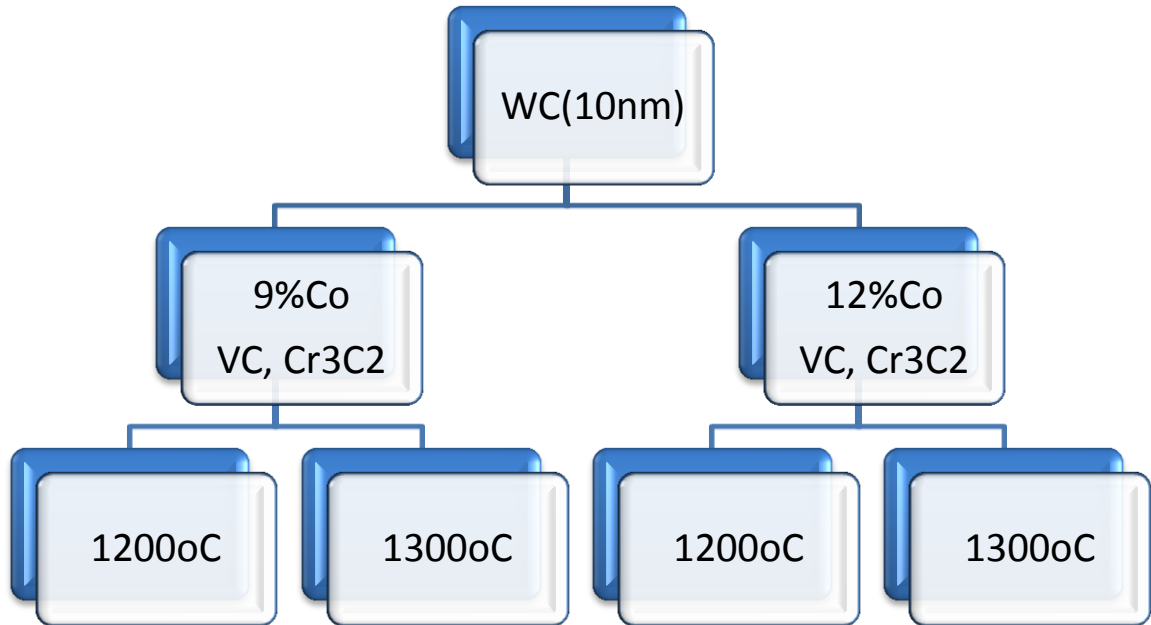


Figure 32 Mapping showing distribution of additives in the composites, after being sintered at 1300°C.

4.7 Effect of adding range of combined Inhibitors to WC-Co Nano composites.



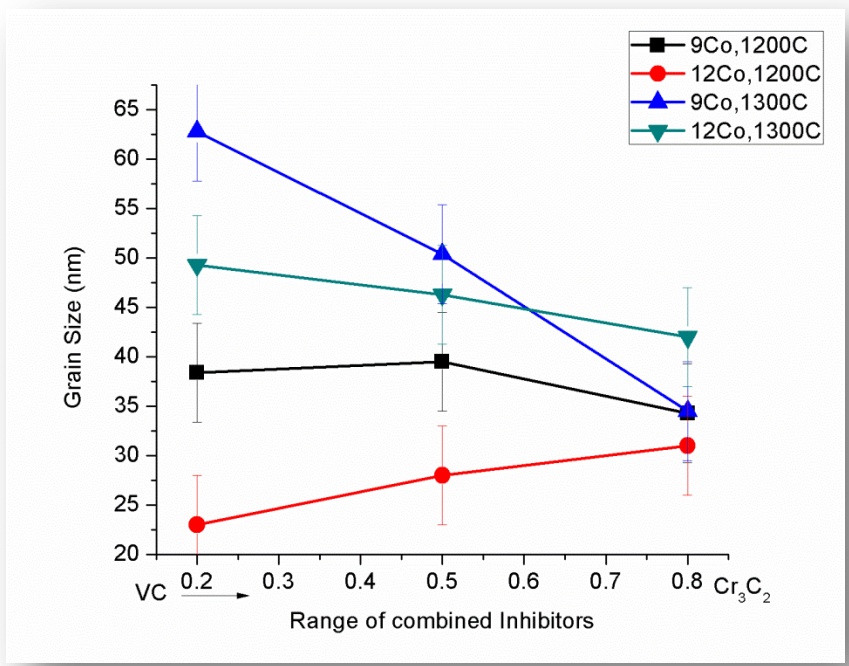
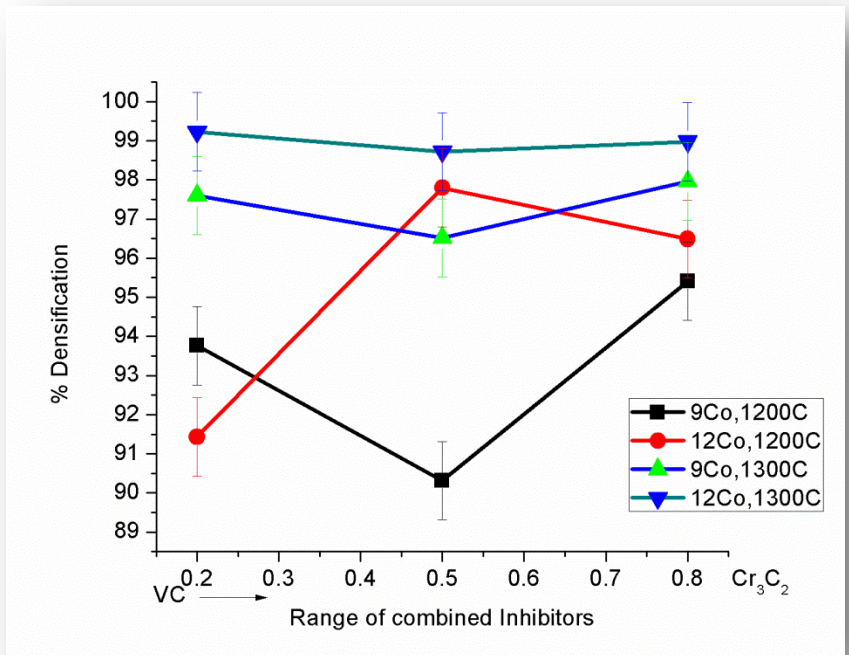
Effect of adding range of combined Inhibitors to WC (10nm)-9,12Co and SPS at 1200°C, 1300°C

Table 10 Experimental input parameters for addition of combination of both inhibitors.

	WC Size	WC-9Co	WC-12C0	VC	Cr3C3	Sintering parameters
sample 4-1	10nm	15		0.5	0.5	1200/50Mpa/10min
sample 4-2	10nm	15		0.8	0.2	1200/50Mpa/10min
sample 4-3	10nm	15		0.2	0.8	1200/50Mpa/10min
sample 4-4	10nm	15		0.5	0.5	1300/50Mpa/10min
sample 4-5	10nm	15		0.8	0.2	1300/50Mpa/10min
sample 4-6	10nm	15		0.2	0.8	1300/50Mpa/10min
sample 4-7	10nm		15	0.5	0.5	1200/50Mpa/10min
sample 4-8	10nm		15	0.8	0.2	1200/50Mpa/10min
sample 4-9	10nm		15	0.2	0.8	1200/50Mpa/10min
sample 4-10	10nm		15	0.5	0.5	1300/50Mpa/10min
sample 4-11	10nm		15	0.8	0.2	1300/50Mpa/10min
sample 4-12	10nm		15	0.2	0.8	1300/50Mpa/10min

Table 11 results for combined addition of inhibitors to Nano-scaled WC-Co

	Hv30	K1c	%densification	grain size(nm)
sample 4-1	847	11.72	90.31	34.3
sample 4-2	916	11.85	95.41	38.4
sample 4-3	811	11.39	93.76	39.5
sample 4-4	1375	11.87	96.52	34.5
sample 4-5	1485	15.92	97.96	62.8
sample 4-6	1514	11.2	97.6	34.5
sample 4-7	1012	12.1	97.8	31
sample 4-8	884	13.1	96.49	23
sample 4-9	913	12.25	91.43	28
sample 4-10	1555	17.5	98.72	42
sample 4-11	1640	11.17	98.98	49.3
sample 4-12	1642	18.29	99.23	46.3



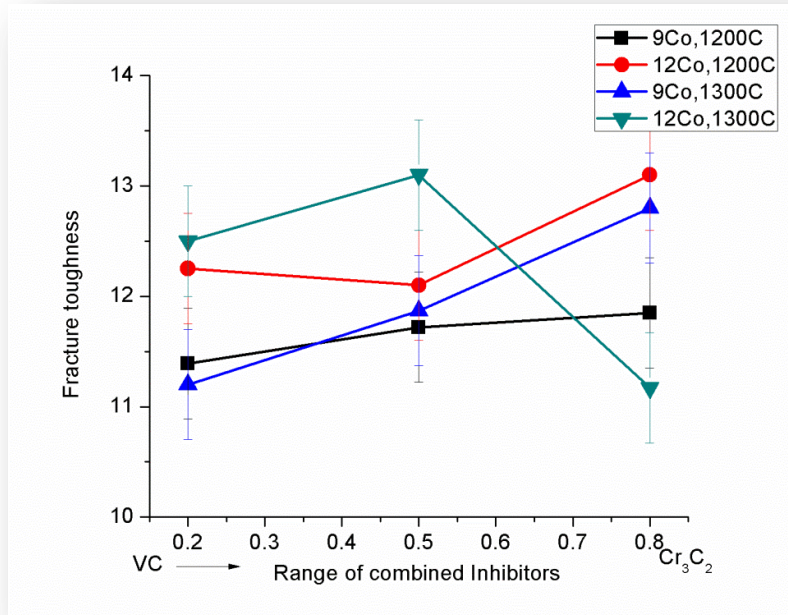
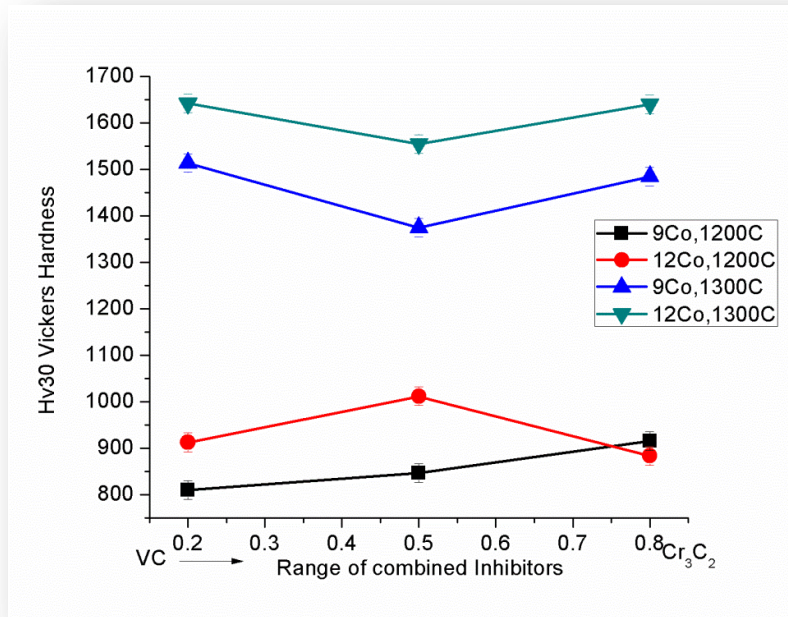


Figure 33 Graphical representation of results from addition of combined effect of inhibitors to the nano composites

It can be noted generally that densification has gone down with the addition of inhibitor. Another general statement, which can be concluded, is that inhibitors have played their role in restricting grains to grow during sintering process. Consolidated samples were analyzed more critically using XRD and peak broadening effect have been studied using sherrer equation to measure the final attained grain sizes. The results show that grains have been refined by the addition of VC/Cr₃C₂ inhibitors, as can be seen more particularly in samples 4-4 and 4-6. The sudden increases in grain size of sample 4-5 are abnormal and are not understood. However the expected grains growth in samples 4-10 to 4-12, which were sintered at high temperature was not noticed. This probably be due to increase in solubility limit of inhibitors in the liquid binder at high temperature, and thus would have comparatively better control over the grain growth, rather than re-precipitation which would rather have happened over the WC/Co boundary. This effect at high temperature has ended in almost same grain sizes which were rather attained at low sintering temperatures. It can also be noted that VC has been found comparatively more active in restricting grains to grow and hence higher quantity of VC has shown finer grains in the consolidated composite, as noticed in samples 4-11. Reducing grain sizes means higher grain boundary area between WC and cobalt which ends with thinner layer of existing cobalt in the composite. So trans granular crack will come across comparatively smaller portion of softer material, which will show decreases in toughness value. Secondly inter granular crack, will have longer routes which consumes larger energy and thus reduces fracture toughness of the composite, as shown in sample 4-11. This has been explained by [51], who reports that Cr₃C₂ mainly exists in binder phase and its addition to binder phase creates distortional stresses in the material, which

restricts its plasticity and hence strengthened the binder phase. Addition of Cr₃C₂ quantity has therefore shown particular increase in Hv30 values, as shown in Table 11 for samples, with high cobalt quantity. Powder composition containing higher content of Cr₃C₂ has shown increase in fracture toughness of the composite, due to the binder strengthening effect, where propagation of crack in the samples will be difficult, and thus have resulted in higher fracture toughness of the composite, as show in 4-10 and 4-1.

Low sinter-ability of nano WC with 9%CO has already been explained in detail in Section 4.3, however it didn't show any improvement in hardness or densification beside the addition of grain growth inhibitors, when sintered at lower temperatures. This can be seen in samples 4-1 to 4-3. However with the same cobalt quantity, and sintered at high temperatures have shown improvement in hardness values. Secondly It can be noted that addition of higher VC content have resulted in lower densification and hence increase porosity in the composite. These micro pores in the composites may act as stress concentration and hence a source of crack initiation and thus reduces fracture toughness of the material, as shown in sample 4-11 Higher cobalt content at higher sintering temperature have shown increases in densification. This can be explained by low viscous binder phase at higher temperatures, which can flow easily into nano pore structure of the material and further can accommodate more WC grains, which helps these grains and added inhibitors to re-arrange themselves easily and hence promotes densification kinetics which results in higher densification.

CONCLUSION:

1. Initial crystallite size of WC plays a vital role in attaining desired mechanical properties of WC-CO cemented carbides. Planetary ball milling process has been can effectively used in reducing WC particle size, as well in homogenizing particle size distribution. Initial crystallite size have been reduced from 78nm to 10nm through ball milling, which increased to almost 92nm after sintering in SPS. However addition of 0.6%Cr₃C₂ has successfully retarded WC grain size to 71nm with almost full densification and 9.23 Mpam^{1/2} and hardness value of 1592Hv30.
2. It was found that change in initial particle size of WC powder in the mixed composition effected the final attained crystallite lite of the resulted composite.
3. It was found through this study that increase in particle surface area, due to finer particle size of WC, must be compensated with increase in binder quantity, to fully bind and dandify all the powder during sintering process. However this quantity must not exceed more, which otherwise may decrease hardness at the expense of fracture toughness. However increasing sintering temperature for the same amount of Cobalt, in a WC-CO composition, has been shown to cover the deficiencies. Higher pressures during SPS may probably increase the mechanical properties of the resultant composite.

4. Addition of inhibitors have played their role in inhibiting the grain sizes, where it is inhibited from 92nm to 40nm after consolidation. Although densification was noticed to reduce.
5. It was found during the study that 0.6VC is the saturation point in WC(10nm)-9Co, when sintered at 1200°C. After saturation densification was found to de-grade. However this saturation point was not noticed at higher amount of cobalt as binding material.
6. This study further strongly emphasizes over the controlling parameters, especially inert gas, during milling process, or otherwise the probable adsorption of oxygen and water droplets may results in decarburization and hinders the flow of binder during sintering process. This would probably help in attaining higher dense nano crystallite carbides with improved hardness value while maintaining higher fracture toughness.
7. Addition of inhibitors was found useful in reducing ultimate grain size of the composite, although densification was found to decrease.
8. VC has been found to be more active in refining the grains, however samples containing more VC were found to have more micro porosity, cause of early crack initiation.
9. However Cr₃C₂ was found more active in increasing hardness, densification and fracture toughness of the composite. Although it was found comparatively weaker in controlling grain growth during sintering process.

10. Further using combined effect of both inhibitors has been found to be more effective, rather than individual in attaining higher mechanical properties along with minimum grain sizes. . This is because VC has been found more effective in restricting grain growth, while at the same time has been found to end up with comparatively lower densification and lower fracture toughness value. However Cr_3C_2 has been noticed to increase effective hardness value of the composite. It also was found to comparatively have higher densification.

Future Recommendation.

1. Cobalt added should be allowed to mill for long hours along with WC from the very beginning Homogeneous
2. Use of spray conversion prepared powder, possibility of different gases being absorbed, which will hinder flow of liquid cobalt.
3. Effect of using Higher pressures during \SPS can be studies in future.

Publications.

1. *Effect of consolidation mechanism on the properties of micro-nanostructured WC-6, 9, 12 wgt%co hard metals.*
2. *Influence of initial powder surface area over the consolidation behavior of WC-9Co hard material by spark plasma sintering and their mechanical properties.*
3. *Influence of temperature and binding material over microstructural behavior of fine grained WC-Co-VC/Cr₃C₂ composite produced by ball milling assisted spark plasma sintering technique.*
4. *Effect of type and amount of inhibitor on the microstructural and mechanical properties of VC/Cr₃C₂doped WC-Co nanocomposites.*
5. *Combined effect of VC/Cr₃C₂ over microstructural development of WC-Co nano composited prepared by spark plasma sintering.*

REFERENCES.

- [1] H. Y. S. Z.Z., X. Wang, T. Ryu, K.S. Hwang, "Synthesis, sintering, and mechanical properties of nanocrystalline cemented tungsten carbide," *International Journal of Refractory Metals and Hard Materials*, vol. 27, no. 2, pp. 288–289, 2009.
- [2] K.-M. Tsai, C.-Y. Hsieh, and H.-H. Lu, "Sintering of binderless tungsten carbide," *Ceramics International*, vol. 36, no. 2, pp. 689–692, Mar. 2010.
- [3] Z. Z. Fang, X. Wang, T. Ryu, K. S. Hwang, and H. Y. Sohn, "Synthesis, sintering, and mechanical properties of nanocrystalline cemented tungsten carbide – A review," *International Journal of Refractory Metals and Hard Materials*, vol. 27, no. 2, pp. 288–299, Mar. 2009.
- [4] X. L. and J. Z. S. Zhao, X. Song, C. Wei, L. Zhang, "Effects of WC particle size on densification and properties of spark plasma sintered WC-Co cermet," *International Journal of Refractory Metals and Hard Materials*, vol. 27, pp. 1014–1018, 2009.
- [5] E. J. Fang Z, "Study of Nanostructured WC-Co Composites," *Int J Refract Met Hard Mater*, vol. 13, pp. 297–303, 1995.
- [6] W. P. Sommer M, Schubert WD, Zobetz E, "On the formation of very large WC crystals during sintering of ultrafine WC–Co alloys," *Int J Refract Met Hard Mater*, vol. 20, pp. 41–50, 2002.
- [7] K. B. Cha SI, Hong SH, "Spark plasma sintering behavior of nanocrystalline WC–10Co cemented carbide powders," *Mater Sci Eng*, vol. 351, pp. 31–38, 2003.
- [8] C. Suryanarayana, "Mechanical alloying and Milling," *Progress in Materials Science*, vol. 46, no. 1–2, pp. 1–184, 2001.

- [9] T. C. T. Kagnaya, C. Boher, L. Lambert, M. Lazard, “mechanisms of WC-Co cutting tools from high-speed tribological tests,” *Wear*, vol. 267, pp. 890–897, 2009.
- [10] I. Konyashin, B. Ries, and F. Lachmann, “Near-nano WC–Co hardmetals: Will they substitute conventional coarse-grained mining grades?,” *International Journal of Refractory Metals and Hard Materials*, vol. 28, no. 4, pp. 489–497, Jul. 2010.
- [11] Z. Yao, J. J. Stiglich, and T. S. Sudarshan, “Nano-grained Tungsten Carbide-Cobalt (WC / Co),” pp. 1–27.
- [12] R. R. Berger S, Porat R, “Nanocrystalline materials: a study of WC-based hard metals,” *Prog Mater*, vol. 42, pp. 311–320, 1997.
- [13] M. S. El-Eskandarany, “Structure and properties of nano-crystalline TiC full-density bulk alloy consolidated from mechanically reacted powders,” *Journal of Alloys and Compounds*, vol. 305, pp. 225–238, 2000.
- [14] Y. S. F.] L. Fu, L.H. Cao, “Two-step synthesis of nanostructured tungsten carbide–cobalt powders,” *Scripta Materialia*, vol. 44, pp. 1061–1068, 2001.
- [15] C. J. and J. X. L. Sun, T.e. Yang, “VC, Cr₃C₂ doped ultrafine WC-Co cemented carbides prepared by spark plasma sintering,” *International Journal of Refractory Metals and Hard Materials*, vol. 29, pp. 147–152, 2011.
- [16] Y. M. Kai Egashira, Shigeyuki Hosono, Sho Takemoto, “Fabrication and cutting performance of cemented tungsten carbide micro-cutting tools,” *Precis Eng*, vol. 35, no. 4, pp. 547–553, 2011.
- [17] H.-C. Kim, I.-J. Shon, J.-K. Yoon, and J.-M. Doh, “Consolidation of ultra fine WC and WC–Co hard materials by pulsed current activated sintering and its mechanical properties,” *International Journal of Refractory Metals and Hard Materials*, vol. 25, no. 1, pp. 46–52, Jan. 2007.

- [18] a. Michalski and D. Siemiaszko, "Nanocrystalline cemented carbides sintered by the pulse plasma method," *International Journal of Refractory Metals and Hard Materials*, vol. 25, no. 2, pp. 153–158, Mar. 2007.
- [19] J. V. Huang, S.G., K. Vanmeensel, L. Li, O. Van der Biest, "Tailored sintering of VC-doped WC-Co cemented carbides by pulsed electric current sintering," *International Journal of Refractory Metals and Hard Materials*, vol. 26, no. 3, pp. 256–262, 2008.
- [20] H. Kim and I. Shon, "Consolidation of ultra fine WC and WC – Co hard materials by pulsed current activated sintering and its mechanical properties," *International Journal of Refractory Metals & Hard Materials*, vol. 25, pp. 46–52, 2007.
- [21] S. Zhao, X. Song, J. Zhang, and X. Liu, "Effects of scale combination and contact condition of raw powders on SPS sintered near-nanocrystalline WC–Co alloy," *Materials Science and Engineering: A*, vol. 473, no. 1–2, pp. 323–329, Jan. 2008.
- [22] R. B. Almond EA, "Identification of optimum binder phase compositions for improved WC hard metal," *Mater Sci Eng A*, vol. 105/106, no. 237–48, 1988.
- [23] M. Mahmoodan, H. Aliakbarzadeh, and R. Gholamipour, "Sintering of WC-10%Co nano powders containing TaC and VC grain growth inhibitors," *Transactions of Nonferrous Metals Society of China*, vol. 21, no. 5, pp. 1080–1084, May 2011.
- [24] A. . R. A Calka, "Universal high performance ball-milling device and its application for mechanical alloying," *Materials Science and Engineering: A*, vol. 134, pp. 1350–1353, 1991.
- [25] S.-J. L. Kang, "Sintering: densification, grain growth, and microstructure," *published by Butterworth-Heinemann Ltd*, vol. ISBN 97807, 2004.
- [26] G. S. Upadhyaya, "Some issues in sintering science and technology," *Materials Chemistry and Physics*, vol. 67, no. 1–3, pp. 1–5, 2001.

- [27] J. R. Groza, "Nanocrystalline Powder Consolidation Methods," *Nanostructured Materials, Second edition, ed. C.C. Koch, William Andrew Publishing, Norwich, NY*, pp. 173–233, 2007.
- [28] O. MortezaOghbaei, "Microwave versus conventional sintering: A review of fundamentals, advantages and applications," *Journal of Alloys and Compounds*, vol. 494, no. 1–2, pp. 175–189, 2010.
- [29] I.-J. S. Kim, H.-C., D.-Y. Oh, "Sintering of nanophase WC–15vol.%Co hard metals by rapid sintering process," *International Journal of Refractory Metals & Hard Materials*, vol. 22, pp. 197–203, 2004.
- [30] L. Ding, D. P. Xiang, Y. Y. Li, C. Li, and J. B. Li, "Effects of sintering temperature on fine-grained tungsten heavy alloy produced by high-energy ball milling assisted spark plasma sintering," *International Journal of Refractory Metals and Hard Materials*, vol. 33, pp. 65–69, Jul. 2012.
- [31] N. A. R.M. Govindarajan, "Deformation processing of metal powders: Part I—Cold isostatic pressing," *International Journal of Mechanical Sciences*, vol. 36, no. 4, pp. 343–357, 1994.
- [32] M. F. A. . D. Turner, "The cold isostatic pressing of composite powders—I. Experimental investigations using model powders," *Journal of ActaMaterialia*, vol. 44, no. 11, pp. 4521–4530, 1996.
- [33] S. T. Srivatsan TS, Woods R, Petraroli M, "An investigation of the influence of powder particle size on microstructure and hardness of bulk samples of tungsten carbide," *Powder Technol*, vol. 122, pp. 54–60, 2002.
- [34] J. S. Sun, J., F. Zhang, "Characterizations of ball-milled nanocrystalline WC-Co composite powders and subsequently rapid hot pressing cermets," *Materials Letters*, vol. 5, no. 2003, 2003.

- [35] M. I. O. . Belmonte, J. González-Julián, P. Miranzo, “Spark plasma sintering: A powerful tool to develop new silicon nitride-based materials,” *Journal of the European Ceramic Society*, vol. 30, pp. 2937–2946, 2010.
- [36] N. Saheb, Z. Iqbal, A. Khalil, A. S. Hakeem, N. Al Aqeeli, T. Laoui, A. Al-Qutub, and R. Kirchner, “Spark Plasma Sintering of Metals and Metal Matrix Nanocomposites: A Review,” *Journal of Nanomaterials*, vol. 2012, pp. 1–13, 2012.
- [37] “The electro-discharge compaction of powder tungsten carbide-cobalt-diamond composite material,” *Advances in Sintering Science and Technology*, vol. Bordia and, 2010.
- [38] W. Liu, X. Song, K. Wang, and J. Zhang, “A novel rapid route for synthesizing WC–Co bulk by in situ reactions in spark plasma sintering,” ... *and Engineering: A*, vol. A 499, pp. 476–481, 2009.
- [39] W. D. S. and B. L. B. Wittmann, “WC grain growth and grain growth inhibition in nickel and iron binder hardmetals,” . *Int J Refract Met Hard Mater*, vol. 20, pp. 51–60, 2002.
- [40] D. Sivaprahasam, S. B. Chandrasekar, and R. Sundaresan, “Microstructure and mechanical properties of nanocrystalline WC–12Co consolidated by spark plasma sintering,” *International Journal of Refractory Metals and Hard Materials*, vol. 25, no. 2, pp. 144–152, Mar. 2007.
- [41] S. G. Huang, K. Vanmeensel, L. Li, O. Van der Biest, and J. Vleugels, “Influence of starting powder on the microstructure of WC–Co hardmetals obtained by spark plasma sintering,” *Materials Science and Engineering: A*, vol. 475, no. 1–2, pp. 87–91, Feb. 2008.
- [42] V. Huang SG, Li L, Vanmeensel K, Van der Biest O, “VC. Cr₃C₂ and NbC doped WC–Co cemented carbides prepared by pulsed electric,” *Int J Refract Met Hard Mater*, vol. 25, pp. 417–22, 2007.

- [43] R. M. Da Silva AGP, De Souza CP, Gomes UU, Medeiros FFP, Ciaravino C, “low temperature synthesized NbC as grain growth inhibitor for WC–Co composites,” *Mater Sci Eng A*, vol. 293, pp. 242–6, 2000.
- [44] K. S. C.W. Morton, D.J. Wills, “The temperature ranges for maximum effectiveness of grain growth inhibitors in WC–Co alloys,” *Int J Refract Met Hard Mater*, vol. 23, pp. 287–293, 2005.
- [45] B. S. H.] X.Q. Wang, H.L. Guo, “Inhibition of WC grain growth during sintering of cemented carbide,” *J Shanghai Univ (Nat Sci)*, vol. 9, pp. 312–316, 2003.
- [46] V. Bonache, M. D. Salvador, V. G. Rocha, and A. Borrell, “Microstructural control of ultrafine and nanocrystalline WC – 12Co – VC / Cr 3 C 2 mixture by spark plasma sintering,” *ceramics Internatoinal*, vol. 37, pp. 1139–1142, 2011.
- [47] W. Z. N. Li, Y.X. Qiu, “Influence and function of inhibitor VC/Cr3C2 on the grain growth in super fine WC–Co cermets,” *Rare Met Mater Eng*, vol. 36, pp. 1736–1766, 2007.
- [48] L. B. Schubert WD, Bock A, “General aspects and limits of conventional ultrafine WC powder manufacture and hard metal production,” *Int J Refract Met Hard Mater*, vol. 13, pp. 281–96, 1995.
- [49] C. DF, “Sintering and microstructural development in WC/Co-based alloys made with superfine WC powder,” *Int J Refract Met Hard Mater*, vol. 17, pp. 123–32, 1999.
- [50] V. Bonache, M. D. Salvador, a. Fernández, and a. Borrell, “Fabrication of full density near-nanostructured cemented carbides by combination of VC/Cr3C2 addition and consolidation by SPS and HIP technologies,” *International Journal of Refractory Metals and Hard Materials*, vol. 29, no. 2, pp. 202–208, Mar. 2011.
- [51] B. Zhan, N. Liu, Z. Jin, Q. Li, and J. Shi, “Effect of VC/Cr3C2 on microstructure and mechanical properties of Ti(C,N)-based cermets,” *Transactions of Nonferrous Metals Society of China*, vol. 22, no. 5, pp. 1096–1105, May 2012.

CURRICULUM VITAE

Khwaja Mohammad

Current Address

Research Assistant, Mechanical
Engineering Department, King Fahd
University of Petroleum and Minerals,
Dhahran Dammam.

Email: wawakhan@kfupm.edu.sa
wawa_khan90@yahoo.com

Permanent Address

Haji Abad, Eid Gah Road
Mardan City, Khyber
Pukhtoonkhwa, Pakistan.

Email: wawakhan@kfupm.edu.sa
wawa_khan90@yahoo.com

M.Sc.
(Engineering) Material and Manufacturing (Mechanical
Engineering), King Fahd University of
Petroleum & Minerals (KFUPM), Dhahran,
Saudi Arabia. (February'2011–till date).

Education

B.Sc.
(Engineering) Metallurgy And Materials Engineering,
Ghulam Ishaq Khan Institute Of Engineering
Sciences And Technology, Topi Swabi,
Pakistan.
(Sept. 1995 – May 1999).

Work

Experience

Feb. 2001
May'2001 Teaching Assistant at Ghulam Ishaq Khan
Institute of Engineering Sciences and
Technology, Pakistan.

May 2001-
Dec'2006 Jr. engineer (Research & Development),
Powder Metallurgy, Lab. Pakistan.

May 2006-
Feb'2011 Sr. Engineer (Research & Development),
Powder Metallurgy Lab. Pakistan.

Feb.2011- till
date Research Assistant, Mechanical Engineering
Department, KFUPM, Saudi Arabia.

Certificates

1. Member of materials society for Engineering, Pakistan.
2. Java computer programming skills, Certification from IT track, Karachi.
3. Post graduate computer orientation course certification at Islamabad, Pakistan.
4. Adventure foundation of Pakistan.

Technical skills

Development of low- dense high thermal ceramic insulation through Powder Metallurgy, Developed high temperature 1700oC Sintering furnace, Development of different Ceramic Alloys, Porous Ceramics, Ferrite Materials, worked on Microwave Furnace, de-binding cycles, sintering behaviour, Glass coatings over Alumina based substrates in air and under reducing environment, Zirconia-Toughened Alumina.

Recent Area of Research

WC-Co nano composites, synthesis, analysis by FESEM, XRD, micro indentation, Fracture toughness and Hv30 for improving mechanical aspects. Nano-structural control by grain growth inhibition using VC and Cr₃C₂ as inhibitors. Consolidation by Spark plasma sintering. Micro and nano Al₂O₃ based high tech-Ceramics, Development and characterization of Advanced Materials, Surface Engineering, Advance coatings. Corrosion study of re-inforced steel in concrete.

Publication and conferences

K. Muhammed, M. Islam, M. I. Qureshi, A. A. Khan « Development and Characterization of Ceramic Foams/Filters from Commercial Grade Alumina » Proceedings of 6th Int. Symp. on Advanced Materials, 19-23 Sept. 1999, Islamabad, Pakistan, pp 47-50. (Published).

K. Mohammad, T. Laoui, S. Nouari, A. S. Hakeem, K. Abdullahi, N. Al-Aqeeli “Influence of initial powder surface area over the consolidation behavior of WC-9CO hard material by spark plasma sintering and their mechanical properties.” 2012.(Ready to be submitted).

K. Mohammad, T. Laoui, S. Nouari, N. Al-Aqeeli “Effect of type and amount of inhibitor on the microstructural and mechanical properties of VC/Cr₃C₂ doped WC-Co nano composites. (Under preparation).

N. Al-Aqeeli, K. Mohammad, T. Laoui, S. Nouari “Influence of temperature and binding material over microstructural behavior of fine grained WC-CO-VC/Cr₃C₂ composite produced by ball milling assisted spark plasma sintering technique.”(Ready to be submitted).

N.Al-Aqeeli, K. Mohammad, T. Laoui, S. Nouari “Combined effect of VC/Cr₃C₂ over microstructural development of WC-Co nano composited prepared by spark plasma sintering.” (Under preparation).

T. Laoui, A. S. Hakeem, K. Mohammad, K. Abdullahi, S. Nouari, N. Al-Aqeeli “Effect of consolidation mechanism on the properties of micro-nanostructured WC-6,9 12 wgt%Co hard metals 12-10-2012_Abbas (1).” 2012. (Ready to be submitted).